A review of nanoparticle material coatings in passive radiative cooling systems including skylights

Gangisetty, Gopalakrishna; Zevenhoven, Cornelis A P

Review

A Review of Nanoparticle Material Coatings in Passive Radiative Cooling Systems Including Skylights

Gopalakrishna Gangisetty [ID] and Ron Zevenhoven *[ID]

Process and Systems Engineering, Åbo Akademi University, 20500 Turku, Finland
* Correspondence: ron.zevenhoven@abo.fi; Tel.: +358-2215-3223

Abstract: Daytime passive radiative cooling (DPRC) has remained a challenge over the past decades due to the necessity of precisely defined materials with a significantly high emissivity of thermal radiation within the atmospheric transparent window wavelength range (8–13 μm) as well as high reflectivity in the solar spectrum (0.2–3 μm). Fortunately, recent advances and technological improvements in nanoscience and metamaterials are making it possible to create diverse metamaterials. This enables the production of DPRC in direct solar irradiation. The development of a material that is appropriate for effective DPRC is also a noteworthy development in this field of technology. This review gives a thorough introduction and discussion of the fundamental ideas, as well as the state-of-the-art and current trends in passive radiative cooling, and describes the cutting-edge materials and various photonic radiator structures that are useful in enhancing net cooling performance. This work also addresses a novel skylight window that offers passive cooling developed at the Åbo Akademi (ÅA) University, Finland. In conclusion, nanomaterials and nanoparticle-based coatings are preferred over all other approaches for commercialization in the future because of their low cost, the ability for large-scale production, simplicity in fabrication, and great potential for further increasing cooling performance.

Keywords: daytime radiative cooling; skylight; atmospheric window; solar irradiation; photonic radiators; nanoparticles; surface coatings; energy savings; building thermal management

1. Introduction

The two greatest threats to human life posed by climate change in many parts of the world in recent years have been energy scarcity and global warming. A major contributor to climate change is anthropogenic greenhouse gas (GHG) emissions. In a study conducted by the International Energy Agency (IEA), buildings currently utilize 20–40% of the world's energy with conventional HVAC systems engrossing most of its primary energy [1]. There are numerous applications, including domestic, commercial, and industrial, where cooling requires a substantial quantity of energy. Major reasons for the high-energy usage of cooling are the growing population, improved living standards in developing countries—particularly in hot climate regions—and industrial development [2]. Conventional cooling systems utilize 15% of the world's electricity and result in 10% of GHG emissions. The global CO_2 concentration is now 147% higher than it was before industrialization, and rising. Emissions of gaseous refrigerants are predicted to make up 45% of all GHG emissions by the end of 2050 [3]. Therefore, there is a pressing need for innovation in cooling technologies to reduce both energy usage and GHG emissions.

The current ubiquitous vapor compression-based cooling technologies are facing issues with energy usage and the global warming effect due to the refrigerants used, e.g., hydrofluorocarbons (HFCs), which consequently cause environmental problems. The increased spotlight on the energy crisis and environmental concerns has upsurged an interest in enhancing the efficiency of existing cooling systems and monitoring various cooling technologies. Analysis of various cooling processes suggests that passive radiative

cooling (PRC) is the most effective way to cool buildings. Further, PRC is a technology that provides cooling alternatives to heat pumps. Recently, PRC techniques and their potential applications have gained noticeable attention for energy-saving applications. The PRC technique that cools with no power required could therefore make an exceptional difference in energy usage and the reduction in emissions that cause global warming. The general principle of passive cooling is the dissipation of heat from buildings to an environmental heat sink. Many research studies address PRC strategies under different climatic conditions. This technology can be used to reduce energy usage in both buildings and automobiles, solve urban heat islands, and tackle water issues [2,4]. In spite of the possibility that PRC approaches might be useful in building design, they are not widely used. Two cited challenges in this area are technical and cost problems. Technical problems are low cooling capacity, expensive specialized manufacturing techniques or suitable materials, challenging system implementation, issues with durability, and maintenance concerns [5].

Thermal radiation depends on spectrum characteristics due to Kirchhoff's law of heat absorption, which links emittance to absorptance. A significant application of this technology is that it is possible to alter the rate of radiative heat transfer between objects by changing the spectral absorption or emissivity of these, which is dependent on how electromagnetic waves interact with them. Increased reflectance on a surface, for example, reduces heat absorption and hence prevents a temperature gain, which is critical in a radiative cooling scenario. Reduced reflectance and greater absorption of incident power, on the other hand, result in temperature increase, which is critical in radiative heating applications. Accordingly, good thermal radiation control results in greater system efficiency and lower maintenance costs of temperature control systems due to increased component lifespan because of reduced thermal loads [6].

The field of radiative cooling has been the focus of many authors since the mid-20th century. Nonetheless, it appears as if radiative cooling research has fallen very short of its potential due to a lack of researchers engaged in this area, as well as a lack of complete analysis of its diverse technological scope [7]. This idea provided the impetus for the compilation of a review paper that includes thorough and methodical mathematical descriptions of radiative cooling, information updates on various leading-edge radiator materials, and introduces novel applications of PRC [8]. The research work conducted by Lu et al. [9] concentrated on advancements in the PRC of buildings, including the formulation of theoretical models and calculations, the structural design and configuration of cooling systems, and the forecasting of potential and prospects. Muntasir et al. [10], Sun et al. [11], and others later introduced the concept of radiative cooling from basic fundamental principles, materials, and radiators. In their work, the main topic was the progress of sophisticated materials and radiators that provide radiative cooling during both day and night, together with metamaterials and photonic radiators. Sergi et al. [12] conducted a thorough analysis of the PRC theory and nocturnal radiators, with particular emphasis on atmospheric radiation and selective radiative emitters. Furthermore, their work also covered several numerical simulation methods and radiative cooling prototypes, but they did not address how to realize commercial applications. Researchers are still having trouble sufficiently improving cooling performance during the daytime towards implementation in a consumer product because it is impossible to ignore direct solar irradiance. A substantial amount of research is yet to be undertaken on diurnal radiative cooling, which is more challenging than nocturnal radiative cooling [13–15].

In fact, this article also provides a comprehensive analysis of the fundamental physics underlying PRC, considering radiation to the atmosphere and space beyond that. Several other variables, in addition to the incoming atmospheric radiation, have an impact on a radiator's cooling capacity. For instance, the effect of non-radiative heat transfer gain from the environment (conduction and convection heat gain) on radiative cooling must be taken into account [16]. Correspondingly, it has been possible to compile modern radiative structures and exotic materials [2,9,17–19] which are discussed in further sections. The main distinction between this work and others is demonstrated by an example provided in it,

namely a passive skylight window design that provides a passive cooling skylight prototype developed at Åbo Akademi University (ÅA) in Finland [20]. This skylight provides passive cooling at a rate of 100 W/m^2 without external power. The core concept of that PRC skylight, realized using widely accessible materials, could enhance the performance of current cooling systems, which will enable next-generation thermal management of buildings. Further sections concentrate on providing a brief overview of the nocturnal (nighttime) and diurnal (daytime) materials as well as information on various investigations based on the experimental findings for each structure and material to enhance net cooling performance. The following sections go over advanced radiator types, metamaterial developments, recent research on nanophotonic structures and nanoparticle-based techniques, challenges and potential application developments and improvements in this technology, as well as opportunities for radiative cooling. Finally, the discussion includes informative ideas and suggestions for commercializing this technology. There are a few points to keep in mind when promoting PRC technology on a large scale, such as the low energy density, low cooling capacity, and constrained sky-facing area hampers the large-scale application of PRC technology [2,21–23]. It is undeniable that further research into this technology is required in order to develop a new generation of PRC coolers with high efficiency, less energy usage, and the capability of maximizing net cooling performance at all times.

1.1. Passive Radiative Cooling

PRC is the phenomenon that reduces the temperature of a system by promoting heat transfer with the sky. Our planet earth must eventually reemit all solar radiation absorbed by it into space through heat radiation. If not, the earth would continue to heat. Figure 1 shows average heat flows in the earth–atmosphere energy balance. The average incident radiation is 341.3 W/m^2, of which the atmosphere reflects 79 W/m^2 and the surface absorbs 161 W/m^2. As shown in the figure below, radiative cooling transfers all heat from the earth to space [20].
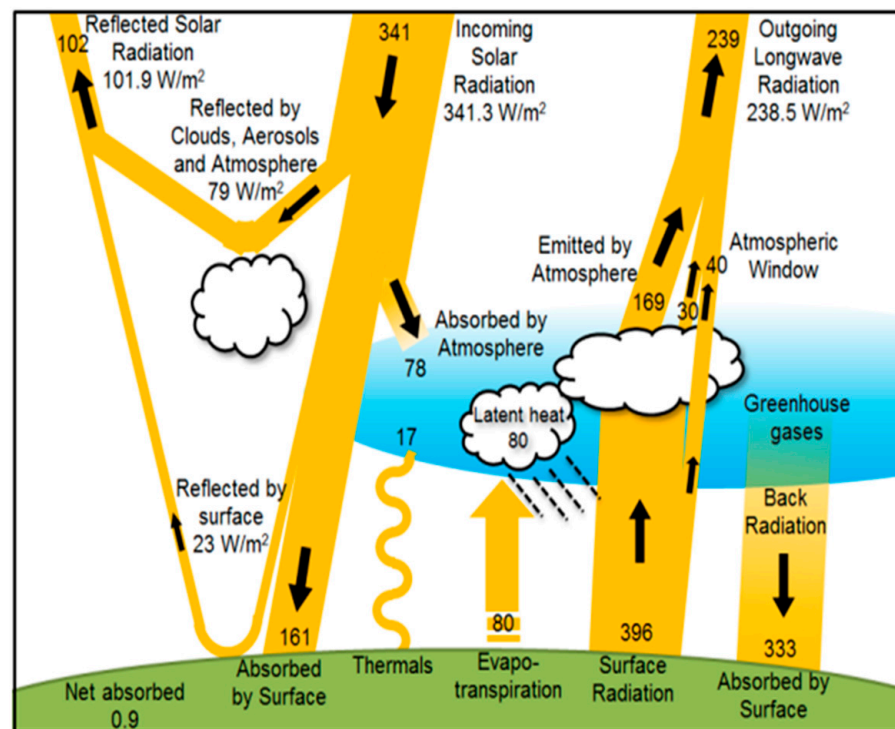

Figure 1. Representation of earth–atmosphere energy balance [24].

Considering that the earth's surface temperature is around 300 K, and the universe is blackbody radiation at 3 K, it is possible to use this large temperature difference acting

as a main driving force to cool the surface by radiating thermal infrared radiation to the universe via the atmosphere. The atmosphere, which consists of several gases located between the planet's surface and the universe, participates in PRC via the superposition of radiation to and from its constituent elements. A benefit is that our earth's atmosphere has an "atmospheric window"—a region from 8–13 µm where it is highly transparent. Different gases can absorb and emit heat radiation in various parts of the spectrum. The primary atmospheric gases' absorption spectra are shown in Figure 2 sub-pictures. The atmospheric window's wavelength range can still fit into these various spectra. Due to its limited transmittance in most wavelength bands, the atmosphere blocks heat radiation from the earth's surface to the universe. Regardless, the atmosphere serves as a semi-transparent medium for radiative cooling applications [20].
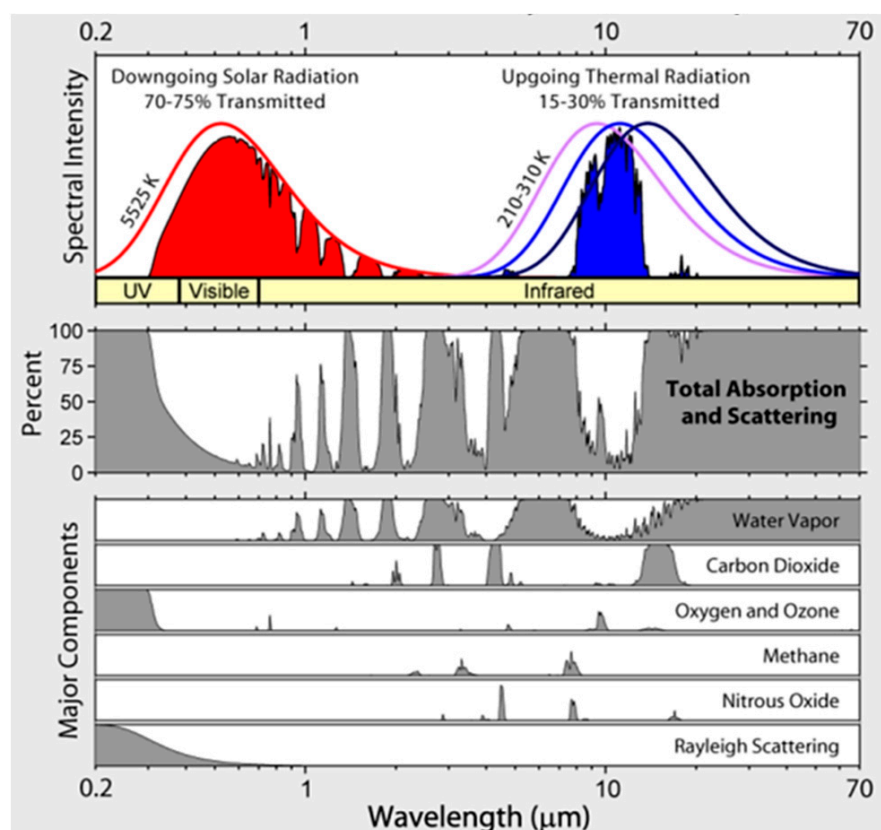

Figure 2. Thermal radiation transmission by the atmosphere [25].

The principle of PRC relies on the fact that the atmosphere transmits about 87% of the outgoing radiation from the Earth in the "atmospheric window" region. Surfaces can exchange heat with cold space (3 K) through this atmospheric window region. If surfaces (or participating gases, for that matter) experience a mismatch between outgoing and incoming thermal radiation, they can reach a lower steady-state temperature than the ambient due to strong emission in this wavelength region and strong reflection outside of it [26].

Fortunately, the wavelength of the atmospheric window falls within the black body's peak thermal radiation region at room temperature (300 K), as defined by Plank's law. This property allows a passive cooling mechanism for a terrestrial body to operate at room temperature by removing heat through the atmospheric window. The Earth's atmosphere acts as a huge thermal reservoir that allows radiation to escape into space directly. Consequently, any terrestrial object with a high emissivity in the atmospheric window can radiate heat into space effectively. Even so, a number of factors, such as geographical location, cloudiness, and humidity levels, affect atmospheric window transmittance. When the sky is clear and dry, the atmospheric window transmittance is high [8].

When the sky is clear at night, PRC can produce around 100 W/m^2 of net cooling power, which suggests that a relatively large surface area is required to deliver significant cooling power of a few kilowatts (kW) or more. Demanding a larger surface area in building applications certainly leads to the development of sophisticated material technology to produce suitable radiators, which entails high installation and production costs, and maintenance issues [5]. The main problem, however, is material science, i.e., finding practical window materials for effective cooling during day and night that can afford outstanding performance at a lower cost; this technique will be a challenging solution to PRC acceptability.

1.2. Classification of PRC

PRC research falls into two main categories: radiative cooling at night (nocturnal) and radiative cooling during the day (diurnal). The design of PRC systems typically involves adjusting the spectral reflection, emission, absorption, and transmission at various wavelength intervals. While radiative cooling is difficult in the daytime, nocturnal cooling has been an established practice for centuries. A considerable amount of research has been conducted on nocturnal PRC materials, as well as on the potential uses of nocturnal radiative cooling. According to Eriksson and Granqvist [27], the initial scientific study to investigate the effects of nocturnal cooling in 1828, Arago revealed the existence of this phenomenon. Arago recorded a temperature drop of 6–8 °C below the surrounding air for the small amount of grass, cotton, and quilt placed outside in a tranquil environment during the night. Later, Alan K [28] made the first suggestion for selective infrared (IR) emitters to enhance PRC's performance at night. Since then, several strategies have been developed to improve radiative cooling.

There are actually two types of conventional radiators in use for overnight radiation cooling. A thermal blackbody emitter is the first kind of radiator to have a high emissivity in all thermal radiation bands. A selective radiator is another form of radiator that emits significant heat solely through the atmospheric window wavelength. There is experimental evidence that it is possible to achieve nocturnal cooling up to around 100 W/m^2. Under cloudless skies, radiative heat flux from a thermal blackbody emitter at near ambient temperatures can reach up to 120 W/m^2 [29]. The ability to reach a minimum temperature below the surroundings is limited by the inverse effect of radiative thermal absorption outside the 8–13 μm wavelength, which makes it difficult to attain temperatures lower than 6 and 8 °C below the ambient. Thus, alternative methods for mitigating adverse thermal absorption at sub-ambient temperatures include using metallic mirrors (typically aluminum or silver) surrounded by thin layers of material that only absorb/emit within the atmospheric window and are transparent to other wavelength regions. Metallic mirrors reflect undesirable solar irradiation, while emitters transfer thermal energy to space by emitting radiation within the range of the atmospheric window. For the top portion of the emitting materials, a wide variety of materials have been suggested, including polymers, pigmented paints, metal oxides, gas slabs, multilayer semiconductors, and metal–dielectric photonic and plasmonic structures [30].

However, the challenge with daytime cooling is solar irradiation, and exposure to direct sunlight during the daytime (around noon) reduces the effectiveness of the devices and systems due to the need for much larger cooling power (up to 1000 W/m^2). Around noon, a small amount of solar absorption of 1000 W/m^2 might be sufficient to counteract the surface temperature dependent on the outgoing radiative cooling power of between 100 and 150 W/m^2. The solar spectral region, which has shorter wavelengths between 0.2–3 μm, and the atmospheric transparency window, which has wavelengths between 8 and 13 μm, need to be addressed simultaneously in the development of effective high-performance DPRC materials [2] (see Figure 3).

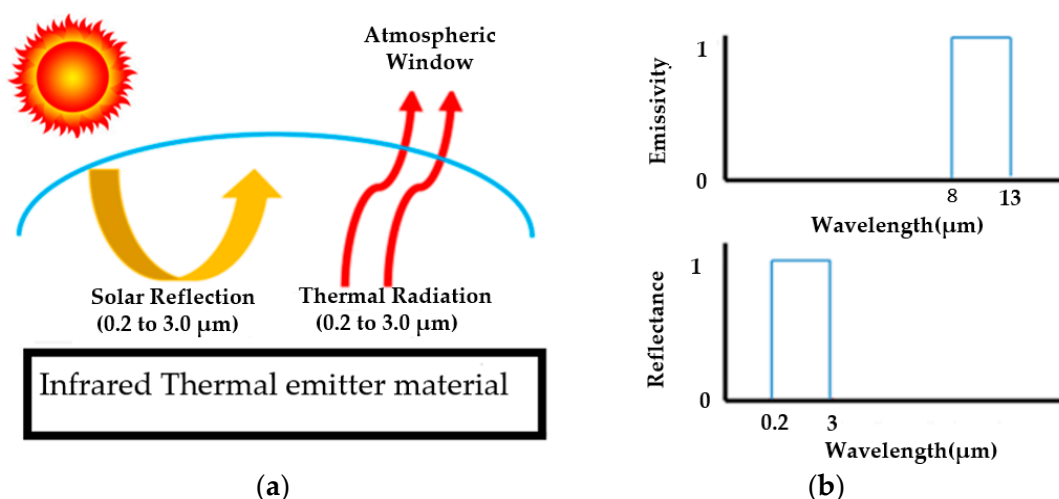**Figure 3.** (**a**) Radiative cooling: Schematic presentation. (**b**) Radiative cooling properties of materials for ideal reflection and emission (adapted from [31]).

To limit solar heating during the day, these materials must have low absorption (100% reflectance) in the solar spectrum. In addition, they should also have high emissivity ($\approx$1) in the atmospheric transparency window in order to transfer excess heat effectively to the sky and, eventually, to outer space as the final heat sink of radiative cooling. In the early attempts to obtain these specific characteristics, a radiative cover shield was fixed at the top of the radiative cooler. During the day, the radiative cooler beneath the cover shield can emit radiation into space because it reflects solar radiation while remaining transparent to long wavelengths inside the atmospheric window. Various researchers have contemplated polyethylene foils covered or doped with TiO_2, ZnS, and ZnO for this application [32–34]. Nevertheless, it is difficult to achieve high solar reflectance and high IR transmittance simultaneously. Furthermore, PRC systems are based on various materials and structures such as bulk media (painted metal and gypsum), thin films (ZnS, CdTe, SiO, PbSe, MgO), and gases (ammonia, ethylene, ethylene oxide), including functional films coated with SiO and Si_3N_4, have been explored and tested. Although these radiators also emit large amounts of radiation into the atmosphere, these materials perform poorly and have limitations when exposed directly to sunlight during the daytime. So none of the experiments using these materials and techniques has succeeded in obtaining sub-ambient temperatures when exposed to direct sunlight [35].

Fortunately, the recent demonstration of effective DPRC under direct sunlight through the development of innovative classes of selective infrared radiators, combined with metamaterials, nanophotonic structures, nanoparticle methods, also cutting-edge design methodologies enabled the fabrication of precise structures with tailored radiative properties for various energy applications. This also results in daytime cooling that results in temperatures below ambient. During the daytime, these novel radiators provide significant diurnal radiative cooling due to their high reflection capability within the range of solar radiation and strong emissivity within the atmospheric wavelength.

The importance of this research has grown steadily over the past decade. In 2013, Raman et al. [36] published the first theoretical design of a metal–dielectric planar photonic structure for DPRC based on adjusting the spectral behaviour/responses of the material. Later, in 2014, ref. [37] they achieved DPRC for the first time experimentally using a precisely designed nanophotonic structure radiative cooler. In this photonic radiative cooler, seven alternate dielectric layers are deposited onto a silver mirror, allowing it to cool to 4.9 °C below the surrounding temperature by reflecting 97% of incident solar irradiance while selectively emitting in the wavelength of the atmospheric transparency window.

Another effective example is the DPRC structure suggested and created by Zhai et al. [38] using a polymer embedded with micron-sized dielectric spheres on top of a silver (Ag)

substrate as the back reflector In spite of this, many photonic structures are not widely used due to their high production cost, production complexities, and other complicated manufacturing techniques [21,30,39]. Besides emissive properties, a DPRC must have adequate heat-insulating properties to keep the temperature differential with the surroundings. Currently, the most prominent strategies combining the DPRC techniques are to be solar irradiance backscattering, thin film forming, cooling coating, pumping of mid-infrared thermal radiation from the radiator, and phonon control, all of which result in continuous sub-ambient cooling during the day and at night. Backscattering is the most popular method for obtaining material for DPRC, based on reflection [40]. It is possible to achieve this by incorporating Titania (TiO_2) and silica (SiO_2) particles in high concentrations (40–50% Wt) into a paint or coating. Several potential pigments, including TiO_2, ZrO_2, ZnS, ZnSe, and ZnO, were tested with a pigment fraction of 0.10–0.15 in 400-μm-thick polyethylene. In terms of radiative cooling properties, ZnS performed better, which had 84.9% solar reflectivity, but due to peak solar radiation, they were unable to achieve daytime cooling at noon. TiO_2 has higher solar reflectivity but absorbs UV radiation due to bandgap overlap, whereas ZrO_2 is lossless in UV but has a lower refractive index and thus reflects less than titania. Many of the proposals suggested in the application of PRC in buildings are still lacking research and development, mostly regarding the transmissivity/emissivity of the material or the use of PRC to maximize net cooling performance. Inclusive of the above, daytime radiative cooling still has three significant issues. To begin with, it is unclear which structures are essential for radiative cooling to perform at it is their best. Secondly, it is difficult to avoid the heat losses produced by the different available coolers, which restricts both cooling power and temperature drop to less than 105 W/m^2 and 10 °C, respectively. Therefore, these materials should have substantial emissivity in other wavelengths, preferably within the atmospheric window, while having extremely low absorptivity in the intense solar spectrum [5,22].

1.3. Fundamental Physics of Radiative Cooling

Developing dynamic and efficient radiative coolers for specific applications requires accurate engineering and design. This subsection discusses the design issues for radiative coolers and the physics involved in PRC as described by the heat-transfer balance equation (see Figure 4). In fact, estimating the incoming spectrum irradiation on a terrestrial body is crucial for determining the cooling capability of radiative coolers. Generally, a terrestrial body may partially absorb, reflect, or transmit the radiation. A body's absorption (α), reflection (ρ), and transmission (τ) are related as follows: $\alpha(\lambda) + \rho(\lambda) + \tau(\lambda) = 1$. Kirchhoff's law states that absorptivity and emissivity (ε) are equal $\alpha(\lambda) = \varepsilon(\lambda)$ for every object in thermal equilibrium in all directions and for all wavelengths [30].

Let us consider a material that has similar absorption qualities to a black body with $\alpha = \varepsilon = 1$. It can predominantly absorb incident light from the surroundings and achieve complete absorption across all spectral regions. Kirchhoff's law would thus predict that the material would also possess excellent thermal radiation emission properties. Consequently, the following Equation (1) [41] represents spectral radiation from a black body at temperature T:

$$I_{BB}(T,\lambda) = \frac{2\pi hc^2}{\lambda^5} \frac{1}{\exp\left(\frac{h.c}{\lambda kT}\right) - 1} \qquad (W/m^2) \qquad (1)$$

where I_{BB} represents the radiation intensity of the blackbody at a given temperature T (K), and wavelength λ, h is a Planck's constant and its value is 6.626×0^{-34} J·s, k = 1.381×10^{-23} J/K is Boltzmann's constant, and c = 3×10^8 m/s is the speed of light.

For a given temperature, certainly, a black body emits energy into its surroundings, according to Equation (1). Furthermore, it may be possible for heat from the material to be transferred by conduction and convection besides thermal radiation. To compute the net

cooling impact of a radiative cooler, it is necessary to consider all heat transfer mechanisms, which can be determined by using the formula below from Equation (2): [41]

$$P_{net} = P_{rad} - P_{atm} - P_{nonrad} - P_{solar} \qquad (W/m^2) \qquad (2)$$

where P_{solar} represents the power density of the sun (say, 1000 W/m^2) and P_{rad} is the Radiative power emitted by the radiative cooler, given by the following:

$$P_{rad} = 2\pi \int_0^{\pi/2} \sin\theta \cos\theta \int_0^\infty I_{BB}(T_{rad}, \lambda) \varepsilon_{rad}(\lambda, \theta, d\lambda) \, d\theta \qquad (W/m^2) \qquad (3)$$

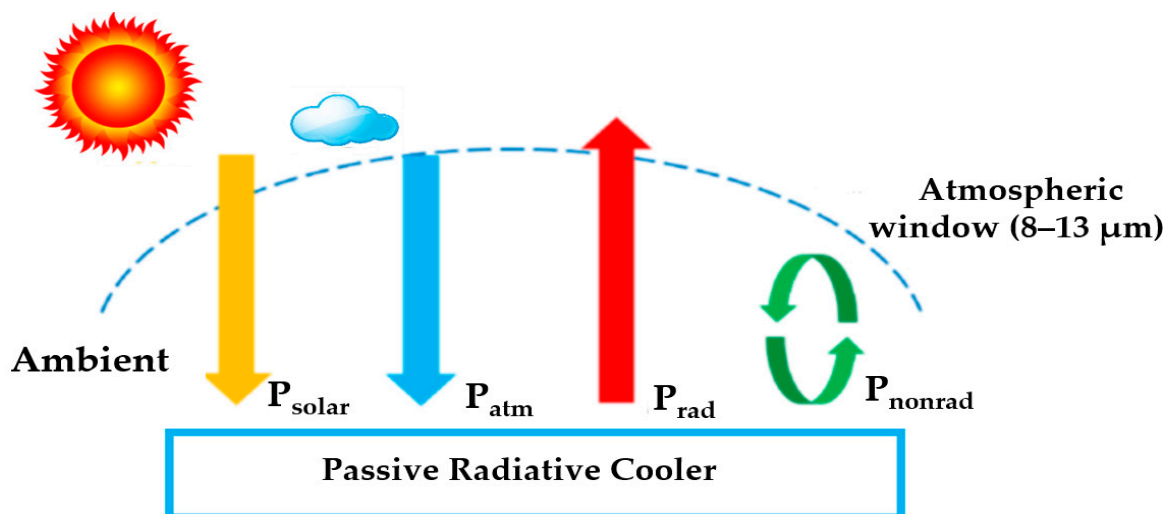θ represents the zenith angle in the above equation.

Figure 4. Schematic representation of radiative cooling surface (adapted from [42]).

Based on the above equation, the thermal radiative intensity of an object directly correlates with its structure and shape as well as the temperature. It is therefore possible to use the shape and structure of the object to improve the thermal radiative power throughout the effective area and control the emissivity $\varepsilon_{rad}(\lambda, \theta)$ of the radiative cooler in the appropriate wave band to achieve an optimal cooling capacity [21]. A radiative cooler's performance, however, will be significantly impacted by weather factors like humidity and clouds [41].

1.4. Impact of Solar Irradiation on DPRC

Solar radiation has a significant impact on how effectively radiative cooling operates throughout the day. A cooler's cooling power also referred to as its total cooling heat flux, is the first determinant (P_{net}). The emissivity of the structure should be close to that of a blackbody emitter in the 8–13 μm range and near zero at wavelengths where the atmosphere is strongly emitting. During the day, however, the structure's solar absorptivity is the dominating factor that determines its cooling efficiency. Therefore, it is crucial that the structure's solar heat absorption remains well below 10% during the daytime in order to achieve meaningful cooling. Another important criterion is the temperature difference that can be achieved by a radiative cooler ($\Delta T = T_s - T_a$), where T_s represents the surface temperature and T_a is an ambient temperature. The temperature at which P_{net} reaches zero is the lowest temperature difference that can exist (the cooler's heat fluxes are then balanced between absorbing heat and emitting heat) [30].

Let us consider that if solar radiation is 800 W/m^2, a radiator with a 5–10% solar absorption will absorb 40–80 W/m^2, which is close to or may exceed a radiator's cooling capacity. Accordingly, the performance of the radiative cooler will decrease as more sunlight

is absorbed by the cooler. The power of the radiative cooler for absorbing solar radiation (P_{solar}) can be determined using the following expression: [8]

$$P_{solar} = A \int_0^\infty \alpha(\lambda, \, 0) \, I_{AM1.5}\,(\lambda) d\lambda \qquad (W/m^2) \qquad (4)$$

where $I_{AM1.5}(\lambda)$ stands for the typical sun spectral irradiance (1000 W/m^2) distribution for reference and AM1.5 represents 1.5 air masses as the path through the atmosphere. A global spectrum profile of AM1.5 is shown in Figure 5; the yellow color illustrates the sun's spectrum across various wavelengths together with the atmospheric window (blue) region. In principle, the cooler must have high reflectivity in order to provide PRC during the day by reducing the absorption of solar energy [21].
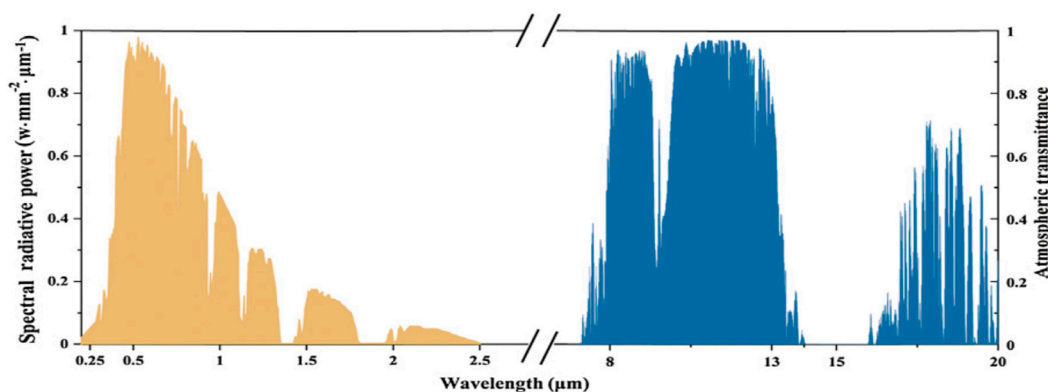

Figure 5. AM1.5 standard solar spectrum (Yellow in color), Atmospheric window (Blue in Color 8 to 13 μm) [21].

The spectral energy of the solar spectrum can be measured experimentally using spectro-radiometers. Later, by using the global AM1.5 spectrum, it is possible to validate the applicability of this experimental method to local weather conditions [8]. On the other hand, one of the accepted methods is the ASHRAE clear sky radiation model, which can be used to determine the solar heat flux that eventually needs to be cooled from a surface or from a volume of participating gas [43].

1.5. Influence of Atmospheric Radiation

The atmosphere between the surface of the earth and space is intricate; atmospheric radiation is the result of the superposition of radiation from elements that exist in the atmosphere. Nitrogen (N_2) and oxygen (O_2), the atmosphere's gas composition, also consists of water vapor, carbon dioxide (CO_2), ozone (O_3), hydrocarbons, nitrogen oxides (NOx), etc. Therefore, it is in the atmosphere's capacity to absorb/emit different infrared wavelengths between 3 and 50 μm radiation that limits the cooling effect, inhibiting the process of thermal radiation from terrestrial objects to space. Water vapor emits/absorbs substantially at 6.3 μm and 20-μm. For CO_2 the main IR emission characteristic is a broadband-intensive emission band primarily focused at 15 μm. While water vapor and carbon dioxide obscure most of the ozone emission bands in the infrared region, a narrow emission bandwidth at 9.6 μm is eminent [30].

The atmospheric radiation in the zenith direction (AM1.0) is minimum. When the air is dry in the wavelength range of 8–13 μm, the so-called atmospheric window allows for practically complete transmission across the atmosphere without absorption. Mainly, the CO_2 and water vapor emission bands, however, are responsible for an overall emission/absorption effect in this range [30]. Sky emission in the atmospheric window wavelength is also highly dependent on air moisture content, ambient temperature, and dew point temperature. Usually, the sky emissivity is greater at larger zenith angles because of the longer path length. Further, the second and the less considerable transparent

window for low concentrations of water vapor in the atmosphere is present in the 16–22 μm range. Atmospheric window transparency is only high in good weather. Moreover, if the atmospheric window is blocked by clouds, rain, or humid conditions, radiative cooling will have a lower cooling effect [30].

Then, in accordance with the thermal radiation theory, P_{atm} is power absorbed by the radiative cooler from the incident atmospheric radiation and is given by,

$$P_{atm} = 2\pi \int_0^{\pi/2} \sin\theta . \cos\theta \int_0^\infty I_{BB}(T,\lambda) \varepsilon_{atm}(\lambda,\theta) \, d\lambda \, d\theta \qquad (W/m^2) \qquad (5)$$

Furthermore, both the angle and the wavelength have an impact on atmospheric emissivity. The following Equation (6) emerges, by applying Kirchhoff's rules.

$$\varepsilon_{atm}(\theta,\lambda) = 1 - \tau_a(\lambda)^{1/\cos\theta} \qquad (6)$$

$\varepsilon_{atm}(\theta,\lambda)$ represents the spectral directional emissivity of the radiator, and $\tau_a(\lambda)$ denotes the transmittance of the atmosphere in a specific direction [21].

Moreover, the atmosphere is almost a blackbody radiator with a temperature of 1–2 °C below ground level ambient temperature for a cloudy sky, according to the measurements on spectral atmospheric radiance made by Bell et al. [32]. This renders the PRC effect for cloudy skies inappropriate. The atmosphere emissivity of a sky under various conditions is a crucial consideration when evaluating PRC systems in order to assess the accuracy of the radiative model. The two most significant variables in calculating sky radiation, besides sky emissivity, are spectral emittance profile and atmospheric temperature. Imagine the atmosphere to be a gray-emitting body at temperature (T_a), with an effective emittance $\bar{\varepsilon}_a$ value of for a total hemispheric emittance (i.e., the ratio of the material's total emissive power to the total emissive power of an ideal black body). Atmospheric radiative heat flux is then as follows [30]:

$$P_a = \varepsilon\sigma T_a{}^4 \qquad (W/m^2) \qquad (7)$$

Following Zevenhoven et al. [44], one shortwave (SW) band < 4 μm plus three longwave (LW) bands, including 4–8 μm, 8–13 μm (the atmospheric window), and >13 μm, can be used to describe how thermal radiation travels through the atmosphere. The atmosphere's transmittance is $\tau_{ai} = 1 - \varepsilon_{ai}$, (i = 1 to 4) for zero reflectance. Consequently, for all four bands, the approximate atmospheric emittance values are with the values $\varepsilon_{a1} = 0.26$ for SW radiation and $\varepsilon_{a2} = 1$, $\varepsilon_{a3} = 0.55$, 0.65, and $\varepsilon_{a4} = 1$, respectively [16], can used for LW radiation. With the exception of wavelengths between 8 and 13 μm, Kondratyev treated the atmosphere as opaque. Using the correlation shown below, a value for ε_{a3} was determined here using Equation (8), [44]

$$\varepsilon_{a3} = 1 + \frac{107,952 \times (1 - \varepsilon_a)}{T_a^2 - 680.0 \times T_a + 73,594.9} \qquad (8)$$

In recent years, several researchers have used empirical correlations to estimate the atmospheric hemispherical emittance more precisely. Such relationships depend on direct measurements of sky radiance and empirical equations to fit experimental observations. For instance, Catalanotti et al. as well as other researchers also report approximate measurements for the atmospheric emittance values. They endorsed total emittance values for clear skies of 0.5–0.6 for arid areas at high elevation, 0.8–0.9 at sea level, and close to 1.0 for cloudy skies. Brunt et al. developed the following mathematical equation for the sky's total emittance based on the partial water vapor pressure in the atmosphere [30]:

$$\varepsilon_a = A + B\sqrt{(p)} \qquad (9)$$

where p stands for partial water pressure (mbar), and A and B are empirical constants with values ranging from 0.34 to 0.71 and 0.023 to 0.110, respectively.

Later, Murray [30], derived an empirical equation for total atmospheric emittance by considering dew point temperature (T_{dp} in °C) and ambient temperature (T_a in °C). It is given by the following:

$$\varepsilon_a = 0.741 + 0.0062T_{dp} \; (-) \tag{10}$$

$$T_{dp} = 273.3 \times \frac{\ln(RH) + axb}{(a - \ln(RH)) + axb} \; (K) \tag{11}$$

a and b are considered empirical constants in the above Equation (11), and their values are as follows: a = 1.727, $0 \leq RH \leq 1$, and b = $T_a/(T_a + 273.3)$, where T_a = ambient temperature.

Similar to this, Martin and Berdahl [30] presented an empirical equation for the relationship between wavelength (λ), zenith angle(θ), and total sky emittance in the case of spectral sky emittance.

$$\varepsilon(\theta, \lambda) = 1 - (1 - \bar{\varepsilon}_a.[t(\lambda)/t_{av}].e^{b(1.7-1/\cos\theta)} \quad (-) \tag{12}$$

$$\varepsilon_a = 0.711 + 0.56(\frac{Tdp}{100}) + 0.73\left(\frac{Tdp}{100}\right)^2 \quad (-) \tag{13}$$

The values are $t(\lambda)/t_{av}$, b implicitly dependents shown in tabular form in [30], valid for $-13 < T_{dp} < 24$ °C, $\bar{\varepsilon}_a$ = total sky emittance, and T_{dp} = dew point temperature (°C). The above Equations (7)–(13) above are most commonly used to properly assess atmospheric emittance and its parameters.

The use of the effective total emittance value ($\bar{\varepsilon}_a$) and modeling the atmosphere as a gray body at an ambient temperature mainly have two implications according to studies conducted by a number of researchers (T_a). The first one is that, initially, many studies made the wrong assumption that the sky emits as a black body outside the range of atmospheric wavelengths. This led to inaccurate estimates of the high cooling capacities for blackbody emitters used as nocturnal PRC. The second point of concern is that experimental measurements presented in [30] showed that the amount of moisture and the zenith angle have a significant effect on directional sky radiation within the atmospheric window wavelength. The variation in atmospheric emissions caused by differences in water vapor amounts, as well as their directional dependence, are greatly reduced when the sky is seen as a gray body.

1.6. Non-Radiative Heat Transfer (Conduction and Convection)

Heat conduction and convective heat transfer affect radiative cooler performance, in addition to its own heat radiation, solar radiation, and atmospheric heat radiation. Convectional and conductional heat transfer from the surroundings is represented by the P_{nonrad}, which is given by,

$$P_{nonrad} = h \cdot (T_{rad} - T_{atm}) \quad (W/m^2) \tag{14}$$

The cooler temperature and atmospheric irradiance temperature are T_{rad} and T_{atm}, respectively, and h stands for the non-radiative heat transfer coefficient (W/m^2K) that results from the heat transfer mechanisms (natural plus forced convection and typically much smaller conduction of heat) from the radiative cooler to its surroundings. A well-controlled h value ranges from 2.0 to 6.9 W/m^2 K. A higher value for non-radiative heat coefficient (h) indicates greater conductive and convective heat exchange with the ground level environment, and a radiative cooler (P_{nonrad}), which results in less cooling power for the fixed temperatures T_{rad} and T_{atm}. To obtain the highest cooling power (P_{net}), it is mandatory to increase the radiative power emitted by the radiative cooler (P_{rad}), while reducing the power absorption from the incident atmospheric gains for effective radiative cooling, $P_{rad} >> P_{nonrad}$. Thus, from the perception of the optimum radiative cooler design, zero absorption (i.e., nearly 100% reflection) across the entire solar spectrum, selective and nearly total absorption/emissivity across the wavelength region from 8 to 13 μm matching the atmospheric transparence window, and reduced excessive energy dissipation

by conduction and convection are the important factors [41]. In addition, several researchers have put forth some of the equations for the radiative cooler's non-radiative heat transfer coefficient. The equations h = 5.7 + 3.8 V and h = 2.8 + 3.0 V, respectively, where V is wind speed in m/s, have been suggested to describe a radiative cooler without the windshield and with the windshield in [41]. Based on the outcomes of the simulation for a particular case with the windshield, Rephaeli et al. [45] and Zhu et al. [36] determined that h = 6, 12, and 40 [W/m^{2}K] for the velocities at V = 1, 3, and 12 m/s, respectively. The values of h are presented for the case of a radiative cooler without the windshield in [46] and [47], where h = 1 + (6 V$^{3/4}$) and h = 1.8 + (3.8 V), respectively—valid if V lies between 1.35 and 4.5 m/s.

Zeyghami et al. [30] calculated and compared the cooling characteristics of a broadband IR radiator and ideal IR emitter by considering three cooling surfaces in two scenarios for surface temperatures $T_s \leq T_{amb}$ and $T \geq T_{amb}$. Cooling heat fluxes up to 80 W/m^2 have been determined for a broadband IR radiator and an ideal IR emitter at room temperature. The cooling heat flux decreases until zero as the surface temperature gradually decreases. The ideal IR emitter has a ΔT_{min} of -9 °C and the broadband IR radiator has a ΔT_{min} of -6 °C, i.e., when a radiative cooler is intended to produce cooling effects at a temperature below ambient, non-radiative heat transfer has a significant impact on the surface ability to cool. Reaching ΔT_{min} -14 °C for a broadband IR emitter and ΔT_{min} -43 °C for an ideal IR emitter is possible by eliminating non-radiative heat transfer completely in the case of $T \geq T_{amb}$. A value $P_{net} = 490$ W/m^2 was calculated for the broadband IR radiator at $\Delta T = 20$ °C higher than the surrounding temperature. A cooling heat flux of up to 405 W/m^2 was found for an ideal IR emitter under similar circumstances. It makes sense that the non-radiative cooling effect would take over as the dominant cooling phenomenon at higher surface temperatures. Similar research findings by Granqvist and co-workers demonstrated that for an ideal IR emitter, increasing ambient temperature and or a lower air humidity would improve the radiative cooler's performance and raise P_{net} and ΔT_{min} values [43].

However, the majority of current studies on radiative cooling assume that the cooler surface temperature is the same as the ambient temperature and disregard non-radiative heat transfer (P_{nonrad}). In real-world situations, this temperature difference is significant, which lowers the cooling effect. Maintaining the temperature drop achieved by cooling with radiant coolers that require effective heat convection insulation is crucial. In conclusion, DPRC performance can be improved or optimized by utilizing four different ways. (1) Improving the radiator's ability to radiate heat effectively. (2) The radiative cooler's ability to reflect more sunlight. (3) Adjusting thermal radiation's wavelength to focus in the range of 8–13 μm. (4) Lastly, controlling the radiation of heat from the radiative cooler to the environment, i.e., the sky through the atmosphere. When developing an ideal radiative cooler, it is crucial to take the material, the structure, and the shape into consideration. By choosing the right materials (today's challenge is also from the material resources availability point of view), the radiative cooler should have high solar reflectivity. However, the power of the sun's radiation, the amount of water in the air, the speed of the wind, and the pressure of the cloud cover all have a significant impact on how efficient radiative coolers are. Certainly, it is essential to take into account the local climatic conditions when developing future radiative coolers [21].

2. A Comparison of Active and Passive Daytime Cooling Technologies for Buildings

Solar energy can be used to provide electricity, heat, light, and cooling for both residential and commercial buildings without harming the environment, apart from the effects of constructing the equipment. In order to brighten the indoor environment, it is possible to gather solar energy as daylight. A passive daytime system often also collects and distributes sunlight for efficient interior building lighting. Daytime passive cooling systems give both daylighting as well as cooling in order to achieve the goal of low-energy buildings [48].

Solar light is gathered and dispersed in a variety of ways; passive and active daylighting systems are extricated based on how light is gathered and dispersed. Skylight windows, sliding glass doors, static waveguides, etc., are just a few examples of the non-tracking, static designs used as part of passive daytime cooling systems to capture, reflect, and disperse the sunlight into a building's interior. In daylighting systems that actively collect sunlight, mechanical and optical devices are equipped with sun-tracking mechanisms that move with the sun and then distribute it through waveguides into buildings' structures [49,50]. The tracking device in an active daylighting system makes it functional when daylight begins early in the morning and lasts until the evening, giving it an edge over stationary passive daytime systems. An active daytime system does have a drawback, though, in that it has a high initial installation cost, related maintenance, and operating costs [48]. The use of passive daytime systems in sustainable building design has a number of benefits, including affordability, simple installation, and aesthetic design (good visual appearance). The following advantages can be mentioned:

(1) All types of buildings can have DPRC installed, and existing construction projects can even use it at a reduced cost.
(2) Daytime cooling systems improve the quality of the indoor air because they do not use forced air systems.
(3) The lack of mechanical components makes passive daytime systems easier to maintain than active daylighting systems.
(4) Savings on electricity-driven cooling and heating expenses are among the long-term advantages of passive cooling during the daytime [48,51].

Passive daytime cooling systems are little more expensive than buildings made only of concrete and bricks, though they will end up costing less over time, according to specialists in passive solar design. The incorporation of passive daytime systems into sustainable building designs presents a number of difficulties:

(1) Due to the fact that glass types and qualities can vary widely, picking the right glass to meet DPRC specifications can be challenging. When choosing materials for passive daytime cooling homes, choosing the wrong glass or other high SW transmittance material is an expensive mistake. The location (north, south, east, or west) and climate of a building will determine the best type of glass to use.
(2) A strong connection exists between daylight and heat. The use of daytime lighting during the summer or in areas where the climate is warm all year can increase the amount of energy used by the air-conditioning systems.
(3) A poorly designed passive daytime system can produce a glare on household items and appliances (furniture, televisions, refrigerators, and laptops). As a result, the placement of items in the home necessitates careful consideration [48].

2.1. Technical Description of Passive Daytime Systems

Passive cooling skylights are used in buildings that do not have enough wall openings so that sunlight can enter through the roof or other horizontal surfaces. Examples of passive daytime cooling techniques include louvers, tubular daylight, skylights, slope glazing, roof windows, solar lights made from soda bottles, windows, light shelves, reflectors, and sawtooth roofs. This section describes a variety of skylight types and their advantages since it is hard to list all kinds of passive daytime systems [52].

2.2. Types of Skylights

A skylight is a usually covered opening in a roof that allows sunlight to penetrate a building from above and brighten it. The material selected for making skylights can have a significant impact on both the quality of daylight and the energy efficiency of the building structure. Polymers and glass in a range of colors and thicknesses are popular skylight glazing materials. Installing pitched or dome-shaped skylights at the same height as a building's roof is standard practice. Light wells are an essential component while designing the skylight. Light wells direct daylight into the building before it enters the interiors by

channeling it via the roof and ceiling. A light well accomplishes two tasks: it diffuses light and protects the observer from direct sunshine [53].

Fixed unit skylight: Generally, this type of skylight typically lacks ventilation and has a structural perimeter frame that supports the light-transmitting portion, which is generally constructed using plastic or glass [48].

Operable skylight: Residents can reach this type of skylight if it is accessible through the roof. It rotates at the top and resembles a single-window frame that opens a few inches higher to allow for greater air circulation and sunlight. Skylights that are operated manually may feature manual locks that allow them to open and close at a specific level [48].

Tubular daylighting device: This fixed unit roof skylight captures sunlight and transfers it to a light-diffusing element via some type of light conveyance optical conduit. This system absorbs and transmits solar light via a roof-mounted dome measuring 0.254 m to 0.559 m in diameter. The building's dome gathers light beams, which are then scattered by a system of aluminum tubes and spread throughout it by a number of specular reflections. The size of the dome is determined by the building's size and is made of acrylic or polycarbonate to block UV light [48].

Retractable skylight: This type of skylight is made up of a single retractable window frame or a group of retractable window frames positioned on top of a roof. When the window is controlled, it slides out of the frame and onto a set of rails, enabling a full opening to the exterior for direct sunshine or ventilation of the building's interior. They use a mechanical cable system to retract left and right as well as up and down [48].

Straight and splayed skylight: There are two types of skylights, straight and splayed. Both of them allow light to enter the building from the rooftop. The spread skylight design spreads light more widely across the building than the straight skylight design, which is how these two designs differ from one another. On the other hand, spread skylights must be closer together than straight skylights to produce the same amount of light [48].

Sloped glazing: When designing and developing sloping glazing assemblies for a specific project, sections are often used. They combine several infill panels in a frame structure. Single clear glass, single glazing with gray tint, double clear glass, double glazing with gray tint, double glazing with selective tint, double glazing with reduced emissivity (Low-E), and triple glazing with Low-E are some of the glazing types that are frequently used in residential windows. It becomes more difficult to select the ideal glazing material when both energy savings and natural light are taken into account simultaneously [54–56].

3. Transmissive Radiative Cooling Skylights

The structural and material engineering for PRC studies is essential, as discussed above, and has been proposed and investigated since the second half of the 20th century. As the first design of a radiative cooler in the 1980's, silicon compounds like silicon dioxide (SiO_2) and silicon nitride (Si_3N_4) were produced on aluminum (Al) film-coated glass substrates using the vacuum deposition technique. These designs successfully achieved PRC, which in practice obtained a net cooling power of about 100 W/m². Following the pioneering work and looking for window materials for skylights allowing passive cooling [57], ÅA has developed and tested a skylight that offers nocturnal PRC up to ≈100 W/m².

The possibility of running water through a double-glass window for simultaneous water heating and air conditioning was presented by a few researchers in the past [58]. However, little research has been conducted concerning the use of so-called participating gases inside skylights that interact with thermal radiation in specific, preselected wavelength bands. Since then, ÅA has been researching PRC strategies to improve cooling performance using skylights during the daytime, an approach that has received little attention. So far, ÅA has investigated and published the fundamentals and possibilities of this technology and its viability through simulations and experimental results [20]. See Section 3.1 of a skylight filled with a participating gas that absorbs and emits thermal radiation, with necessary high absorption, emission, and transmittance of gases and window materials in the atmospheric window range of 8–13 μm.

3.1. ÅA Skylight Prototype

This skylight model, the design and function of which was developed at ÅA, was assessed for effectiveness as both a passive cooler during summer and a thermal insulator during winter. The $10 \times 10 \times 10$ cm^3 small skylight setup for proof-of-concept experiments is shown in Figure 6. Acrylic plastic (non-transparent for long-wavelength thermal radiation, i.e., >4 μm) is used for the construction, except for two zinc sulfide (ZnS) windows as top and bottom cover. The central window (which guides the convective heat flow inside skylight) is constructed of acrylic plastic, which has a reflection coefficient of $\rho = 0.9$ at all wavelengths. The central window divides the skylight into two sections that absorb from below, emitting heat to the atmosphere and space above via thermal radiation-driven (natural) convection while minimizing turbulence.
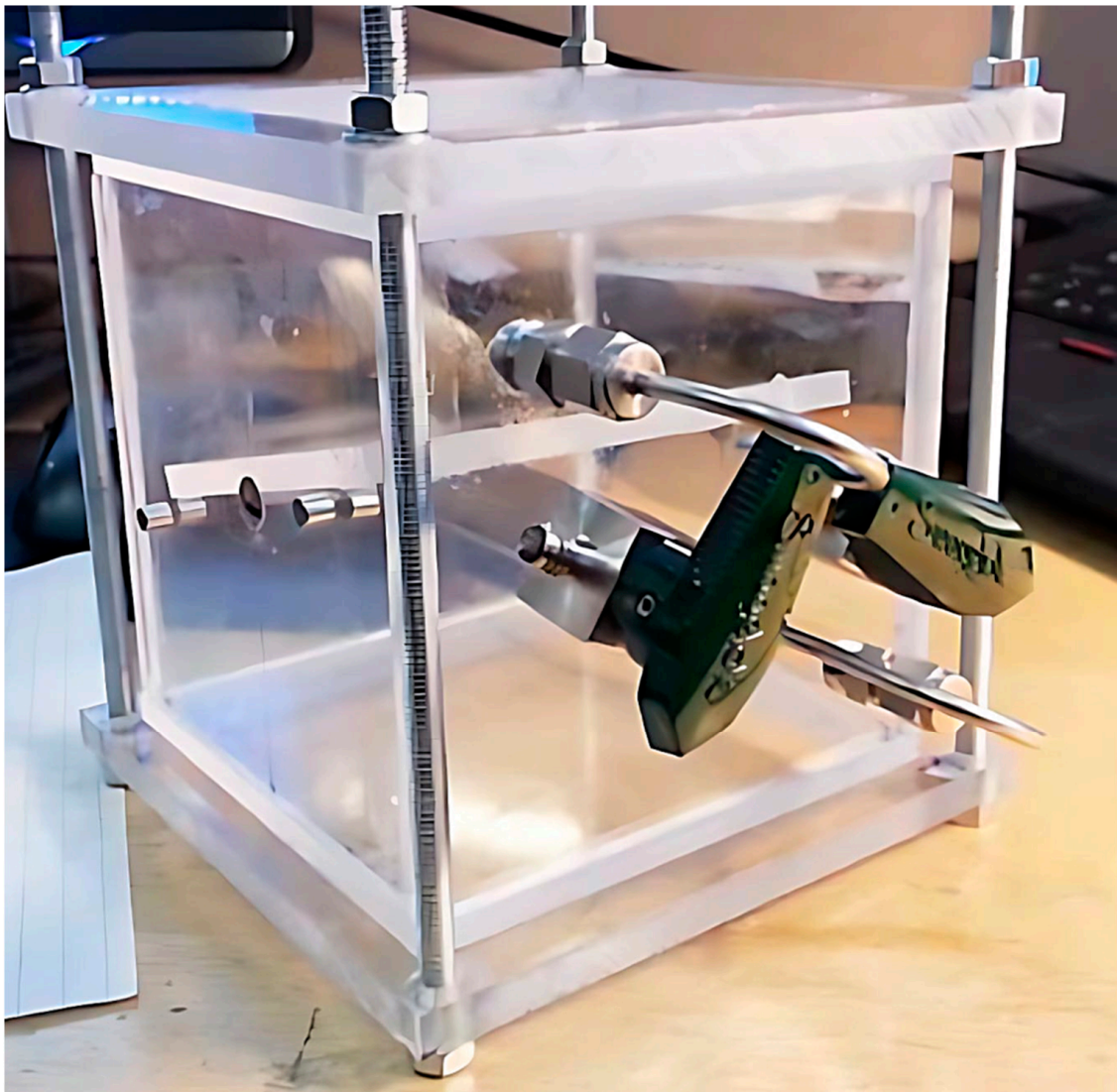

Figure 6. Skylight prototype at the ÅA University, PST laboratory [20].

The circulation provides cooling to a room beneath the skylight. When this circulation is interrupted, the skylight functions as a thermal insulator. The spaces between these three windows are filled with GHGs, such as pure CO_2, HFC-125, or NH_3, other than air. Therefore, the following are sections that provide detailed information about selecting the proper gas and window materials.

3.2. Selecting Participating Gas for Passive Skylight

When selecting a suitable participating gas, it is critical to take the following measures:

- The radiative pathway in the gas must be long enough for it to be capable of radiating enough heat.
- The gas must have high absorptance in the spectral range of the atmospheric window and highly transparent at visible wavelengths.
- In order to achieve adequate convective cooling, the gas thickness must be both large enough to permit and small enough to inhibit convective heat transfer.
- The viscosity of the gas should be as low as practical in order to reduce fluid convective flow limitations
- It is important that the gas has a heat conductivity that is low enough and to give conductive heat transfer << convective heat transfer. Moreover, the gas needs to have a high thermal capacity to minimize mass needed.
- It is critical that a gas's boiling point (BP) is significantly lower than the lowest temperature inside the skylight [20].

Health and safety standards: Consider any leaks near the skylight window in terms of health and safety laws. It is necessary to carefully select gases for skylight windows. The gas cannot be toxic or combustible. Therefore, according to the standards set forth by the International Institute of refrigeration (IIR), gases classified as A2L are appropriate for this application [59].

Effect of the gas on the environment: The potential threats of ozone depletion and global warming from the gas need to be taken into account. Gases that damage the ozone layer are outlawed with strict enforcement, especially in Europe. Consequently, the gases required for a skylight should have a higher global warming potential (GWP) while preferably being sensitive to conversion into harmless species if eventually released into the environment and have no effect on the ozone layer. At ÅA, CO_2 and HFC-125 were considered; it was possible to compare the two gases (see Figure 7) by filling the skylights with CO_2 and HFC-125. The results from the experiments revealed that HFC-125 may achieve temperatures lower than the surrounding air and has a noticeably larger cooling effect compared to CO_2 [60].
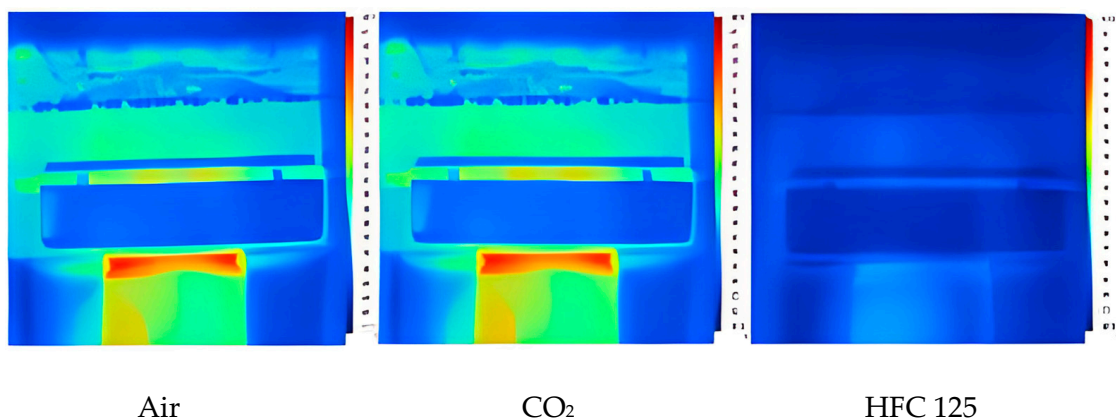

| Air | CO$_2$ | HFC 125 |

Figure 7. Thermal infrared images of skylights after testing with air, CO_2 and HFC-125 [20].

For CO_2 gas to reach temperatures below the ambient, an elevated pressure may be recommended which, however, would require thick glass with consequently lowered transmissivity. In response to this, this led to the choice of HFC-125 refrigerant for skylight construction. Other mixed refrigerants such as NH_3 (strong pungent smell), HFC-32, HFC-134A, HFC-143A, and SF_6 were also studied or considered, but their flammability and other safety reasons preclude their usage. Due to the recent phase-out of HFC-125 [61], R-32, R-410a, R454b, and R449A are likely to be considered for the further scale-up of the skylight window prototype at the ÅA-PST laboratory.

3.3. Selection of Suitable Window Material

The basic and primary function of window materials is to keep the outside weather from affecting the interior climate. A skylight should last for decades, and window material should be mechanically sturdy enough to withstand exterior weather conditions (e.g., it should be resistant to severe winds and snow, and it should not be soluble in rainwater). In addition, direct sunlight must not damage the material. Zinc selenium (ZnSe), despite its viability, was not chosen as a window material for ÅA skylight due to its high cost. Actually, before we found the Cleartran, thin, low-density polyethylene sheets (LDPE) were used as window materials [20]. Later, ZnS was a preferred material since it is transparent to both long-wave and visible light heat radiation. It also possesses a transparency of about 80% [62] in the atmospheric window region. Thus, this material can be used as a several-mm-thick glass sheet that is similar to normal window glass.

3.4. Working Principle and Design Changes for Improving Passive Skylight

With a prototype skylight that contains a GHG-filled inter glazing space, it was shown to be possible to control the radiative heat flux from a building to the sky and ambient surroundings. The third center window and the gas regulate the balance between insulation and cooling while its angle can be used to regulate the (natural) convection for minimal turbulence.

The central window, as previously mentioned, divides the skylight into an upper and a lower portion. The gas functions as the working fluid in a heat exchanger that "connects" the room with the sky. An appropriate participating gas must have a higher thermal emittance value in the atmospheric window's wavelength (8–13 μm) range. The developed skylight can be adjusted to work in either a cooling mode or an insulating mode (see Figure 8) [20].
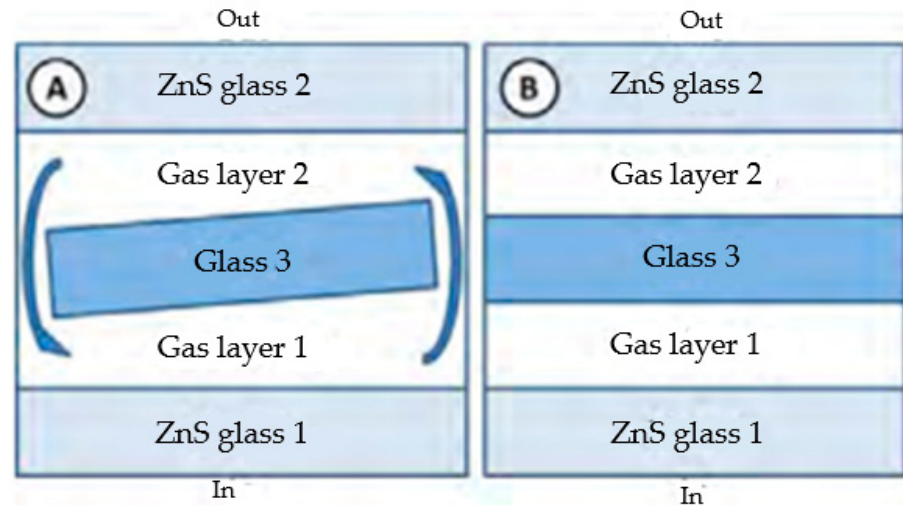

Figure 8. Different skylight configurations Ⓐ cooling mode Ⓑ insulating mode [20].

When the skylight is in its cooling mode, heat from the below room is transferred to the gas via the lower window (ZnS glass 1) via radiation, conduction and natural convection. Due to the decrease in gas density, the heated gas travels to the upper compartment. The radiative heat transfer through this makes it travel to the lower compartment from the upper window (ZnS glass 2) and the atmospheric window to the cooler air masses in the upper atmosphere, which cools the gas in the upper compartment. Additionally, above the skylight, forced convective heat transfer typically occurs between the upper portion of the skylight and its direct surroundings because of wind. The impact of this heat transfer depends on the ambient temperature. When cooling is not required, the connection between the two gas areas (gas layer 1 and gas layer 2) is closed, causing the roof's components to act as thermal insulators rather than passive radiative coolers.

Figure 9a illustrates a side view of the ÅA proof-of-concept passive cooling skylight presented recently. Its performance is comparable to that of a roof paint or other covering material that, in addition to reflecting thermal radiation, has a high emissivity in the wavelength range for the atmospheric window, as illustrated in Figure 9b [63].
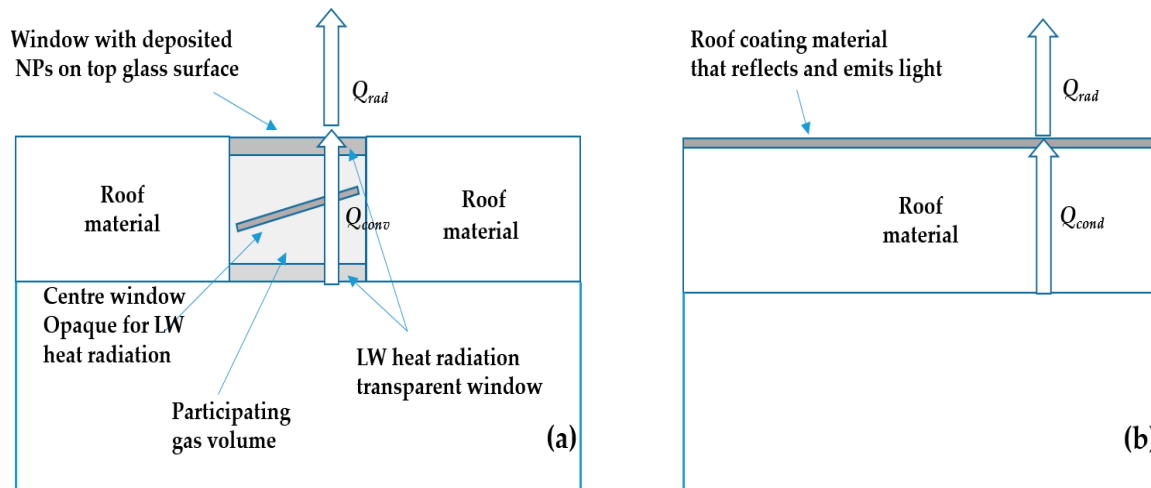

Figure 9. (**a**) A skylight design with reflective NPs on a ZnS substrate and (**b**) compared with a rooftop reflecting and emitting coating material [63].

The skylight provides more heat transfer (per square meter) from the building envelope to the outside top surface, which is governed by convective circulation heat transfer inside the skylight. This is stronger than conductive heat transfer via the material of the building roof ($Q_{conv} \gg Q_{cond}$), and eventually the limiting heat flow will determine the heat radiation to the sky (Q_{rad}). Therefore, the building's top surface must have direct visual contact with the sky (and beyond that, this enables the skylight to illuminate the room). The center window will no longer be necessary for future ÅA skylight designs (ongoing work).

As said earlier, ZnS is widely used in long-wave infrared systems as an infrared transmitting window material. Skylight passive cooling applications benefit from Cleartran's material's excellent thermal, mechanical, and optical properties over a wide range of wavelengths. Because of its non-hygroscopic nature, high refractive index, thermal conductivity, and thermal expansion, this substance was exceptional and frequently used in engineering design applications [64]. However, difficulties with ZnS identified are as follows: (1) it requires an external sunshade to minimize the solar radiation absorbed by the radiative cooler because of its noticeably high solar absorptivity of ≈ 0.13. (2) When exposed to direct solar irradiation, ZnS heats the radiative coolers. Thus, ZnS is not ideally effective for establishing DPRC as intended, particularly during the day (around noon), and therefore tough challenge persists. Further investigation into finding suitable materials is necessary in order to create surface coatings such as single-layer/multi-layer radiative cooling coatings or additives on ZnS glass.

The development of sustainable PRC technology demands a significant amount of research work, and efficient methodologies must be refined, possibly through experiments, mathematical modeling, and validation of the obtained experimental data by building the models using numerical simulation software (Ansys Fluent/Comsol Multiphysics). Another motivating factor is the fact that PRC applications have developed significantly and ingeniously in recent years. As a result, ÅA PST is currently developing a PRC skylight that should be capable of dissipating a few 100 W/m^2 of cooling during daytime, which can be used to lower the energy required to meet a building's heating and cooling needs. It is possible to classify PRC methodologies into two Groups:

Group 1: fundamental principles such as the emissivity properties of radiative cooling surfaces and the wavelength dependence of radiative cooling surfaces. The main goal here is to find a suitable PRC method—even though many studies focus on cooling technologies, there is a scarcity of research offering PRC approaches that lower energy usage. As a result, the focus of this study is on enhancing the impacts of PRC strategies to increase building energy performance [2].

Group 2: this is a practical research phase. The second area of research focuses on finding suitable materials with preferred radiative properties, investigating diurnal cooling for energy-saving applications (such as cooling of residential and commercial buildings, and solar cells), and maximizing net cooling power. The idea is to use the most recent developments in material technology to design and fabricate a skylight using various metamaterials, photonic structures, and thin films with precisely designed nanoparticles (TiO_2, SiO_2, Al_2O_3, and $AgNO_3$) dispersed on the surfaces [2].

According to previous research by a few researchers, PRC systems made of various materials are capable of influencing system performance, and it is a notable technique to achieve perfect sub-ambient radiative cooling. Although the research is progressing toward a more comprehensive and coherent theory for developing PRC technologies, the findings remain diverse and even fragmented.

Motivated by such considerations, ÅA PST's current research activity will involve finding the suitable material used as top and bottom window glass surface for reasonable PRC during both daytime and nighttime, and then combining the materials in a design that can turn into a commercial product.

One benefit is that this skylight PRC system could reduce the need for conventional cooling systems, resulting in savings, but is also applicable for the refrigeration of food products and vehicle applications. In addition, it is very likely to expand this PRC skylight to provide engineering designs for passive cooling systems for cars or trucks parked in the sun. ÅA [65] has already reported work on this. That research showed that the passive cooling effect of almost 27 W/m^2 from the vehicular skylight is achievable for the summer season in Finland. Therefore, when a car is equipped with a skylight for passive cooling, its annual energy usage may decrease while it is inside temperature is controlled, also while being parked in the open air under solar irradiation.

4. Radiative Cooling Materials

The concept of radiative cooling has been largely limited to nocturnal radiators thus far. Natural materials typically exhibit poor radiative cooling efficiency and do not have both a significant high emissivity in the atmospheric window and very high reflectivity in the solar spectrum wavelength. That means a lucrative DPRC structure should have a solar reflectivity much higher than 90% (preferably > 97%) together with a large emissivity value (>0.9) in the atmospheric window. The ability to modify a material structure at the nanoscale and enhance electromagnetic radiation emissivity and spectral absorption, however, is now possible due to the most neoteric developments in material science and the rapid upgrading of nanofabrication technologies. There is speculation that a variety of photonic structures, including multilayer planar photonic thin films, metamaterials, 2D and 3D photonic devices, and plasmonic structures, can be adapted to increase either emissivity of the material in the atmospheric window or increase reflectivity in the solar spectrum [66–68].

While solar radiation at high intensity is present during the day, many of the proposed photonic structures have been able to operate at temperatures lower than ambient temperatures. These radiators, designed to reduce costs and complexity in polymer photonics, use electromagnetic resonators that are generally excited inside a polymer surface, resulting in a very high emissivity in the wavelength of 8–13 μm. Conversely, more recently developed PRC systems—like advanced paints—attempt a high potential for radiative cooling at a significantly lower cost. However, problems that need to be resolved include optical aging brought on by dust accumulation, other atmospheric constituents adhering to paints, and unwanted cooling during the heating period [69]. Due to the extensive research focused

primarily on advanced photonic and plasmonic surface technologies, metamaterials led to the development of sub-ambient DPRC. It appears that these developed technologies can indeed increase buildings' daytime cooling capacity.

There are, as said, two kinds of PRC materials to provide cooling for nocturnal and diurnal periods. During the night, achieving sub-ambient temperatures is very straightforward, but under direct sunlight, it is quite challenging due to the material requirements. Thus, this section aims to summarize materials for PRC during the day and at night. Nevertheless, it mainly focuses on highlighting the most significant advantages and disadvantages of DPRC materials and their potential applications in building cooling. Besides that, their scalability as well as various materials' effectiveness are investigated for producing diurnal and nocturnal PRC capabilities. The following section covers more detail on the materials and structural categories [19].

4.1. PRC Materials for Nighttime (Nocturnal) Cooling

In the past few decades, most nocturnal PRC research has focused mainly on a particular surface in the atmospheric window to reach higher sub-ambient temperatures. The following are some types of materials:

4.1.1. Polymer-Based Materials, Including Paints Made from a Polymeric Binder and Various Pigments, Composite Polymer Materials, and Polyvinyl Chloride (PVC), Polymethyl Methacrylate (PMMA), and Modified Polyphenylene Oxide (PPO) Resin

A thin layer of polymer and a reflective metal are typically the components of polymer-based radiative cooling materials (e.g., aluminium). Prior to now, Catalanotti et al. [70] developed a 12.5-µm-thick polyvinyl-fluoride (PVF) film with an aluminum back coating.

The results revealed strong emissivity within the atmospheric window (8–13 µm) and high IR reflectivity for other wavelengths. This PRC was able to cool to almost 15 °C below ambient temperature using a thermally insulated box covered in IR transparent PE film. Certain polymer films, such as PPO and polymethyl pentene (PMP or TPX), also demonstrated their effectiveness at nighttime cooling [2].

Likewise, composites that combine nanoparticles and IR-transmitting polymers have the potential to produce polymer-based materials. Due to the narrow absorption bands that these nanoparticles typically have within the atmospheric window, the composite material can have its absorption spectrum completely within the atmospheric window by adjusting the nanoparticle concentration. Amorphous silicon carbide (SiC) nanoparticles were doped into a 25-µm PE film at a 20% concentration (see Figure 10) in a composite material created by Gentle et al. [71]. Nanoparticles produce a considerably higher absorption in the 8–13 µm range in comparison to a pure PE film (highly transparent) in the atmospheric window. Besides $Si_2N_2O_3$, SiO_2, and carbon-based nanomaterials such as nanodiamonds and multilayer carbon nanotubes, carbon black also served as effective materials [72–74].

4.1.2. Thin-Film Inorganic Coatings of Materials Such as Silicon Monoxide (SiO), Silicon Dioxide (SiO_2), Silicon Oxynitride (SiO_xN_y), Silicon Nitride (SiN) and White Pigmented Paints

Since the Si-N and Si-O bonds are both absorptive at 11.5 µm and 9.5 µm, respectively, silicon-based oxide and nitride thin coatings (SiO, Si_3N_4, and SiO_xN_y) have a relatively high mid-IR emissivity [75,76]. SiO film that is 1 µm thick is optimized to reduce IR reflection through destructive interference while increasing emissivity [77]. A bilayer of SiO_2 and $SiO_{0.25}N_{1.52}$ on aluminum is depicted in Figure 11 as an example of computed spectral reflectance in the 5 to 25 µm wavelength range [78,79].

Ceramic materials with PRC capabilities include lithium fluoride (LiF) and magnesium oxide (MgO), when supported by an IR-reflective layer, silicon-based thin film. A nearly 20 °C sub-ambient cooling temperature was observed on the 1.1-mm-thick MgO film during a dry, clear sky night [80].
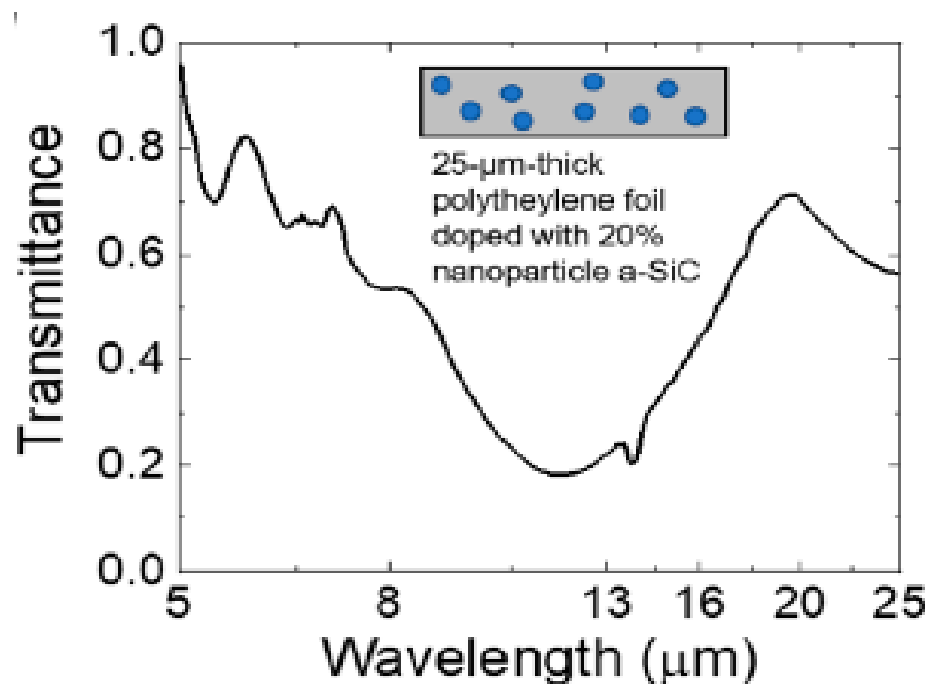
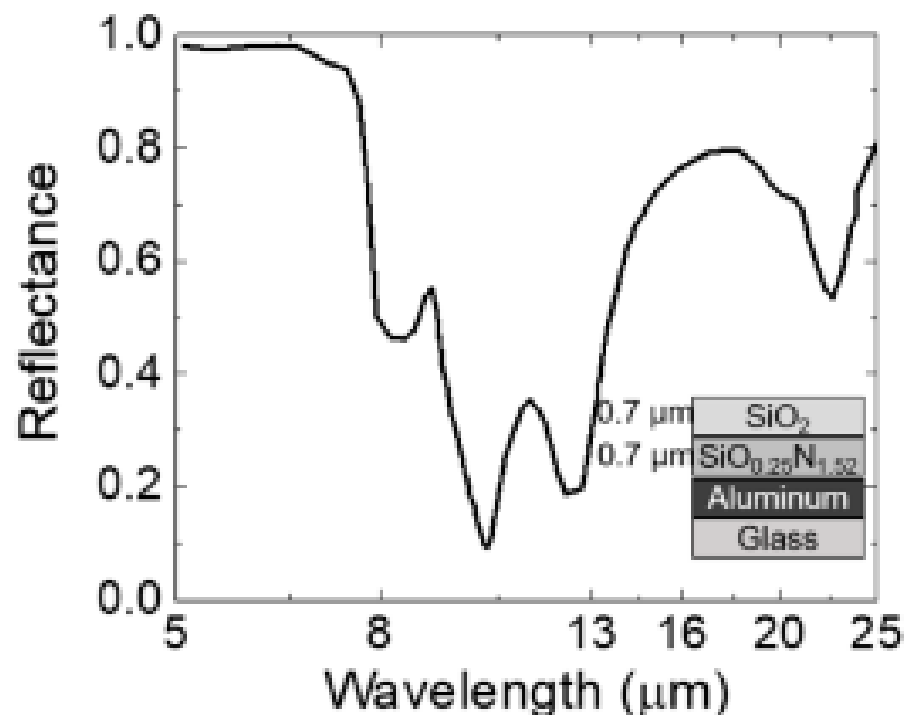**Figure 10.** Polyethylene (PE) thin film with amorphous SiC nanoparticles [71].

Figure 11. Silicon oxide and Nitride film on Aluminium [2].

4.1.3. Ammonia (NH_3), Ethylene (C_2H_4), and Ethylene Oxide (C_2H_4O) Emit IR When Enclosed in an IR Transparent Container, Which Makes IR Emissivity Possible

To produce spectrally selective infrared emissivity, a slab of selectively infrared-emitting gas can be contained within an infrared transparent container. Strong infrared absorption is obtained for certain molecular stretching and rotation modes within the 8–13 μm wavelength. For instance, the C = C bond absorbs the light strongly between 10 μm and 12.5 μm. As C-O and C-N stretching bonds absorb from 8 to 10 μm, and as OH deformation vibration absorbs between 8 and 10 μm, these bonds emit IR absorption [81,82].

Granqvist et al. looked into the viability of using various confined gases, such as NH_3, C_2H_4, and C_2H_4O, or mixtures of them, as PRC materials [82,83]. Figure 12, which shows the optical transmission spectrum for C_2H_4 with a good level of a thickness (up to a few cm), suggests that these molecules could be suitable PRC candidates.
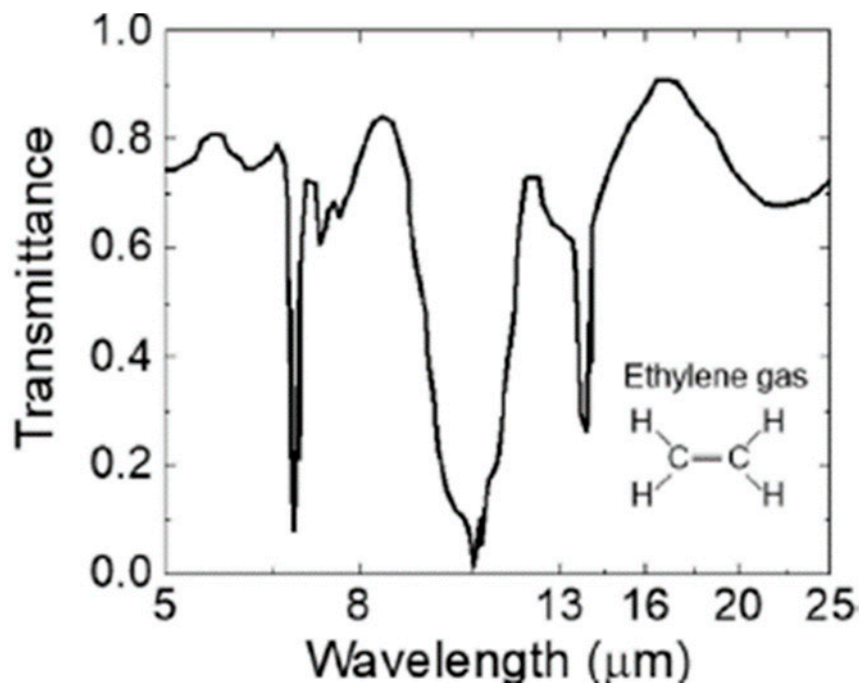

Figure 12. The slab of selectively infrared emitting ethylene gases [83].

When the solar light is shaded during the day, experimental results showed that 12–18 °C sub-ambient cooling is possible. The key benefit of using such a gas slab on a solid PRC surface is that no additional heat transfer fluid is required to build an efficient cooling device [84]. The aforementioned materials demonstrate that selective emitters have been developed and successfully tested for nighttime radiative cooling at both ambient and below-ambient temperatures. However, the inherently low cooling power density of radiative coolers makes them inefficient for nocturnal applications.

4.2. Nocturnal Cooling Structures for Energy-Efficient Buildings

Due to its outstanding PRC capabilities, this DPRC technology hopes to have a significant influence in a variety of fields, including those pertaining to energy-efficient buildings, also known as smart buildings. It has been extensively studied and used in practice to use nocturnal PRC systems. The building incorporated PRC systems fall into two categories based on how the cooling process operates, as shown below [8].

4.2.1. Air-Based Cooling (ABC) Systems

The ABC system, which uses air as the heat exchange medium, is a straightforward way to integrate PRC with a building cooling system. It is mainly composed of a connection loop, a driving fan, and a radiative cooling surface. Prior to entering a building, either the air is cooled naturally or using a fan-driven sky radiant cooler attached to the roof [9,85]. In these systems, it is actually necessary to have a small air passage beneath the radiator and a large surface area in order to cool the exchange the air effectively.

Illustrated by Figure 13, Lu et al. [9] compared three different ABC systems with various system configurations. While Figure 13b,c incorporate an air conditioning system for auxiliary cooling, Figure 13a is a relatively straightforward system that directly cools the roof by using it as a radiator.
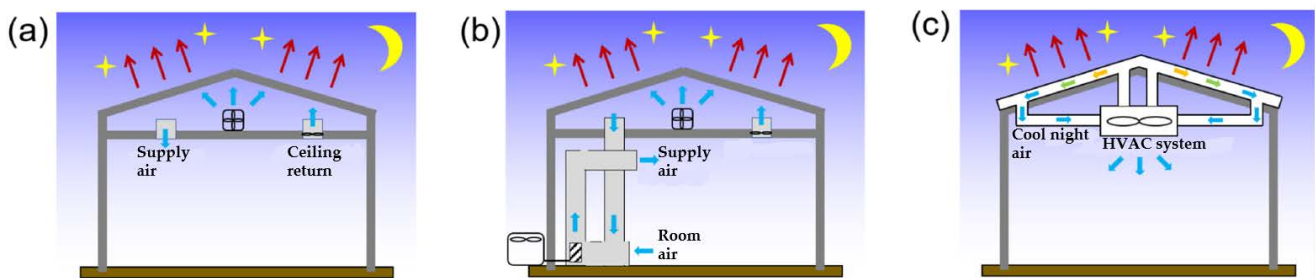
Figure 13. Different air-based system configurations [2].

Kimball et al. [86] developed a PRC-based air box convector. The component comprises two heat exchangers connected in series with a fan for cooling and dehumidification in tropical climates. Their experimental findings showed that this innovative system, when used in conjunction with PRC, could reduce the energy used to maintain an ideal indoor environment by 14–18%. Likewise, The National Solar Test Facility (NSTF) of Canada tested various transpired solar collectors to evaluate the volume of air that could be cooled at night and the temperature difference from ambient as measured. The experiments demonstrated that nocturnal PRC reduces ambient air temperatures by up to 4.7 °C [87]. The patented ABC system invented by the company Conserval Engineering comprises perforated metal panels that operate at night through radiant cooling and in the daytime through above-the-sheathing ventilation [9]. In a theoretical study, Zevenhoven et al. presented the idea of regulating passive skylights for cooling purposes via radiative cooling, and the performance was tested using weather data from Helsinki [88].

Overall, ABC is a concise design that offers instant cooling. Additionally, if it combines well with PRC material and has the advantage of reduced installation and maintenance costs. However, due to the air's poor heat transfer efficiency and low specific heat capacity, it is challenging to meet the building's cooling needs when using natural air circulation. There might be a slight cooling enhancement by including a driven fan, but only by 20–30 W/m² [89]. When it comes to cooling large buildings, a simple combination with an air-based ventilation system can be difficult. Due to the substantial occupied space, as well as the introduction of ducts and other hardware, the integration of the ABC systems in buildings is also inferior. Its usage is currently restricted to the upper floors of multi-story or residential buildings.

4.2.2. Water-Based Cooling (WBC) Systems

Some studies recommended using PRC in conjunction with WBC systems because ABC systems, as discussed in 4.1.1, are insufficient to meet most buildings' needs. A WBC system can provide around 40 W/m² of cooling. Again, depending on how they operate, these cooling systems can be defined as either closed-loop or open-loop systems. An open-loop system such as a rooftop pool transfers heat between the interior and exterior via thermal radiation and phase change evaporation. However, in arid areas, open-loop water-based systems can only be used to a certain extent [8,90].

According to Figure 14, a closed-loop cooling system integrates closed pipes in a flat plate radiant system to cool water using water as a heat carrier [91]. Pumps typically move the cooling water back and forth between the storage tanks and pipes. Sodha et al. [92] and Nahar et al. [93] studied the water cooling of an open-air roof pond system with movable thermal insulation through evaporation and nocturnal radiation, experimentally and analytically.
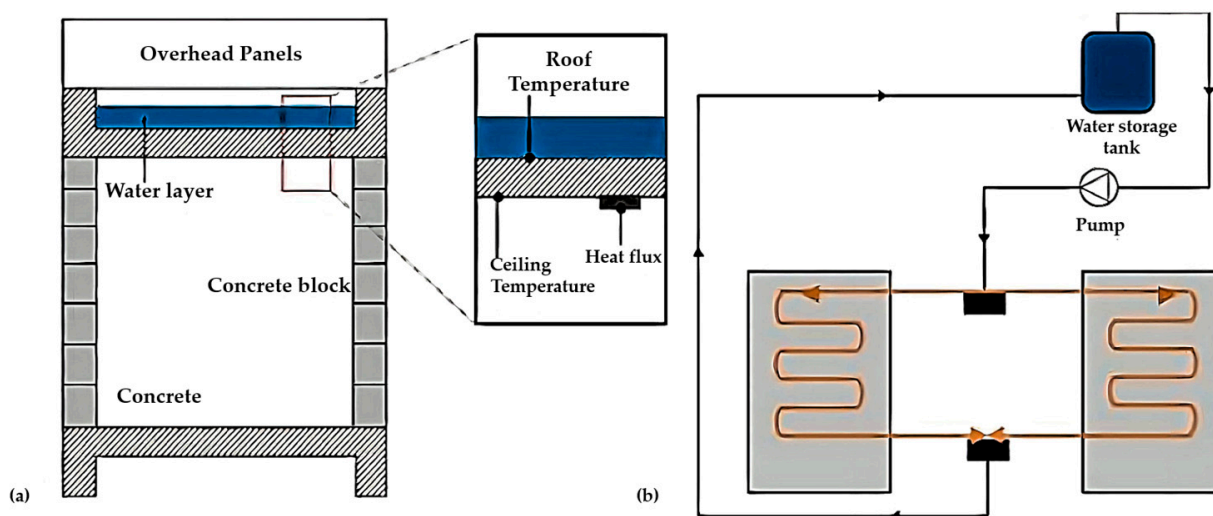
Figure 14. (**a**) Open-loop cooling system [90] and (**b**) Closed-loop cooling system [91].

With the aid of experiments, Chen et al. validated the model set up of a roof pond that was connected directly to a room where water was sprayed over floating-coated insulation [9]. In a roof pond consisting of gunny bags floating on the water's surface, Tang et al. [94,95] presented the theoretical analysis and experimental study of WBC systems by use of night sky thermal radiation and evaporation. To increase the efficiency of the WBC systems, Spanaki et al. [96] introduced 12 different types of rooftop pools, inspected their benefits and drawbacks, and went over the detailed design requirements. Roof ponds may be one of the more effective PRC methods, but there are still a number of significant problems limiting their widespread use.

Meiret et al. [15] used an open-loop radiative system in Oslo that consisted of a 5.3 m^2 radiant and a 280 L tank to confirm that it can provide the cooling requirements of the majority of standard homes, with the exception of the midsummer time when relative humidity is high. Despite the fact that these are affected by outside humidity, open-loop cooling systems are still capable of achieving efficient PRC. However, according to Givoni [88], the wet-bulb temperature (WBT) of the environment must be less than 20 °C for the system to work effectively. This led to a further study of closed-loop WBC systems. In the intervening years, Goldstein et al. [97] proposed a non-evaporative water-cooled panel system with a cooling power of 40–70 W/m^2 and a temperature of the water reduction up to 3–5 °C for particular water flow conditions. The installation of this system in a two-story building can cut summertime electricity usage by 21%. The system suggested by Zhao et al. [98] produces water that is 10.6 °C cold under direct sunlight with the use of glass polymer. This system's nocturnal cooling capacity was found to be 1296 W at a rate of 64% to 82% energy savings. WBC systems use nocturnal radiation to store energy and produce cold water for DPRC. Although achieving a lower outlet temperature and pursuing a greater cooling intensity conflict, a lower outlet temperature results in inadequate cooling of cold water, which limits the application. Two processes of heat transfer are involved in the space's heat dissipation in WBC systems: first, heat is transferred to the water in circulation, and then, via the radiator, heat is released into the atmosphere. Therefore, WBC systems are frequently integrated with other advanced technologies because of these factors.

A summary of the materials, structures, and radiative properties of the radiators designed for nocturnal cooling can be found in Table 1.

Table 1. An overview of the material composition, structures, and characteristics of a radiator designed for nocturnal cooling.

Authors	Structure of Radiative Cooler	$\Delta T_{below\ ambient}$ /P_{net}	Results
Zou et al. [68]	This kind of metamaterial/plasmonic emitter, mounted on a silver back reflector, contains phosphorus-doped n-type silicon cubes coated with silver.	$\Delta T = -10\ °C$	The emittance outside the 8–13 μm is high according to the measurement results, which are nearly ideal according to simulation results.
Miyazaki et al. [99]	A thin layer of Si_2N_2O was applied to an Al substrate.	$\Delta T > -1\ °C$	The structure's ability to keep cool at night was tested for topcoat thicknesses ranging from 6.5 to 35 μm. The findings indicate ineffective cooling.
Hossain et al. [100]	A 7-layer, 2D, alternating germanium (110 nm thick) and aluminum (30 nm thick) metal–dielectric conical nanostructure on an aluminum substrate.	$\Delta T = -12.2\ °C$ and $-9\ °C$ during night & day, respectively, $P_{net} = 116.6\ W/m^2$	The requirement to assemble a broadband mirror on the structure and use it for DPRC is not practical, even though the reflectivity profiles provided show high potential for nighttime PRC.
Tazawa et al. [101]	Bilayers of tungsten-doped vanadium dioxide ($V_{1-x}W_xO_2$) and silicon oxide on an aluminum substrate.	Not Available	The findings showed that the developed material could reach a stable surface temperature that is based on the $V_{1-x}W_xO_2$ film's transition temperature.
Diatezua et al. [79]	Multilayer SiO_2 and SiO_xN_y structures are applied to an aluminum substrate.	Temperature drops are 52, 48, and 56 °C (from T_{amb} of 27 °C),	Corresponding calculated maximum cooling heat flux ranges are 125, 118, and 119 W/m^2, respectively.
Kimball et al. [102]	Black paint and TiO_2 white paint	$\Delta T = -6\ °C$ for Black Paint and $\Delta T = -11°C$ for TiO_2 paint	In the IR thermal range, white TiO_2 paint has been reported to have an emissivity that is nearly equal to that of a blackbody.
Eriksson et al. [81]	$SiO_{0.6}N_{0.2}$, a silicon oxynitride thin film (1.3 μm), has been deposited on an aluminum substrate.	$\Delta T = -16\ °C$	Experimental results showed that low temperatures can be achieved with PRC, but they do not represent the full potential because materials are required for effective IR transparent convection shielding.
Eriksson et al. [78]	SiO_2 and $SiO_{0.25}N_{1.52}$ bilayers, each measuring 0.7 μm thick, are applied to an Al substrate.	$\Delta T = -20\ °C$ and $P_{net} \approx 100\ W/m^2$	Depicted with the outcomes for the 1.5-μm-thick $SiO_{0.6}N_{0.2}$ layers that were vapor-deposited. In terms of cooling efficiency, oxynitride clearly outperforms nitride/dioxide bilayers.
Lushiku et al. [82]	Ammonia (NH_3), ethylene (C_2H_4), and ethylene oxide (C_2H_4O) gas slabs with a reflective Al plate backing are available in thicknesses ranging from 0.1 to 50 cm.	$\Delta T = -10\ °C$ in full daylight	Due to the atmosphere's 82% relative humidity, the net cooling capacity is not as effective. Better climatic conditions will lead to better results.
Granqvist et al. [103]	SiO vapor-deposited in a thin (1-μm) layer on an aluminum substrate.	$\Delta T = -14\ °C$ $P_{net} \approx 61\ W/m^2$	The maximum practicable temperature difference is constrained by the non-radiative exchange.

Authors	Structure of Radiative Cooler	$\Delta T_{below\ ambient}$ /P_{net}	Results
Catalanotti et al. [70]	TEDLAR (polyvinyl fluoride plastic) thin film (12.5 μm) coated on an Al substrate produced through vapor deposition.	$\Delta T = -12\ °C$ $P_{net} \approx 100\ W/m^2$	Conducted daytime tests reporting a 15 °C drop in temperature when compared to the substrate that was not covered.
Hu et al. [104]	A combined solar heating and radiative cooling system (SH-RC) based on the composite surface was installed alongside a conventional flat plate solar heating system.	$P_{net} \approx 50.3\ W/m^2$ (clear sky) and $P_{net} \approx 23.4\ W/m^2$ (cloudy sky)	In this case, better performance could be expected if the collector was fitted at a tilt angle of <32°. The traditional flat plate collector for solar heating, on the other hand, had a very poor radiative cooling performance.
Etzion et al. [105]	The material used: Polycarbonate.	$P_{net} \approx 90\ W/m^2$ $\Delta T = -10\ °C$ to $-14\ °C$	Nighttime LWIR in hot and dry climates using Rooftop ponds.
Berdahl et al. [106]	Selective emitters made of 12 μm aluminized PV films are unable to outperform white paint based on TiO_2.	$\Delta T = -5\ °C$	To improve cooling performance, better selective coolers should be developed.
R T Dobson [107]	Radiator panels, a single water tank, indoor air-water heat exchangers with natural convection or convectors, and other components.	$P_{net} = 60.8\ W/m^2$	The use of a special PE cover film to reduce the convective heat transfer coefficient can improve the cooling efficiency of radiator panels.
Dimoudi et al. [108]	Water-based radiator.	Average $P_{net} = 55.9\ W/m^2$ and $t_{water\ drop} = 6.5°C$	If the temperature of the radiator is kept higher than the dry bulb temperature, the cooling capacity can be increased due to the lower convection losses.
Gentle et al. [109]	The performance of a WBC system using a high emittance-radiating surface is evaluated under various atmospheric conditions.	$P_{net} = 55\ W/m^2$ at T_{amb}.	The use of HDPE mesh covers over a radiative cooling system reduces convective heating, which confines the cooling efficiency.
Okoronkwo et al. [110].	Water-based radiator for space cooling.	$P_{net} = 66.1\ W/m^2$ $\Delta T = -1.4\ °C$	The maximum T_{amb} was about 34 °C, the room temperature was kept between 26 and 28 °C.
Gonzalez et al. [111]	The solar passive cooling system (SPCS) under hot and humid climates.	$P_{net} = 19.4\ W/m^2$ (August) and 24 W/m^2 (January).	The roof of one cell is very well insulated, while the roof of the other cell has an SPCS made of a thermal mass (water) that is cooled by evaporation and LWIR night radiation.
Zevenhoven et al. [112]	The passively cooling skylight containing the gas Pentafluoroethane (HFC-125) between two zinc sulfide (ZnS) windows.	$P_{net} \approx 100\ W/m^2$	The skylights made of ZnS windows, CO_2, and HFC-125 were examined. Further demonstrated that the chosen materials were appropriate for nocturnal cooling.
Dartnall et al. [113]	The panel is made of an Al sheet with a surface coating laminated with insulation made of ethylene vinyl acetate foam.	$P_{net} = 105\ W/m^2$ $\Delta T = -13\ °C$	It is possible to use the phenomenon on cold surfaces and/or liquids, which can then be used in air conditioning applications.

Table 1. *Cont.*

Authors	Structure of Radiative Cooler	$\Delta T_{below\ ambient}$ /P_{net}	Results
Gentle et al. [114]	Two different kinds of multilayers: (a) a highly reflective nanolayer and (b) a layer with a significantly higher index than the other. Surface phonon resonance in the desired absorption band is provided by type (a) materials in the form of nanoparticles.	P_{net} = 135 W/m^2 ΔT = 10 °C below ambient	Two different kinds of multilayers: (a) a highly reflective nanolayer and (b) a layer with a significantly higher index than the other. Surface phonon resonance in the desired absorption band is provided by type (a) materials in the form of nanoparticles.
Zhou et al. [115]	Planar polydimethylsiloxane (PDMS)/metal thermal emitter thin film structure fabricated using a rapid solution coating process.	P_{net} = 120 W/m^2 ΔT = 9.5 °C to 11 °C	The estimated cooling power calculated under maximum sun irradiance is 76.3 W/m^2. Suitable spectral materials are indeed required to improve cooling performance.
Cunha et al. [116]	Multilayer design for passive selective radiative cooling made of $Al/SiO_2/SiN_x/SiO_2/TiO_2/SiO_2$ that were produced using a DC magnetron sputtering process.	P_{net} = 43 W/m^2 ΔT = 7.4 °C	The coating's low solar radiation reflectance of 88%, which is insufficient to achieve significant radiative cooling, results in low cooling efficiency.

4.3. PRC Materials for Daytime (Diurnal) Cooling

DPRC is more fascinating than nocturnal cooling, however, it also poses quite a challenge due to the need to design, fabricate, and optimize structures that can reflect sunlight as well as maximum emission within the entire atmospheric window wavelength. Several advanced materials, including metal oxides, nano-photonic structures, bio-mimetic (manmade) materials, polymer-based porous films, metamaterial, paints, and coatings are described that are efficient at meeting sub-ambient daytime cooling under direct sunlight. It is, therefore, the purpose of this section to discuss recent developments in radiative cooling materials, particularly DPRC materials.

Owing to its high reflectivity within the visible wavelength range, a number of metal carbonates and oxides, such as those of aluminum, zinc, titanium, and silver, are found to be suitable for this application [117]. Besides that, a few other researchers tried to study PRC during the day and used various shields to avoid solar irradiation. In many applications, especially those involving large surfaces, it is impractical to shade the radiative cooling surface from the sun. A nanostructured metamaterial, for instance, has the ability to both reflect solar irradiance and emit strong thermal radiation throughout the entire atmospheric window wavelength. Ideal absorbers, reflectors, and spectral filters can now be developed using metamaterials. These artificial structures are capable of realizing a wide range of optical properties that do not exist in nature. In addition, with the competence to collectively activate the electromagnetic resonators within random metamaterial structures to procure ideal emissivity, random optical metamaterials can significantly reduce the temperature during the day by radiative cooling [2,117].

To cope with sometimes extremely high temperatures, certain insects (Saharan silver ant shown in Figure 15a) have thick hairs that are highly reflective at solar wavelengths (0.4–1.7 µm) and emitting at IR wavelengths of 2.5–16 µm (see Figure 15b). The wings of Bistonina butterflies (see Figure 15c) also have special nanostructured patches that emit strongly in the mid IR range to dissipate heat and have high reflectivity across the solar spectrum to keep the wings cool. They rely on the PRC mechanism to survive in hot weather. Another example of daytime PRC is the silk moth cocoon (see Figure 15d), consisting of disordered threads that protect pupae from overheating when exposed to direct sunlight. This shows that nanophotonic structures can have both exceptional optical

qualities and different thermal radiation properties for the progress of daytime radiative cooling [117].
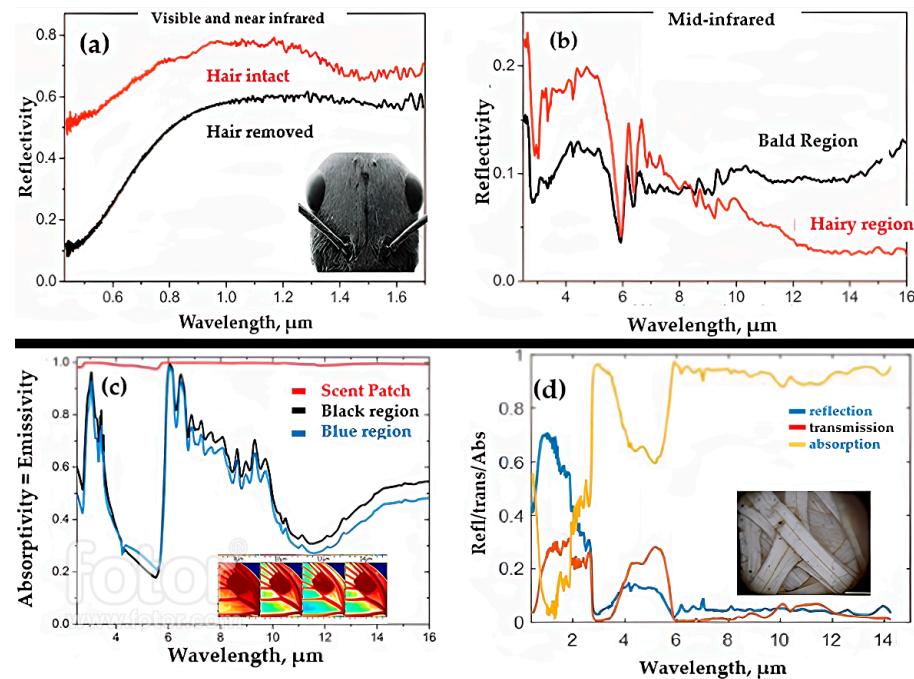

Figure 15. Daytime radiative cooling in nanostructured animals, the body surface of the Saharan silver ant investigated for reflectivity spectra in the (**a**) visible, near infrared (0.4–1.7 µm), and (**b**) mid-infrared (2.5–16 µm) regions, with and without hair, respectively. (**c**) Infrared absorptivity (=emissivity) spectra of various regions of the Bistonina intact forewing. (**d**) Reflection, transmission, and absorption spectra of a cocoon shell from 400 nm to 14 µm, demonstrating high solar reflectance and thermal emittance [118–120].

The thermal radiation properties of nanophotonic structures with structural/optical properties on the wavelength or sub-wavelength scale may be different. Based on this insight, Rephaeli et al. presented a metal–dielectric nanophotonic structure in 2013 and postulated the potential for radiative cooling during daytime. The proposed photonic structure consists of a two-dimensional (2D) periodic column array with quartz and silicon carbide (SiC) as the top two layers over a silver (Ag) substrate coated with high and low refractive index dielectric materials (see Figure 16a).
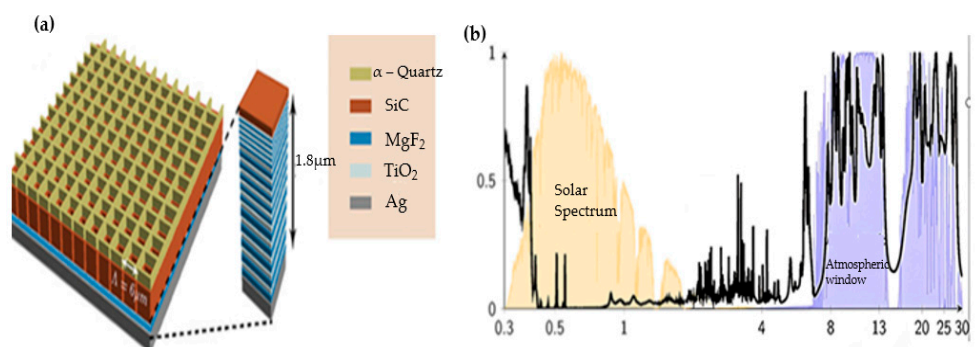

Figure 16. (**a**) DPRC design that consists of two thermally emitting photonic crystal layers (**b**) DPRC emissivity $\varepsilon(\lambda,0)$ is shown in normal incidence (black), with the scaled AM1.5 solar spectrum (yellow) and atmospheric window transmittance (blue) [45].

Due to the phonon–polariton resonance of quartz and the SiC layer, the proposed photonic structure increases the thermal emissivity over the entire wavelength of the atmospheric window, allowing a net cooling power of more than 100 W/m^2 at ambient temperature in the sun [45].

Furthermore, Raman et al. performed an experimental demonstration of sub-ambient daytime radiative cooling in 2014 using a built-in photonic thermal radiative cooler, (see Figure 17). The photonic structure is capable of reflecting 97% of incident sunlight; it consists of seven alternate layers of silicon dioxide (SiO$_2$) and hafnium dioxide (HfO$_2$) stacked at an ideal thickness on top of a silicon wafer coated with silver (Ag) at a thickness of 200 nm. It was found that exposure to direct sunlight exceeding 850 W/m^2 contributed to a 4.9 °C decrease in temperature and gave a net cooling power of 40.1 ± 14.1 W/m^2.
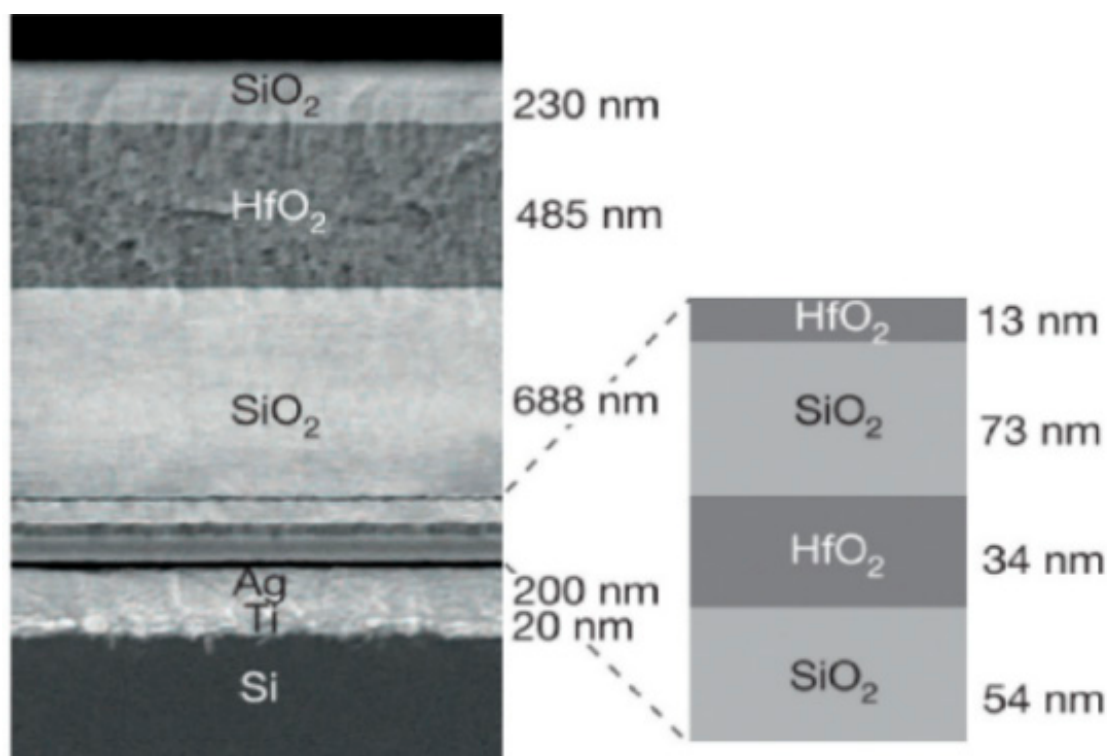

Figure 17. DPRC multilayer structure of SiO$_2$ and HfO$_2$ on the Ag-coated substrate [37].

This work has resulted in a breakthrough in DPRC. HfO$_2$ absorbed little UV light, whereas SiO$_2$ was optically transparent. The top three layers are thicker (designed for thermal radiation), while the bottom four layers are thinner (used for solar spectrum reflection). The figures in [37] show the emissivity and absorptivity of the proposed diurnal radiative cooler in the infrared and mid-infrared ranges.

Intriguing structures, as just described, led some other researchers to investigate nanophotonic structures, such as metal–dielectric multilayer conical pillar arrays, metal-loaded dielectric resonator metasurfaces, multilayer pyramidal nanostructures, metal di-electric metal resonators, and embedded nanoparticle double-layer coatings, which displayed high reflectivity in the solar spectrum and large emissivity in the entire region of the atmospheric window [2].

Min Gu et al. [100] designed and developed a thermal emitter (see Figure 18a) with conical metamaterial pillars comprising alternating layers of aluminum (Al) and germanium (Ge) with a thickness of around 30 nm and 110 nm, correspondingly.
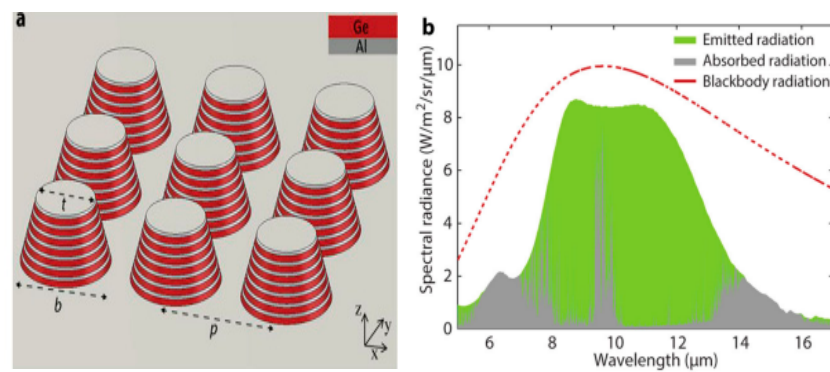
Figure 18. (**a**) Thermal emitter design utilizing multilayer conical metamaterial pillar (CMM) arrays (**b**) Calculated spectral radiance of the CMM structure at 300 K ambient temperature and the percentage of atmospheric radiance that is absorbed within the structure are shown in the shaded green area (shaded gray) [100].

The optical properties of the structures were tested, and the results demonstrated that the designed structures could produce high emissivity in the atmospheric window and low emissivity in other regions. This emitter has the ability to deliver a significantly high cooling power of $\approx$116.6 W/m^2 and to cool to 12 °C below the ambient temperature with the help of a solar reflector that can reduce total solar power absorption by up to 3%.

Takahara et al. [121] have fabricated embedded metal-dielectric-metal (EMDM) structures that have an average absorption coefficient of 0.85 within the atmospheric window, which makes them suitable for use as ultra-wideband absorbers. Their results suggested that these types of periodic 3D EMDM structures are promising candidates for ultra-wideband absorbers and radiative cooling devices.

The unique properties of high order resonance in the magnetic and electric modes of polar dielectric sio$_2$ nanoparticles make them ideal for embedding randomly in TPX polymer to enhance infrared emissions. Zou et al. [68] proposed a dielectric resonator meta-surface (see Figure 19a,b) and demonstrated that this type of meta-surface can achieve strong broadband emissivity over a large angle within the atmospheric window (see Figure 19c,d) and can allow for cooling to 10 °C below the ambient temperature [68].
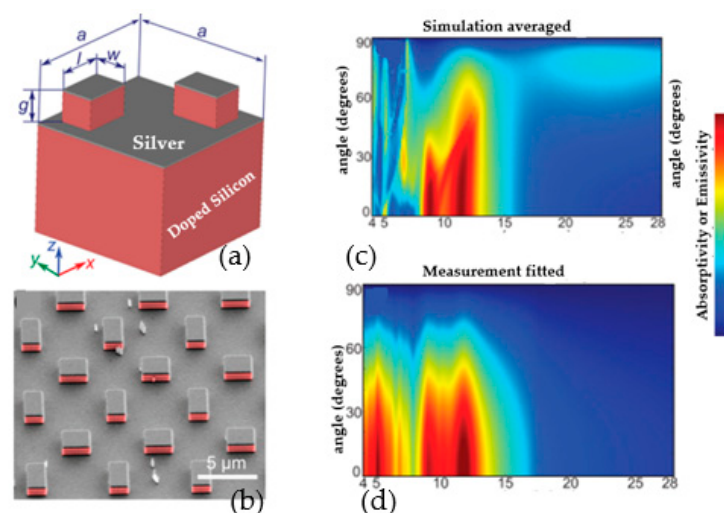

Figure 19. (**a**) DPRC metasurfaces unit cell, with the following measurements: a = 6.9 μm, l = 2.3 μm, w = 1.55 μm, and g = 1.5 μm. Silver-coated layer is 100 nm (**b**) Fabricated sample (SEM image) (**c**) The simulation's result calculated mathematically by averaging the simulated absorptivities (**d**) The angular-dependent absorptivity calculated by fitting the measured results [68].

According to the research by Huang et al. [66], a low-cost two-layer coating with encapsulated nanoparticles can reduce radiant heat both during the day and at night. The acrylic resin that makes up the top and bottom layers of the window's atmospheric transparency contains embedded particles of titanium dioxide and carbon black that, in the wavelength range of 8 to 13 μm, reflect and emit heat, respectively. The black carbon layer is referred to as the black substrate. They investigated various TiO_2 particle sizes for the top layer and found that a radius of 0.2 μm offers the best cooling efficiency. In most directions, the atmospheric transmittance window has an average emissivity > 0.9, reflecting more than 90% of solar irradiation. Furthermore, the results showed that at ambient temperature, a net cooling capacity > 100 W/m^2 obtained during the day and >180 W/m^2 at night.

Dongwu et al. [122] studied a multilayer all-dielectric micro-pyramid structure (see Figure 20a) to gain high mid-IR selectivity in planar photonic devices. The optimized structure achieved an average net cooling capacity of 122 W/m^2, based on broadband selective emissivity in the 8–13 μm wavelength range and very low absorption in the 0.2–3.0 μm range (full solar spectrum).
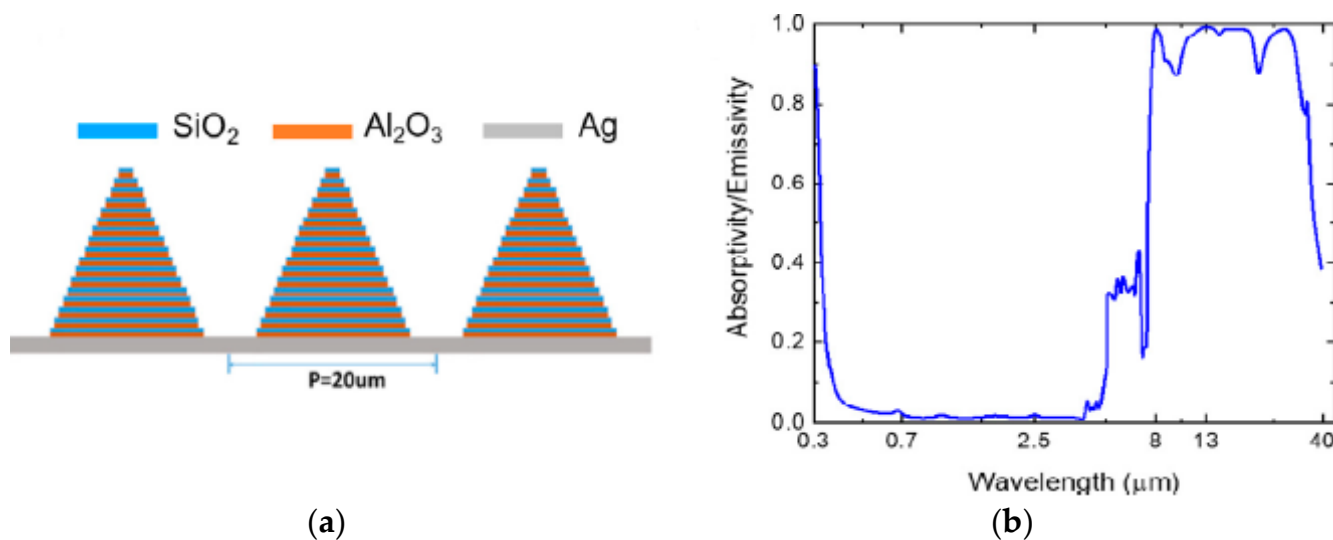
(**a**)   (**b**)

Figure 20. (**a**) Radiative cooling using a micro pyramid structure with multiple layers of all-dielectric material. (**b**) The all-dielectric multilayer micro pyramid structure's absorption/emissivity [122].

Further, considering the cost and scalability of the material, Zhai et al. [38] developed a one-of-a-kind metamaterial—see Figure 21a—using randomized, glass-polymer hybrid metamaterials with SiO2 microspheres randomly distributed in TPX material to exhibit efficient radiative cooling during the day and night. It gives almost zero losses in the solar spectrum with its polymer matrix metamaterial encapsulating SiO2 microspheres (4 μm). This metamaterial emits significant amounts of thermal emission within the atmospheric window and low emissivity in the other infrared ranges due to its strong phonon resonance. The average emissivity of this thin film was greater than 0.93 during the day, with almost 96% of solar irradiance reflected by silver (Ag) as a reflective layer. The average radiative cooling power in a 72-h experiment was >110 W/m^2. Besides that, when exposed to direct sunlight, the hybrid metamaterial thin film of glass and polymer can generate a radiative cooling power of 93 W/m^2 at midday. This device can cool to a temperature of more than 10 °C below the ambient, which is sufficient for commercialization. TPX is also resistant to mechanical and chemical attacks, making it suitable for outdoor applications.
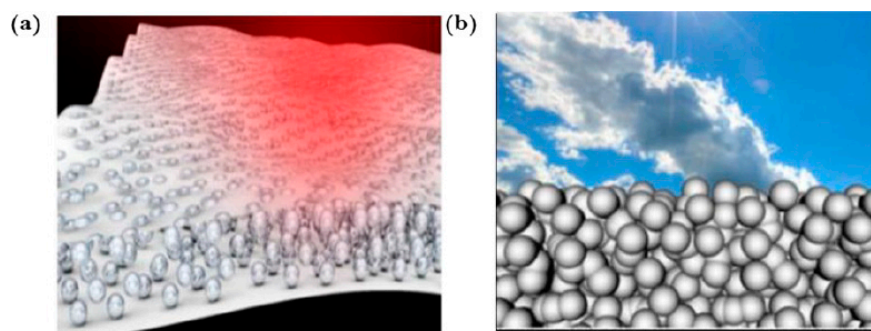
Figure 21. (**a**) Random NP-based designs for radiative cooling using SiO$_2$ microparticles and (**b**) Photonic random media based on SiO$_2$ microspheres [38,69].

For daytime cooling, Atiganyanun et al. [69] developed photonic random media made of SiO2 microspheres that outperform commercially available solar-reflective white paints—see Figure 21b.

Other than thermal radiation, the desirable quality for daytime cooling is to significantly reflect or scatter sunlight to reduce solar heating. The low refractive index of these particles increases emissivity in the atmospheric window wavelength range by reflecting or scattering incident sunlight. Furthermore, under sun irradiation, SiO2 microspheres can drop the temperature of a black substrate below the ambient level by up to 12 °C without the use of costly silver coatings. The coating also reduced the surface temperature by 4.7 °C below that of a commercial solar-reflective white paint during intense solar irradiation.

Gentle et al. [123] demonstrated cooling of 2 °C under direct sunlight without the use of sunshade protection by precisely applying a 200 nm thick layer of silver to a polyester reflector. This roof can be manufactured on a large scale and is referred to as a super cool roof. However, glare was one issue the authors found with this roof. Therefore, additional adjustments are required to reduce the reflection and avoid a glare problem.

A life cycle analysis (LCA) on the use of cool roof paints by Zhang et al. [124] found that annual cooling energy savings of \$33/m^2 are possible. According to another study by Testa and Krarti [125] that examined the benefits of cool roofs, the annual energy costs saved by cool roofs range from \$0.16/m^2 to \$0.36/m^2. The energy-saving benefits are obvious, but there are also the following issues with super cool roofs:

(1)   Cool roofs can make winter heating more effective. This issue is even more serious in regions where the summer season lasts longer than the winter season. The cool roof is less effective at reducing energy usage at high latitudes because there is less solar radiation there. It is crucial to make sure that cool roofs can run all year long, producing good results in the summer and minimal losses in the winter. The cool roof idea is simple to implement at low latitudes where cooling buildings are a crucial factor. A switchable cool roof that can change its reflectance when a building switches from cooling to heating mode is a good solution for high latitudes [124].

(2)   A major disadvantage of super cool roofs is the visual discomfort caused by highly reflective roofs. Research efforts to increase solar reflectance and heat emission, two methods of solving this problem, have not influenced the choice of roof color, which balances aesthetics with lowering roof temperatures [36,126].

(3)   The supercool roof's performance may be affected by dust accumulation over time and material deterioration. Additionally, the inflation of dirt and soot on the roof can reduce solar reflectance by almost 0.15. It is still possible to restore solar reflectance that has degraded due to soiling by washing, but it is usually more difficult to restore degradation brought on by the material itself. The thermal emissivity of the cool roof material, fortunately, does not deteriorate noticeably over time [127,128]. The widespread use of cool roofs can benefit not only buildings but also urban areas by reducing the urban heat island effect. According to Oleson et al. [129], using white

roofs can lower urban daily maximum temperatures by 0.6 °C and daily minimum temperatures by 0.3 °C.

Yang et al. [130] showed that a polytetrafluoroethylene (PTFE) sheet placed on top of a silver (Ag) film creates a double-layered structure that has a 99.1% solar reflectance (see Figure 22a). Here, the PTFE thickness is between 0.24 mm and 1 mm thick. The theoretical analysis sheds light on both the fundamental ideas of the two-layer design as well as the radiation characteristics of sintered PTFE. In addition, PTFE's emittance of 0.9 (see Figure 22b) in the mid-infrared spectrum outside of the solar spectrum is helpful for DPRC.
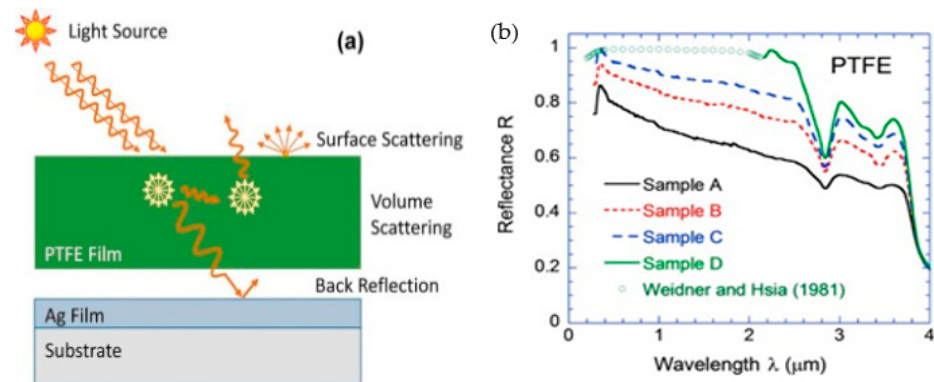

Figure 22. (**a**) PTFE sheet and a back reflector made of the Ag film [130] and (**b**) reflectance of the PTFE sheet for DPRC [130].

Consequently, the two-layer structure enables energy-saving outdoor thermal management and direct sunlight cooling for buildings.

The DPRC mechanism's most affordable and straightforward route is through paints and coatings. Commercial pigments, like white paint, are made of hollow spheres with a low refractive index (RI) of 50–150 μm [131] and titanium dioxide (TiO_2) nanoparticles in the size range of 200–250 nm [132]. In the 8–13 μm, these pigment types have a very high emissivity. There are some restrictions, such as the fact that hollow spheres cannot scatter sunlight as effectively as TiO_2 nanoparticles can because TiO_2 completely absorbs ultraviolet (UV) light.

According to [69], the main determinants of performance in photonic media are silicon dioxide (SiO_2) microspheres with various filling factors and proportions of microspheres (see Figure 23a). The proposed material's highly reflective and emissive qualities were effective in producing diurnal PRC in the sub-ambient. Moreover, their studies noted that elastomer-based materials are necessary for real-world applications that consider resilience and soil resistance.
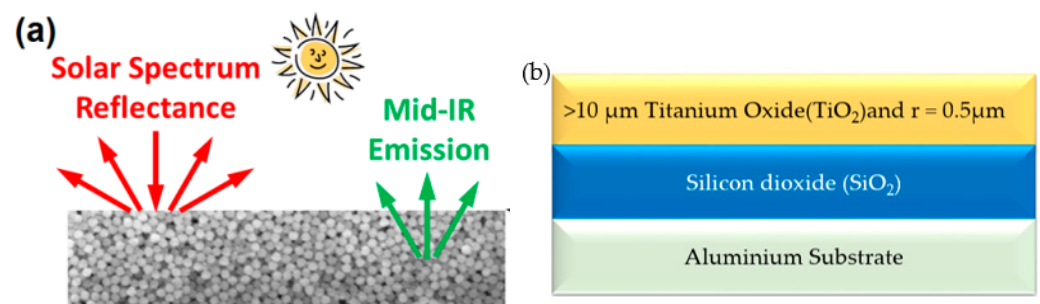

Figure 23. (**a**) Paint-format microsphere-based photonic random media [69] and (**b**) double-layer coating composed of TiO_2 and SiO_2 on a Silver substrate [26].

The method of using a double-layer coating (see Figure 23b) with nanoparticles by Bao et al. [26]. TiO_2, SiO_2, and SiC nanoparticles can be used to make double-layer coatings

with an upper reflective layer and lower-emitting layer that have high solar albedo. These coatings' spectral radiation properties were assessed after being applied to substrates (low and high emissivities). The coating of TiO_2 and SiO_2 on a reflective substrate has excellent selective emission properties for radiative cooling (theoretically) under dry air conditions and assuming convective heat transfer coefficient of h = 4 W/m^{2}K. Despite this, solar absorption remained within the wavelength range of 0.3–0.4 µm. TiO_2 + SiO_2 and TiO_2 + SiC could achieve temperatures of approximately 17 °C below ambient at night and 5 °C below ambient under direct sunlight.

Alden et al. [117] used white silicon-based coatings surrounded by randomly placed microbubbles that, when exposed to direct sunlight, could produce highly effective DPRC. These kinds of surfaces are suitable for rooftop applications where the coating's thickness is less important than its net cooling capacity.

Optimized SiO_2 microspheres for DPRC in the bottom layer and the intrinsic narrow absorption of the plasmonic nanospheres for the color of the thin top layer were used by Meijie et al. [133] to develop a straightforward, affordable, and scalable method to fabricate a colored DPRC coating in two layers. White SiO_2 DPRC coatings can have R_{solar} of 94.2% (see Figure 24a) by adjusting the sphere size. There is a slight reduction in the R_{solar} of colored coatings with Au or Ag layers, to 85.9% and 82.2%, (see Figure 24b) respectively. These coatings have mid-infrared thermal emittances of 0.93 at 300 µm thickness.
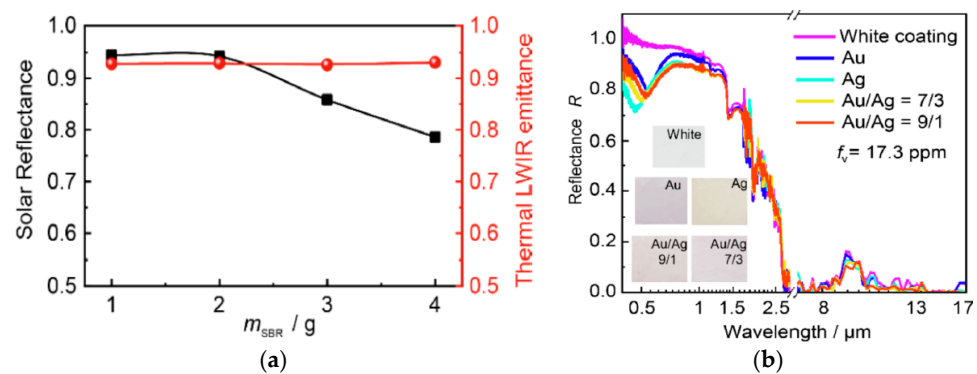

Figure 24. (**a**) Spectral reflectance (R_{solar} = 94.2%) and longwave infrared emissivity (ε_{LWIR} = 0.93) using SiO_2 sphere DPRC coatings and (**b**) Coloured DPRC coatings based on Au-Ag spheres (note: white and colored coatings are 300 µm and 310 µm thick, respectively) [133].

In contrast to the 7.5 °C (with an Au layer) and 5.1 °C (with an Ag layer) temperature reductions that the colored DPRC coatings achieved under direct solar irradiation of 881 W/m^2, the white DPRC coating does so up to 10.9 °C. Compared to a commercial white coating, the DPRC performance of this two-colored Au and Ag coating is better. Its high storage stability is also a result of the SiO_2 coating's optimal radius of 0.4 µm. The coating's high fire resistance, excellent water repellency, and good substrate confirmability also make it possible and practical for use in commercially profitable, sustainable applications.

Within the range of wavelength λ = 0.2–3 µm, R_{Solar} represents the ratio of reflected solar irradiation with respect to total solar irradiation intensity [41]:

$$R_{Solar} = \frac{\int_{0.3}^{2.5} I_{Solar}(\lambda)\rho(\lambda)\,d\lambda}{\int_{0.3}^{2.5} I_{Solar}(\lambda)\,d\lambda} \qquad (W/m^2) \qquad (15)$$

In this equation, $I_{Solar}(\lambda)$ refers to the solar intensity spectrum and $\rho(\lambda)$ represents the coating's spectral reflectance. Similarly, ε_{LWIR} is as follows [41]:

$$\varepsilon_{LWIR} = \frac{\int_{8}^{13} I_{bb}(T,\lambda)\varepsilon(T,\lambda)\,d\lambda}{\int_{8}^{13} I_{bb}(T,\lambda)\,d\lambda} \qquad (-) \qquad (16)$$

where $I_{bb}(T, \lambda)$ refers to the spectral intensity emitted by a blackbody at temperature T(K) and $\varepsilon(T, \lambda)$ denotes the material's spectral emittance.

The possibility of self-adaptive PRC materials at low ambient temperatures (especially at night and during the winter season) when DPRC may not be strongly required is intriguing. By utilizing phase change materials (PCM) with 11 top layers of a self-adaptive photonic structure made of Ge/MgF$_2$, Ono et al. [134] contributed a novel concept of self-adaptive PRC. Figure 25a,b below shows the precise arrangement of the three bottom layers (VO$_2$/MgF$_2$/W). The absorption/emissivity of VO$_2$ changes as it transitions from an insulating to a metallic state, but there is a significant change in the mid-infrared (atmospheric window) wavelength range (8–13 μm), as shown in [134].
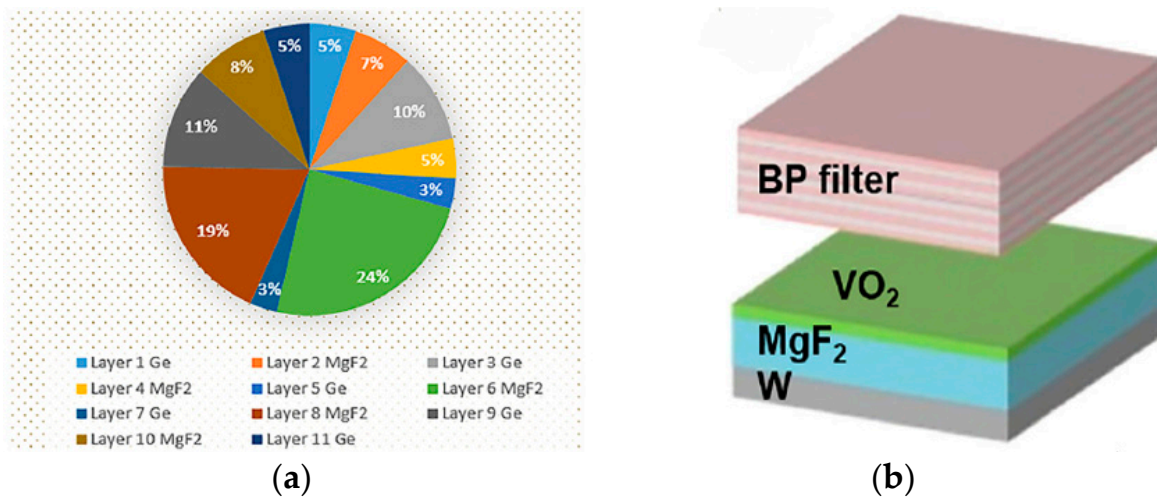

Figure 25. (**a**) Material thickness for the proposed DPRC material and (**b**) self-adaptive diurnal radiative cooling structure [134].

Future daytime radiative cooling metamaterials based on polymers are likely to be used extensively as they provide significant cost and manufacturing efficiency advantages over other non-polymer nanophotonic materials [19]. However, there is still reliability as a pressing issue. It might not be difficult to keep the atmospheric window's infrared emissivity high. The degradation of the polymer and the metallic solar reflectance layer, such as the silver layers shown in Figures 22a and 23b, makes it much more difficult to maintain a high solar reflectance. The functionality of long-term solar reflectance is jeopardized by oxidation of the metal coating caused by oxygen and moisture entering from the front and back surfaces. There are several approaches to dealing with this. One alternative is to use a barrier polymer, such as polyvinylidene chloride (PVDC) or polychlorotrifluoroethylene (PCTFE), to prevent oxygen and moisture from perforating, while another is to increase the thickness of the emissive polymer layer and/or the metal layer [2].

Conversely, a thin layer of barrier material can be applied to the polymer and metal layers. It is worth noting that a study by Mandal et al. [135] showed that high solar reflectivity can be obtained without backing the polymer layer with a reflective metal layer, for instance, by generating micro- and nanoscale pores in polymers that strongly scatter and reflect light in all directions using the phase inversion technique. In contrast to metal-supported radiation-cooled polymeric metamaterials, this type of radiation-cooled polymer may be a better alternative. It must, however, be improved considering its reliability, including dust and moisture penetration issues. The defense of the polymer layer against UV radiation and chemical deterioration is another factor in long-term dependability. Polymer degradation caused by UV is a frequent challenge. Some polymers, like PET and PTFE, are resistant to UV ray deterioration. It is thus possible to make the product more durable by adding anti-UV additives.

A summary of the materials, structures, and radiative properties of the radiators designed for diurnal cooling presented in Table 2.

Table 2. An overview of the material composition, structures, and characteristics of a radiator designed for diurnal cooling.

Authors	Structure of Radiative Cooler	Properties of the Structure	$\Delta T_{below\ ambient}$ /P_{net}
Chae et al. [136]	This DPRC structure has a thin silver layer of 200 nm on a substrate of 1312 nm Al_2O_3, 312 nm Si_3N_4, and 276 nm SiO_2.	$\rho = 0.948$ and $\varepsilon = 0.87$	$\Delta T = 8.2\ °C$ and $P_{net} = 66\ W/m^2$
Li et al. [137]	This multi-layer structure consists of an optimized coating of 1.5 µm overlapping MgF_2 and Si_3N_4 layers.	$\rho > 0.95$ and $\varepsilon > 0.75$	$\Delta T = 6.8\ °C$ and $P_{net} = 62\ W/m^2$
Rephaeli et al. [45]	1D-photonic structure is composed of three groups of five layers of MgF_2 (low-index) and TiO_2 (high-index) on a silver substrate, as well as two laminated SiC and quartz layers.	$\rho = 0.965$ and $\varepsilon = 0.1$ to 0.95	$\Delta T =$ Not Available $P_{net} = 105\ W/m^2$
Lee et al. [138]	The top surface of 200-µm-thick planar polydimethylsiloxane (PDMS) is a pyramid structure (chemically stable and inexpensive).	$\rho = 0.95$ and $\varepsilon = 0.98$	$\Delta T = 6.2\ °C$ and $P_{net} = 20\ W/m^2$
Hossain et al. [100]	Alternating layers of germanium and aluminum make up this metal–dielectric CMM pillar structure.	$\rho = 0.97$ and $\varepsilon = 0.99$	$\Delta T = 9\ °C$ and $P_{net} =$ Not available
Raman et al. [37]	Seven layers of HfO_2 and SiO_2 make up this nanophotonic radiative cooler, which also functions as a thermal emitter and photonic solar reflector.	$\rho = 0.97$ and $\varepsilon = 0.5$ to 0.8	$\Delta T = 5\ °C$ and $P_{net} = 40\ W/m^2$
Kecebas et al. [139]	Thin film coatings with a combination of SiO_2, and TiO_2 layers. Then, significant performance improvements can be achieved by adding Al_2O_3 layers.	$\rho = 0.94$ and $\varepsilon = 0.84$	$\Delta T =$ Not available and $P_{net} = 103\ W/m^2$
Fan et al. [140]	The DPRC structure is an 8 Wt% yttria-stabilized zirconia (8YSZ) coated SiO_2 (glass)/Ag that serves as a reflecting layer.	$\rho =$ not given and $\varepsilon = 0.88$	$\Delta T = 10.3\ °C$ and $P_{net} \approx 95.1\ W/m^2$
Zhang et al. [141]	Tridymite-type $AlPO_4$ powder coating tested performance for DPRC.	$\rho = 0.97$ and $\varepsilon = 0.90$	$\Delta T = 4.2\ °C$ and $P_{net} =$ Not available.
Mandal et al. [135]	Hierarchically porous polyvinylidene fluoride/hexafluoropropylene) [P(VdF-HFP)HP] coatings.	$\rho = 0.96$ and $\varepsilon = 0.97$	$\Delta T = 6\ °C$ and $P_{net} = 96\ W/m^2$.
Xu et al. [142]	Powdered nanoporous crystals $Mg_{11}(HPO_3)_8(OH)_6$, which are applied to the floor tiles, are made up of [MgO6] octahedrons and [HPO3] tetrahedrons.	$\rho = 0.922$ and $\varepsilon = 0.94$	$\Delta T = 4.1\ °C$ and $P_{net} \approx 78\ W/m^2$
Cheng et al. [143]	Single-layer radiative cooling coating mixed with TiO_2 (d = 0.4 µm) and SiO_2 (d = 5.0 µm).	$\rho = 0.956$ and $\varepsilon = 0.95$	Not Available
Liu et al. [144]	TPX bilayer selective emitter film coated with nanosized 15% SiO_2 and 15% $CaMoO_4$ (volume fraction).	$\rho = 0.94$ and $\varepsilon = 0.85$	$P_{net} = 47\ W/m^2$
Zhai et al. [38]	A metamaterial with a polymer layer containing SiO_2 microspheres and a thin silver layer on top of it.	$\rho = 0.96$ and $\varepsilon = 0.93$	$\Delta T = 8\ °C$ and $P_{net} \approx 93\ W/m^2$
Huang et al. [66]	The acrylic resin makes up the top and bottom layers, and it contains embedded nanoparticles of carbon black and titanium dioxide.	$\rho = 0.9$ and $\varepsilon > 0.9$	$\Delta T = 6\ °C$ and $P_{net} \approx 100\ W/m^2$

Table 2. *Cont.*

Authors	Structure of Radiative Cooler	Properties of the Structure	$\Delta T_{below\ ambient}$ /P_{net}
Gentle et al. [71]	This DPRC material is composed of 25 μm PE on aluminum and a blend of 5% SiC and 5% SiO$_2$ nanoparticles.	ρ = 0.9 and ε = 0.35–0.95	ΔT = 12 to 25 °C and P_{net} = 50 W/m^2
Song et al. [145]	Polyvinylidene fluoride-co-hexafluoropropylene (PVDF-HFP) nanofiber membrane using electrospinning technology.	ρ = 0.96 and ε = 0.97	ΔT = 10 °C and P_{net} = 85 W/m^2
Kou et al. [67]	Polymer-silica-mirror produced by coating a 4 in. fused silica wafer with a 100-μm-thick polydimethylsiloxane (PDMS) film as a top layer and a 120 nm thick silver film as a back reflector.	$\varepsilon \approx 1$	ΔT = 8.2 °C (daytime) and 8.4 °C (nighttime) P_{net} = 127 W/m^2

5. PRC Application in Buildings to Enhance Performance

As mentioned in previous sections, advances in nanophotonics and nanomaterials technology have aided in increasing the net cooling capacity of PRC materials. However, in most cases, the material has two parts that need to be improved: (1) emitter material and (2) convection cover material.

5.1. Improvements in PRC Emitter Materials

The three main objectives of research studies based on PRC emitters are to improve performance in humid environments, develop a material that is both affordable and scalable, and improve net cooling performance during the day. The material technologies for PRC were divided into four categories in the work presented by Zhao et al. [8], namely natural emitters, film-based emitters, nanoparticle-based emitters, and nanophotonic emitters. Different emitters can be seen in Figure 15a,c, Figure 21a,b and Figure 24a,b. However, this section discusses only a few materials relevant to the application of radiative cooling in buildings.

According to earlier discussions, thin film-based radiative emitters can cool buildings between 2 and 9 °C during typical sunny weather conditions [115]. Furthermore, direct solar irradiation with a photonic radiator can achieve a net cooling capacity of 110 W/m^2 [146]. Using nanoparticle-based emitters, Liu et al. [144] and Kim and Lenart et al. were able to achieve daytime temperatures that were 25.5 °C and 35 °C below ambient temperature, respectively [5]. The PRC emitters in the research conducted by Jeong et al. [147] achieved an impressive result during the daytime in subtropical (humidity is 60 to 70%) climates, using a multilayer passive TiO$_2$-SiO$_2$ (see Figure 26a) radiator to achieve 7.2 °C below ambient temperature. This PRC radiator, with an average emissivity of 0.84 between the wavelengths of 8 and 13 μm, reflects 94% of incident solar energy. This photonic radiative cooler has a net cooling power of 136.3 W/m^2 at a temperature of 27 °C, a significant improvement of 90 W/m^2 over the photonic radiative cooler made of HfO$_2$ and SiO$_2$. However, when the humidity is high during the day, it is difficult to achieve the desired PRC results [140,148,149].

The 3M Enhanced Specular Reflector (ESR) material [150]—which is a high reflectivity (>98.5%), mirror-like optical enhancement film—multi-layer polymer technology, and non-metallic thin film construction, produced perfect results when tested with PRC materials for highly humid climatic conditions. This material may be better able to cool to sub-ambient temperatures under highly humid conditions and cloudy nights [148,149].

Many researchers, however, have focused on improving PRC performance during the day and at higher humidity levels, while very few have focused on materials affordability. Using a technique called roof radiation trap, Givoni et al. [47] developed an innovative system to improve PRC that consists of a fixed insulation layer between the roof and the fixed insulation, protected by a hinged panel between them. This fixed insulation layer is

safeguarded by a white corrugated metal sheet that can also be used as a nocturnal radiator in the summer [5].
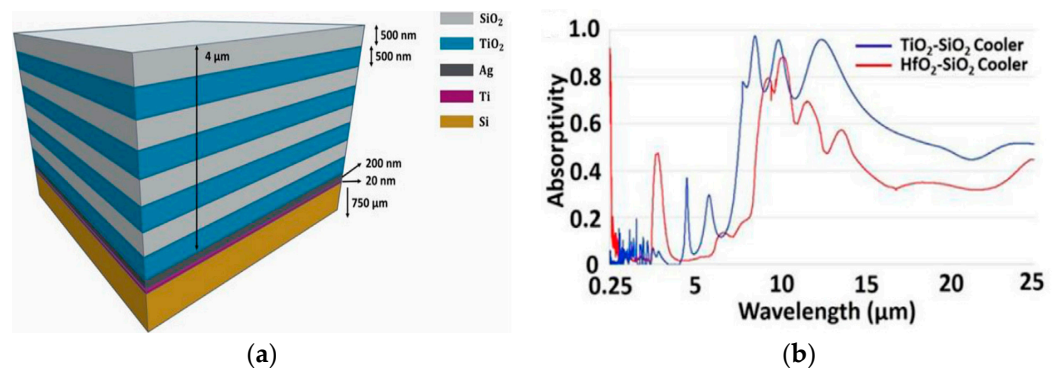

Figure 26. (**a**) A schematic representation of an optimized multi-layered TiO_2-SiO_2 alternating radiative cooler and (**b**) emission spectrum comparison of an optimized 500 nm TiO_2-SiO_2 alternating radiative cooler and a HfO_2-SiO_2 radiative cooler [147].

Erell et al. [151] suggest rooftop ponds for providing thermal comfort in hot and dry climates as a low-cost and efficient method. The nocturnal longwave radiation is responsible for cooling these ponds. In contrast to other materials, their research produced PRCs with poor cooling performance (90 W/m^2) under typical desert meteorological conditions. PRC materials with advanced performance levels are expensive to produce and have a short lifespan. Zhang et al. [141] used aluminum phosphate ($AlPO_4$), an innovative inorganic DPRC material, for improving daytime cooling. A tridymite-type $AlPO_4$ fabricated at 700 °C has a high solar reflectivity of 97% and selective emission with an emissivity of 0.90 across 8–13 μm. When incorporated into the coating, the optimum cooling effect could achieve a temperature drop of 4.2 °C lower than the ambient temperature and 4.8 °C lower than a commercial heat-insulating coating when exposed to intense sunlight.

The cooling performance of PRC in direct sunlight has, as shown, significantly evolved. Non-radiative heat transfer can give a maximum temperature drop of 2–10 °C in cooling performance. Under ambient conditions, cover shields or covering materials are the main contenders for achieving significant PRC performance. For this, the spectral properties of convective covers are being modified, for example by using the chemical solution separation method by Benlattar et al. [152,153]. They developed CdS (1 mm) and CdTe (9.7 μm) thin films (see Figure 27) on silicon substrates that are transparent for IR radiation as well as predicted a temperature difference decrease of 65 K when comparing between covered and uncovered emitters.
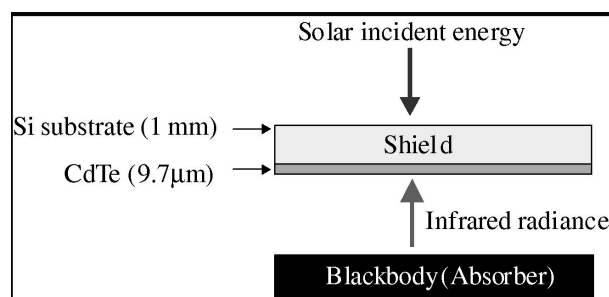

Figure 27. Schematic diagram of convective shielding to improve performance [152].

In a comparison of 30 potential thin-film PRC materials (a combination of 16 different thin-film materials) for passive cooling applications, Naghshine et al. [154] concluded that structures with cubic ZnS multilayers (see Figure 28a) effectively shielded the PRC emitter from parasitic heating loss leaking in both during the day and at night.
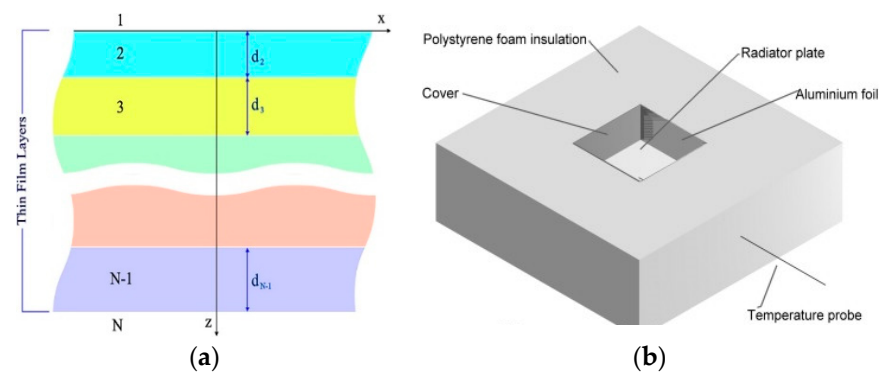
Figure 28. (**a**) An arrangement of thin-film multi-layer structure [154] and (**b**) radiative surfaces protected by cover shields [155].

Research studies conducted by Bathgate et al. [155] on the durability of the convective cover materials found that ZnS, which is mechanically stronger than PE, is a suitable candidate for the PRC emitter cover depicted in Figure 28b.

5.2. Improvements to PRC Material Design

If daytime cooling is the objective, it is essential to improve both the PRC systems' and PRC materials' designs. As a result, researchers have proposed PRC design improvements. The two main areas of the PRC system that need to be improved are emitter isolation and emitter contact with the working fluid. Dimoudi et al. [108] investigated radiative cooling with a prototype roof component consisting of a radiator that uses water as a fluid medium. One of the most crucial features in a roof-integrated PRC system was the concept of emitter insulation, which was created and developed by Khedari et al. [156]. Four types of roof-mounted emitters were constructed using standard building materials. Three different sky types were considered: clear, cloudy, and rainy. Under clear and cloudy skies, the experimental results showed that the various surface temperatures dropped by 1–6 °C below the ambient temperature. However, the temperature of the various roof radiator surfaces and the surrounding temperatures were very similar under rainy skies.

Later, Craig et al. [157] suggested that improving roof RC insulation not only improves performance but that by adapting the roof insulation, a conventional roofing material can acts as a PRC emitter. Figure 29 shows a honeycomb-shaped open-cell insulation that could replace standard insulation. While suppressing convection, the vertical cells would transmit longwave radiation.
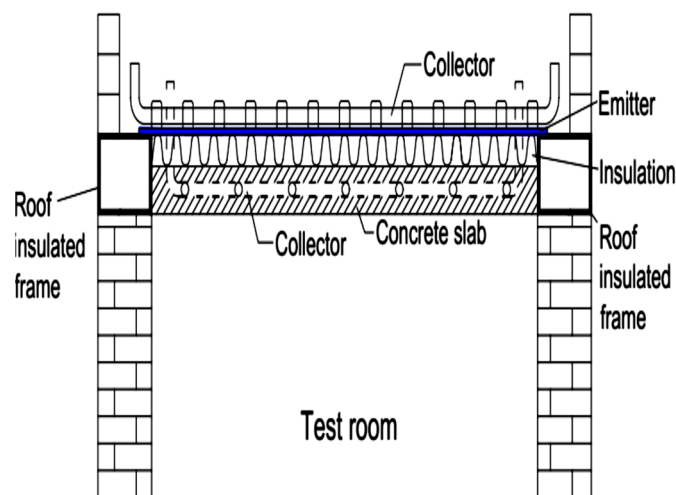

Figure 29. Suggested honeycomb-shaped open-cell insulation for the roof's insulation [5].

In order to reduce the parasitic thermal load on the emitter and safeguard the insulation against convection between the emitter material and the cover shield, some researchers recommended using a vacuum. Indeed, Chen et al. [158] tested an enhanced PRC emitter in a vacuum. The proposed emitter design demonstrated that a selective thermal emitter could reduce the temperature significantly. By removing the parasitic thermal load, it was possible to achieve a maximum temperature of 42 °C below ambient under exposure to solar radiation.

Tso et al. [159] investigated three different PRC designs. Non-vacuum and vacuum systems with seven potassium chloride (KCl) IR-pass windows (heat-absorbing filters) are among the three designs, as is a system with a single KCl IR–pass window. Authors were unable to produce a PRC effect during the day but were able to produce PRC at night in a very humid climate in Hong Kong. Figure 30 depicts their design, which produced a net cooling capacity of 38 W/m^2.
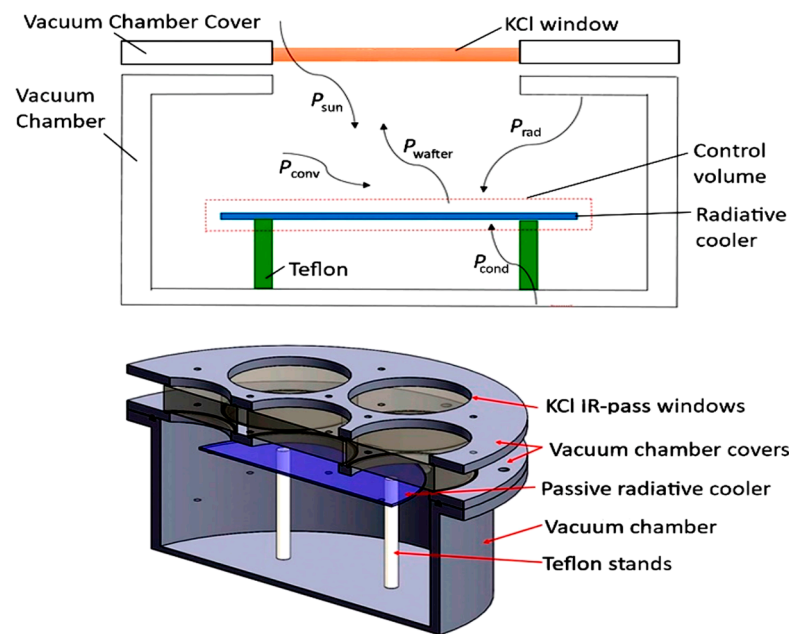

Figure 30. Vacuum chamber design as insulation and part of the convection cover for the PRC radiator [159].

Zevenhoven et al. developed a design (see Figure 31) using a novel approach. A triple-glazed skylight with high absorption capacity was their suggestion. A participating gas inside the skylight reduces heat gain in the building by blocking IR radiation from the sun, while at night heat is released by radiating to space. Subsequently, with this new design, the skylight can be modified according to the desired size without sacrificing performance [160].
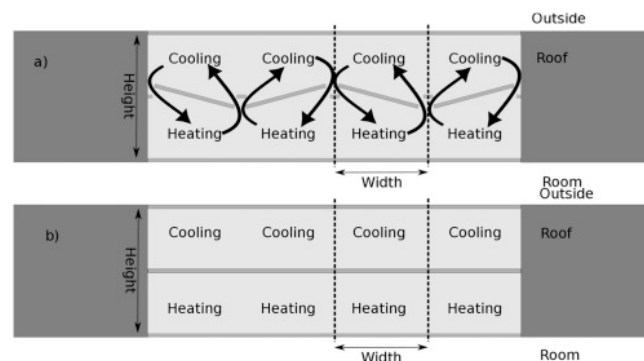

Figure 31. Triple glazing skylight (**a**) in cooling mode (**b**) and in insulating mode [160].

The design appearance of the PRC emitter needs to be appealing to architects and research addresses improving the transmitter's aesthetic quality. Lee et al. [126] and Son et al. [161] fabricated the colored emitters using different techniques. They developed PRC emitters by arranging photonic nanosheets in the form of metal–insulator–metal (MIM) under the emitter.

Based on an optical thin-film resonator surrounded by an effective heat-emitting structure, for aesthetic reasons, Lee et al. [126] introduced the colored passive radiative cooler (CPRC); it has distinctive areas with subtractive primary colors (cyan, magenta, and yellow) on a background of silver, where the former area stands in for a conventional daytime radiative cooler.

The CPRC (see Figure 32a) is made up of an Ag film (100 nm) deposited on a silicon substrate, which serves as the metal reflector, and a selective emitter made of a double layer of SiO_2 (650 nm) and Si_3N_4 (910 nm) materials. To produce radiant colors at desired locations, a thin-film resonator made of a metal–insulator–metal structure (MIM) is positioned underneath the selective emitter. By varying the thickness of the insulator layer, color generation can be precisely controlled. The MIM structure determines each color by intervention in the 1D stacked layers (i.e., SiO_2 cavity). This proposed approach and confirming experiments showed that CPRC can be used to achieve cooling by decreasing the temperature to 3.9 °C below ambient during day.
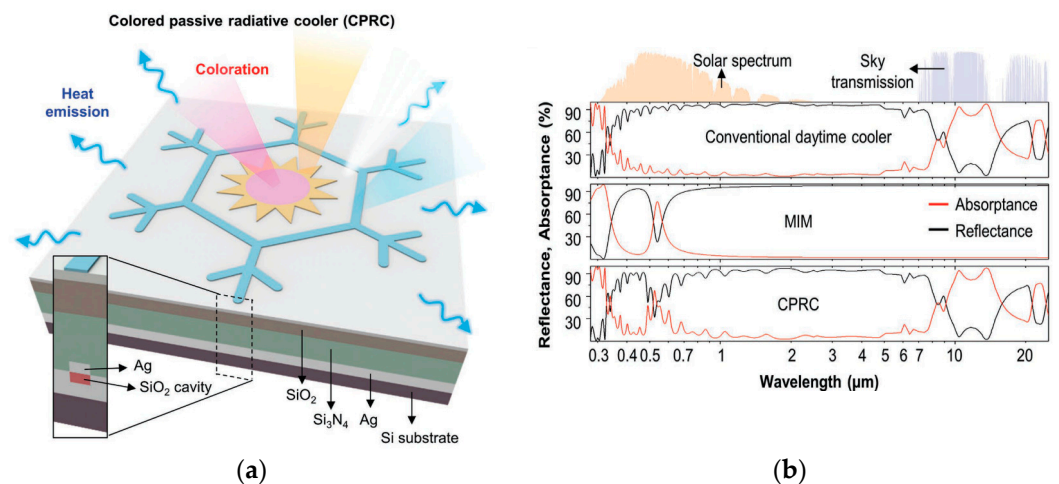

Figure 32. (**a**) Colored passive radiative cooler and (**b**) reflectance and absorption spectra for conventional daytime coolers, MIM, and CPRC from visible to far-infrared wavelength ranges [126].

Son et al. [161] investigated colored radiators (see Figure 33) for improving daytime radiative cooling, which was designed with perovskite nanocrystals embedded in silica and colored with high light–photon conversion in the solar spectrum rather than light–heat conversion, and applied to a white radiator with average IR radiation. When measured outdoors, the fabricated white, green, and red radiators for daytime radiative cooling can give cooling temperatures of 4.2, 3.6, and 1.7 °C below ambient, respectively.

Figure 33. White, green, and red colored DPRC emitter for sub-ambient cooling [161].

6. The Effect of Cover Shields on PRC

Ideally, a cooling power of more than 100 W/m^2 is achieved at ambient temperature, and a very significant temperature reduction of up to 60 °C below ambient should be possible [158]. With a typical maximum temperature of up to 10 °C below the ambient [37], experimental cooling performance is still significantly below average. This is primarily due to non-radiative heat exchange [26]. The most common approach to sub-ambient PRC are infrared-transmissive and convection-suppressive cover shields, which provide better cooling performance [42]. At the same time, it safeguards the radiator's underside by keeping out dust and condensed water vapor [71]. Furthermore, some selective cover shields can act as a solar reflector for the radiator, improving cooling performance and reducing the need for solar reflective radiators [162]. Generally, cover shields fall into three categories: non-selective, mid-infrared selective, or atmospheric window selective [42].

6.1. Nonselective Cover Shields

A non-selective cover shield is the most common type, which can be further divided into single flat films and specially shaped films.

6.1.1. Single Flat Thin Films

The wavelengths at which polyethylene (PE) does not absorb light are 3.4, 3.5, 6.8, 7.3, 13.7, and 13.9 μm, respectively. Moreover, these absorption peaks are smaller, so they have little impact on the radiative cooler [163].

Figure 34 displays the overall transmittance spectrum of PE layers at various thicknesses. It is evident that, aside from the 420-μm-thick PE behaviour, the absorption peaks are nearly identical. The transmittance decreases with PE thickness; it therefore must be thin. The 10-μm-thick PE has the highest average transmittance up to 90% (black curve) [42]. Between the 20-μm- (red curve), 30-μm- (blue curve), and 50-μm-thick (green curve) PE layer, there is no discernible difference with a transmissivity above 80%. The transmittance, however, decreases to 75% for a 100-μm-thick PE (purple curve) [32,155,164,165].
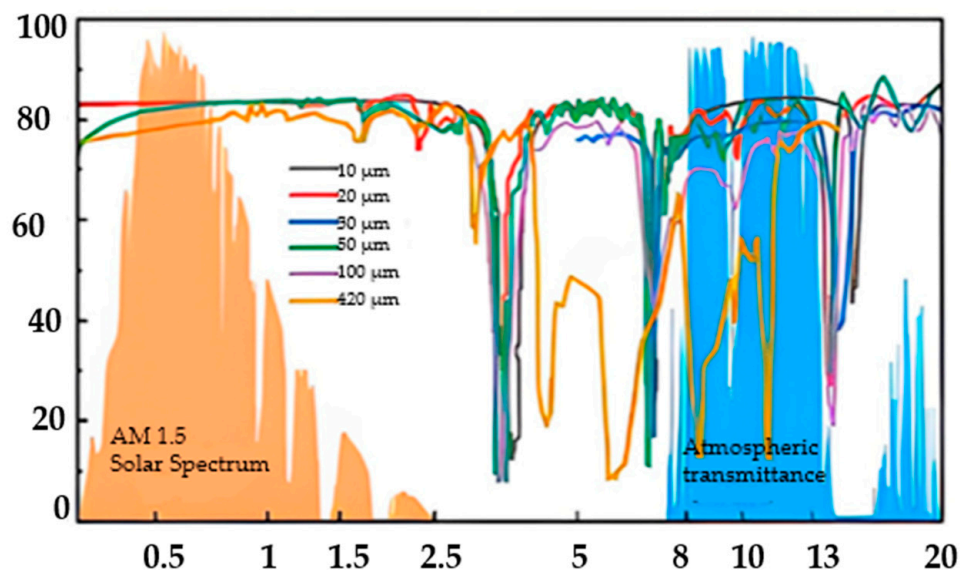

Figure 34. Full-length transmissivity spectrum of PE films at different thicknesses [42].

According to Ali et al. [166], cooling performance increased by 8.6% when the PE film's thickness was decreased from 50 to 25 μm. However, PE films must be both thin enough to transmit IR radiation yet thick enough to withstand extreme weather conditions. The average overall transmittance of 420-μm-thick PE films (yellow curve), in comparison to thin PE films, and is only 50%. There are more absorption peaks, which is likely a result of impurities [42]. To fully understand the durability of PE, Ali et al. also investigated the

effects of aging on the transmissivity of a 50-μm-thick film PE after aging for 5, 30, and 100 days. Average overall transmittance decreased from 72% to 69% and from 57% to 42%, respectively. The cooling performance also decreased by 33.3% over the course of 100 days. In addition, dust buildup and condensation in humid environments may have an impact on PE transmittance [167]. Water condensation reduces PE film transmittance by 9–19%, which lowers the net cooling capacity, according to experimental evidence [168,169].

6.1.2. Special-Shaped Films

Generally, thin film PE is not suitable for areas larger than 0.06 to 0.08 m^2 due to its low durability and mechanical weakness [170]. Researchers, therefore, suggested multilayered films, referred to as "specially shaped films", to allow better outdoor sustainability by withstanding bad weather conditions.

The cover shields are uniquely shaped structures, such as crossed layers of V-waves [32] and wind shields [171]. The self-supporting high-density polyethylene (HDPE) mesh has a porosity of 41.6%, a hole size of 0.8×0.4 mm^2, and a filament diameter of 0.15 mm [170]. This mesh can increase PE's lifespan to more than five years, according to the authors' experimental results. The meshed PE led to a further temperature reduction of 2 °C below ambient and a measured transmissivity of 87.2% [32].

The IR transmissivity of V-shaped HDPE films is 73%, but because of the way the structure is designed, water tends to collect, and PE ages more quickly [32]. By separating the main airflow from the emitter surface, a metal strip windshield shown in [171] was used to suppress the non-radiative heat exchange in order to improve the radiative cooling performance. Passive cooling frequently makes use of the cover shields mentioned above. Despite their daytime cooling capability, this cannot achieve sub-ambient radiative cooling unless a sunshade or other sun reflector is used to reflect direct sunlight.

6.2. Selective or Mid-Infrared Cover Shields

Due to the demands for low transmittance in the solar spectrum and high transmittance in the other wavelength range, particularly in the atmospheric window, selective covers continue to present a challenge. There have been several approaches to achieve spectral selectivity, including pigment-embedded polymers, nanoparticle coating, multilayer inorganic film, and nanoporous material. Therefore, this section focuses only on nanoparticles and nanoporous cover shields shown in Figure 35a,b.
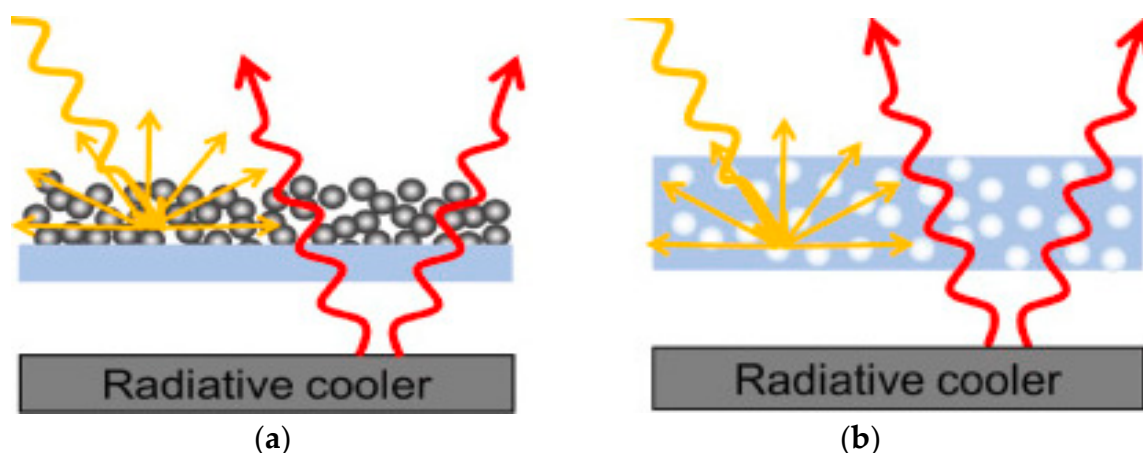

Figure 35. Schematic representation of (**a**) nanoparticle coating cover shields and (**b**) nanoporous PE cover shields [42].

6.2.1. Nanoparticle Coatings

Using particle coatings to achieve spectrum selectivity in cover shields is possible without doping the polymer matrix with solar irradiation (SWIR) reflective particles (see

Figure 35a). Nanocrystalline coatings are much finer (nanoscale) than embedded particles as these can perform as desired in terms of scattering solar radiation.

For instance, the optical spectra of 250 nm TiO_2 particles embedded on polyethylene films are contrasted with those of 60 nm TiO_2 coatings on a PE matrix [172] in Figure 36. As the coating thickness increased, so did the solar reflectance, while the atmospheric window transmittance decreased at the same time. All coatings, however, were more transparent than the pigment-coated sample, whose average transmittance to atmospheric windows was below 40%. The coating that was 1.82 μm thick had the highest solar reflectance, 76%, as well as the lowest transmittance, 54.6%.
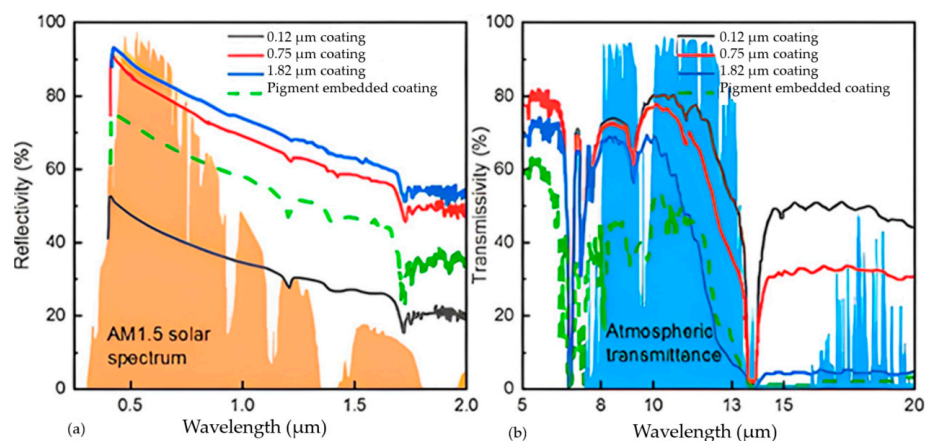

Figure 36. (**a**) Solar spectrum reflectivity and (**b**) the IR transmissivity spectrum of TiO_2 coating films of various thicknesses [42,172].

Furthermore, as shown in Figure 37, BaF_2, ZnS, and PE coatings demonstrated spectral emission selectivity. A 3 cm-thick 150 nm BaF_2 coating with a porosity of 99% should be able to achieve a maximum temperature drop of 35 °C and cooling power of 120 W/m² at an ambient temperature of 300 K during daytime, according to modeling results.
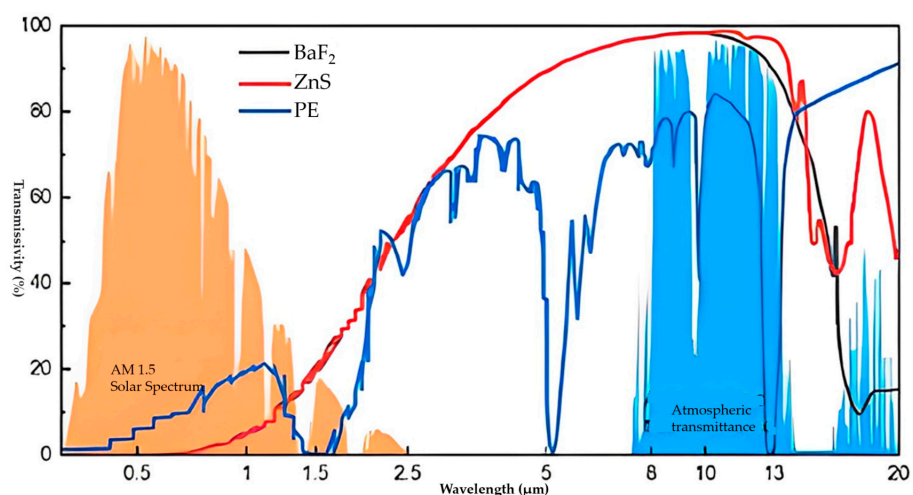
Figure 37. The transmission spectra of BaF_2, ZnS, and PE coatings, as well as a typical atmospheric transmittance, are depicted in orange and blue, respectively [42,173].

6.2.2. Nanoporous Polyethylene (PE) Shields

A polished aluminum direct sunlight reflector was used in conjunction with a double-layer nanoporous polyethylene (NanoPE) film to reduce the effect of incoming diffuse solar radiation, which accounts for about 10% of solar radiation [174]. The total transmittance in the atmospheric window was up to 92%, while the solar reflectance was only about

55%, with a 6.4 mm air gap separating the two layers. Experimentally, the maximum temperature drop was 2 °C higher than a 50-μm-thick LDPE cover shield and 6 °C below ambient temperature ($\rho_{0.25-2.5\mu m}$ = 39%, $\tau_{8-13\mu m}$ = 67%). The modeling results suggest that a maximum temperature drop of 20 °C might be achievable with NanoPE's solar reflectivity (SW) raised to 80% [174].

Two distinct types of customized nanoporous materials made of PE have been developed by Leroy et al. [175], who recommended a thermally induced phase separation (TIPS)-based optically selective and thermally insulating covering. Leroy reported a maximum temperature drop of 13 °C around noon and a maximum net cooling performance of 96 W/m² during the day at ambient temperature, which is 22% better than the coverage previously reported using a 15-μm-thick PE film [98].

Figure 38 displays the optical characteristics of 6-mm-thick polyethylene aerogel sample (PEA). The PEA has a high atmospheric window transmittance of 79.9% and a high solar irradiation reflectance of 92.2%. In spite of this, PEA's mechanical strength may be problematic since it is extremely porous (>0.9). Due to this, it is necessary to attach it to the radiator's surface when used in practical applications.
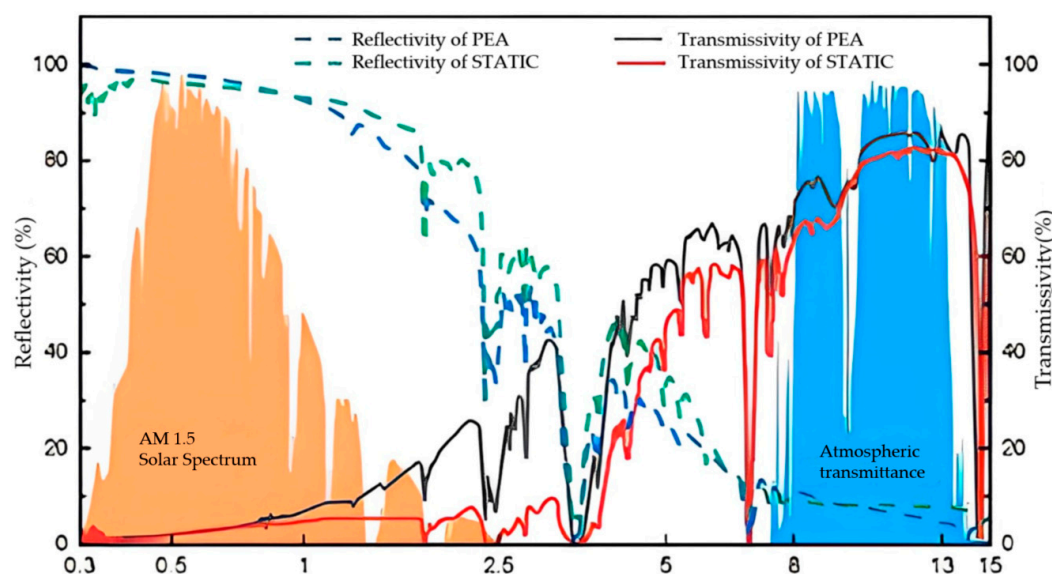

Figure 38. PEA and STATIC transmissivity and reflectivity [42,146,176].

Torgerson et al. also demonstrated a polymer filter, in fact, a spectrally tuned all-polymer technology for inducing cooling (STATIC) that blocks solar radiation while transmitting infrared radiation. Figure 38 also displays the optical characteristics of STATIC. The average solar reflectance of the STATIC 250-μm-thick film is 95%, while the average transmittance in the atmospheric window is more than 75%. A maximum temperature drop of 7.5 °C resulted in a net heat flux of more than 110 W/m² [146].

As mentioned above, the combined requirements for mechanical strength and optical properties of the cover shield limit the development of the cover shield and result in a significant difference between the experimental results and the theoretical potential. As shown in Figure 29, the rigid cover shields provide excellent spectral selection performance, resulting in increased cooling efficiency. In theory, rigid cover shields could operate at ambient temperatures up to 67 °C by suppressing non-radiative heat transfer. To reduce the impact of non-radiative heat exchange on cooling performance, the radiator cooler needs to be properly isolated in a vacuum environment. Suitable candidates for this include ZnSe, ZnS, and BaF$_2$ [42].

So far, convection shields generally consist of the materials mentioned above. However, thin PE films, such as ZnSe, ZnS, or CdS, are not suitable because they require additional sun shading for use during the day. Furthermore, the use of PE in multilayer films, corrugated

structures, and grids is also undesirable, limiting its application. Therefore, Hu et al.'s [177] proposal is a spectrally selective and mechanically robust convection shielding made of a nanoporous composite fabric (NCF) of 200 μm thickness made from inexpensive materials through a scalable fabrication process (see Figure 38).

NCF (see Figure 39) exhibits excellent UV resistance, mechanical strength, hydrophilicity, and thermo-stability in addition to nearly perfect spectral selectivity with 95% solar reflectance and 84% IR transmittance. Additionally, continuous cooling performance below ambient temperature was found to give an average cooling of 4.9 °C below ambient temperature and an average net radiative cooling capacity of 48 W/m^2 over a 24-h period. Furthermore, modeling results revealed that under a direct solar irradiance of 850 W/m^2 a cooling effect of 10 °C and a net radiative cooling capacity of more than 100 W/m^2 could be achieved. The main idea here is that this convection shield can prevent non-radiative heat exchange from a warmer environment [177].
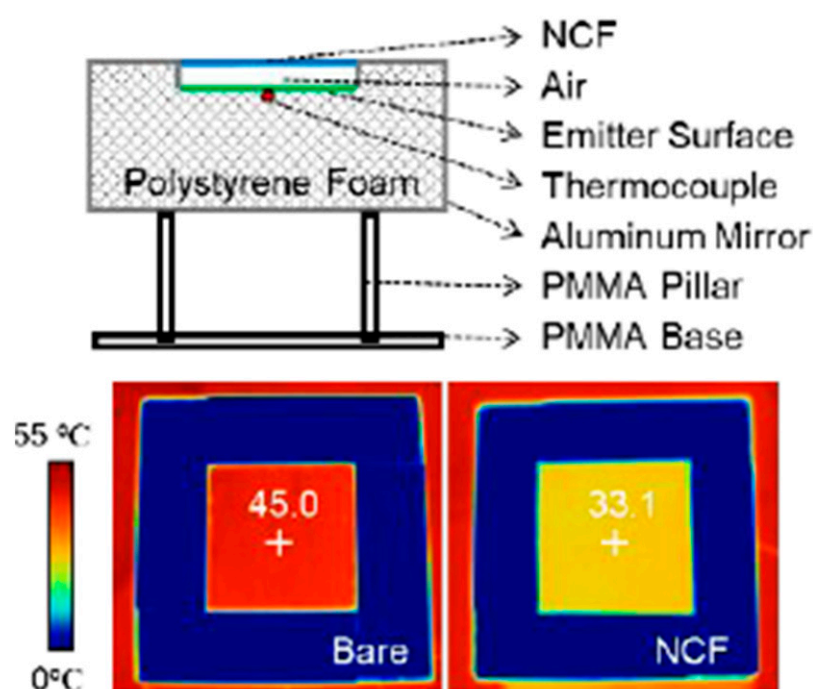

Figure 39. The NCF-based radiative cooler schematic and thermal images of the bare and NCF-based radiative cooling devices [177].

7. Applications and Challenges in Evolving DPRC

A number of DPRC materials and structures have been developed with attractive optical properties, but designing a PRC system requires considering a number of crucial factors, including system configuration and control, end-user cooling load profiles, weather effects, system costs, and payback time. This section discusses a few DPRC applications [35]:

7.1. Cooling of Solar Cells

The effective operation of any thermal system depends on heat dissipation. For instance, higher operating temperatures significantly shorten the service life of photovoltaic systems while also reducing their efficiency. The efficiency of a silicon-based solar cell, which has a 22% efficiency, decreases by 0.1% when the temperature rises by 1 °C because silicon solar cells typically have a negative temperature coefficient of 0.45% [178,179]. The actual spectral range of Si-based solar cells, according to more research, is between 0.3 and 1.1 μm, and the remaining solar energy is transmitted, either reflected or converted into heat, further lowering the conversion efficiency of solar cells. Thus, in photovoltaic systems, thermal management is crucial. The solar cell's operating temperature is greater than the surrounding temperature, making it feasible to dissipate heat without creating a

barrier to non-radiative heat transfer. Simultaneously, due to Si's significant absorption dip around the wavelength of 9 μm, the emissivity of Si-based solar cells can reach 85% in the long wave (LWIR) transmission window [180].

The development of a special DPRC coating that can both strongly reflect solar radiation in the sub-band gap and ultraviolet regions as well as strongly radiate heat by thermal emission is one approach. Utilization of such a cooler with a solar PV module (see Figure 40) has experimentally demonstrated a temperature decrease in the Si cell of more than 5.7 °C.
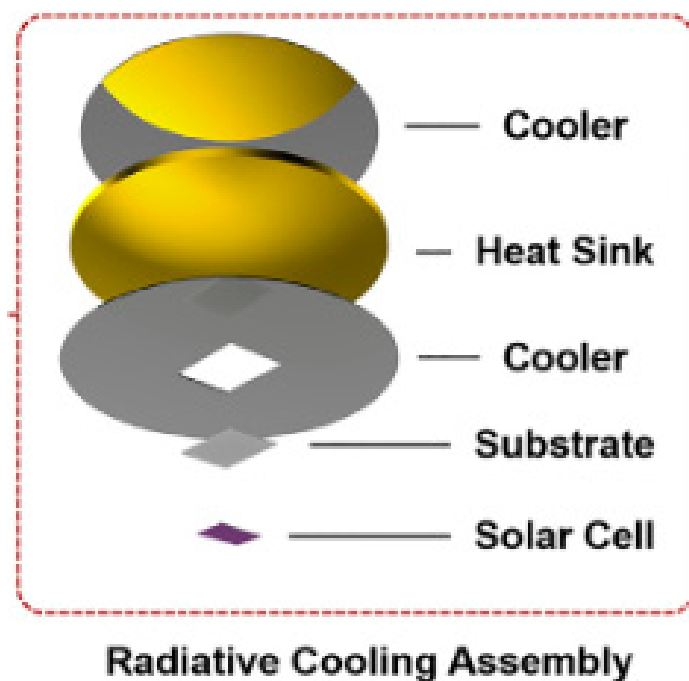

Figure 40. Traditional cooling methods are applied with lightweight DPRC coatings [181].

Due to the high cost and insufficient processing technology for photonic structures, it has been challenging to commercialize photonic selective reflective structures. Another strategy is to use DPRC to remove excess waste heat from solar cells; a thin coat of DPRC can achieve this [35,182–184]. DPRC coatings are traditionally applied to solar cells via a direct method. Following the experimental demonstration that a temperature drop of 36 °C was sufficient for concentration photovoltaics, the open-circuit voltage of gallium antimonide (GaSb) cells increased by 27%, and it was anticipated that the lifespan would increase four to fifteen times [181].

7.2. Power Generation

With DPRC coatings, it is possible to passively lower a surface's temperature, which can be deployed for the generation of electricity. By using thermo-electric (TE) generators, this temperature difference is directly converted into electricity. TE generators have received much attention as a way to generate usable energy from waste heat or from solar heat. The DPRC technology can provide a cold source and be integrated with traditional TE generators to produce electricity, unlike traditional TE generators [185,186]. When photovoltaic systems are not functioning at night, TE can be used in conjunction with the cooling effect in DPRC to produce electricity. Applications for nighttime power generation include sensors and lighting, among many others. A commercial TE generator, for example, has been experimentally combined with a reflective cooling coating to produce 25 mW/m^2 at night, which can be used to light the room (see Figure 41a). Besides that, a spectral-angular-selective radiator (see Figure 41b), which operates close to the thermodynamic Carnot limit, was able to produce a high electrical power density > 2 W/m^2. These findings suggest that

optimizing the radiator will increase the power density for electricity generation based on radiative cooling [187,188].
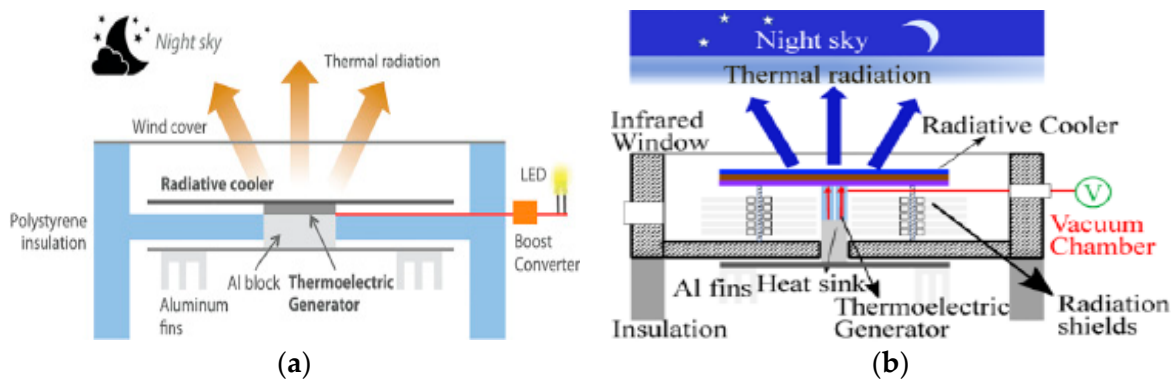

Figure 41. (**a**) Configuration of the main parts of the economical TE generator for the night [187] and (**b**) system design for optimal nighttime power generation [188].

The TE device is equipped with a selective emitter, which has high reflectance/low emissivity in the solar spectrum and high emissivity in the atmospheric window. Additionally, the DPRC continuously cools the top of the TE generator.

As a result, electricity has continued to be generated continuously at a constant rate. If the broadband radiator is attached to the TE device and has high emissivity/absorbance in both the solar spectrum and the atmospheric window, it will be heated by solar absorption during the day and cooled by thermal radiation through the atmospheric window at night. As a result, the maximum temperature gradually rises from night to morning and the temperature difference disappears. The power of TE generation becomes zero then.

The power would also be completely zero due to weather effects like clouds. It is therefore of utmost importance to carefully consider the temperature difference achieved during the day when considering continuous power generation based on radiant cooling and current/voltage intensity. This is yet another way to utilize TE to generate electricity throughout the day (see Figure 42) [189].
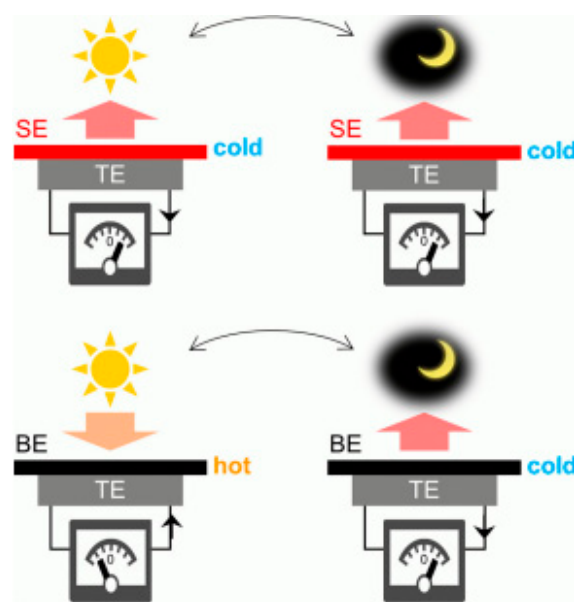

Figure 42. Theoretical illustration of TE devices with a broadband emitter (BE) and a wavelength selective emitter (SE) on top [189].

Thermal control of spacecraft is one of the crucial applications, due to extreme temperature variations. In order to maintain a desired temperature where radiative cooling and heat gain are balanced, temperature control is necessary; typically, this is done at high temperatures. Taylor et al. proposed a switchable coating of metal dielectrics based on VO_2. These structures have a high IR reflectance in wavelength range of 5–25 μm below 341 K and are emitting above it, as shown in [190]. Similarly to this, Sun et al. [191] suggested using aluminum-doped zinc oxide (AZO) instead of traditional rigid quartz tiles for spacecraft cooling because it would be lighter and less expensive to launch.

Hu et al. suggested a combined photo-thermal and radiative cooling module for zero-energy building applications for daytime and nighttime heating and cooling, respectively. The module comprises ultra-white glass glazing and a solar selective absorbing coating, separated by an air tunnel, which transports thermal loads during the day for photo-thermal heating and at night for radiative cooling.

8. Technical Challenges in Commercializing Especially for DPRC

The text given above points out a number of technical difficulties. Prior to implementation, the biggest obstacles were cost, an optimized design, operational reliability, and DPRC material durability. Particularly for developing nations like India, affordability is a crucial factor. Low-cost materials, easy accessibility, and the manufacturing process all contribute to affordable devices. There have not been any studies on the DPRC materials' stability or durability apart from technical limitations. The management and disposal of production by-products and end-of-life waste materials is another challenge. The radiative cooling system faces as main challenges the low energy density and possibly high atmospheric humidity. Low energy density requires a large area of heat transfer fluid to be circulated in an active system, which requires pumping power (resulting in a non-passive system [98].

The short life cycles of the primary developed materials, which must and can be improved by polymers and materials similar to plastic, is a cause for this. Due to higher heating energy requirements and visual inconvenience from mirror reflection, roof-integrated radiant coolers raise energy costs. The albedo/reflection decreases very quickly in the beginning due to dirt accumulation on the open radiant cooling surface. Hand washing with soap can fix this problem, however, the development of a self-cleaning material is still required [127,135].

High humidity and dense clouds hamper the performance of the radiative cooler, so it is less effective along coastlines. According to a study by Bijarniya et al. [192], DPRC is less efficient in coastal cities or in cities with high levels of humidity. This presents a significant challenge because the coastal region is home to many populated cities throughout the world. Due to the relatively high wind speed in coastal regions, minimizing convective heat transfer is another implementation challenge. Another negative effect of radiant cooling can be frost formation. In cold weather, IR emission cooling causes frost to form on car windshields, for example. One method for removing the frost is by heating, but the low-emitting SnO_2 coating does not require heating. The fact that DPRC only reduces temperature makes it unsuitable for most air conditioning systems because both temperature and humidity control is necessary. This is a drawback in commercializing this technology although it applies to most air-conditioning, heating, and ventilation equipment with temperature as the control parameter [22].

Significant challenges also come from maintenance and integration with building infrastructure. Therefore, the ability to achieve a desired PRC effect during the day largely depends on the material itself, and the production of a material that closely resembles the properties of an ideal selective material is still in the coming decades. Increasing solar reflectance while specifically modifying thermal radiation at particular wavelengths offers new possibilities. Additionally, non-reciprocal materials that might defy Kirchhoff's law for different wavelengths can achieve a disparity between directional spectral emissivity and absorptivity by managing thermal radiation, which may offer new insight into achieving significant cooling during the day [193].

The limitations of space and available surface present another technical challenge. When it comes to managing most of a building's cooling load, radiative cooling requires a large amount of surface area. A roof should be horizontal or moderately sloped if the cooling panels are to be merged into it. Due to the low roof-to-floor area ratio in multi-story buildings, this technology is unable to satisfy cooling requirements. Thus, the technology is intended for shorter, smaller, and mid-sized buildings [9]. Other technical issues include the intricate and integrated design of PRC systems, and parasitic energy losses in each heat transfer process, such as those that occur in water storage tanks and between radiating surfaces and heat transfer fluids. Retrofits are often not an option for PRC systems because of their complexity, and building maintenance and operations staff typically find it challenging to fully understand and control the system and its parts [34].

8.1. Limitations via Geographical Conditions

When using PRC systems in buildings, geographic conditions are critical. Some of these, such as atmospheric constituents (e.g., CO_2 and H_2O), sky condition (e.g., cloudy vs. clear), wind speed, and humidity situation, are discussed in the sections above (see Section 2). Water vapor content (see Section 1.5) is the most important factor for atmospheric radiation in the 8 to 13 μm range. By calculating the cooling potential at varying relative humidity at two Australian mid-latitude sites, Hossain et al. [10] investigated the impact of humidity on radiative cooling. Specifically, they found that atmospheric water vapor could significantly affect the performance of selective radiators. Furthermore, when the sky is cloudy, the atmosphere becomes completely IR-impermeable, making effective cooling impossible because of an increased sky temperature. Therefore, low humidity and little cloud cover are the conditions where PRC performs best [10].

The amount of thermal radiation that might potentially pass through the atmospheric window is based on weather conditions, temperature of the sky, and surface objects. As shown in Figure 43, the atmosphere absorbs 30 to 40% of the thermal radiation from black bodies (or gray bodies) between 30 and 60 °C. Furthermore, for radiation emitted from surfaces hotter than 40 °C, the intensity increases from 60 W/m² for cold surfaces to >200 W/m² for hot ones. Zevenhoven et al. [194] tested their passive skylight during the night and concluded that in a country like Finland, with very short nights during the summer, the nighttime passive cooling potential is limited.
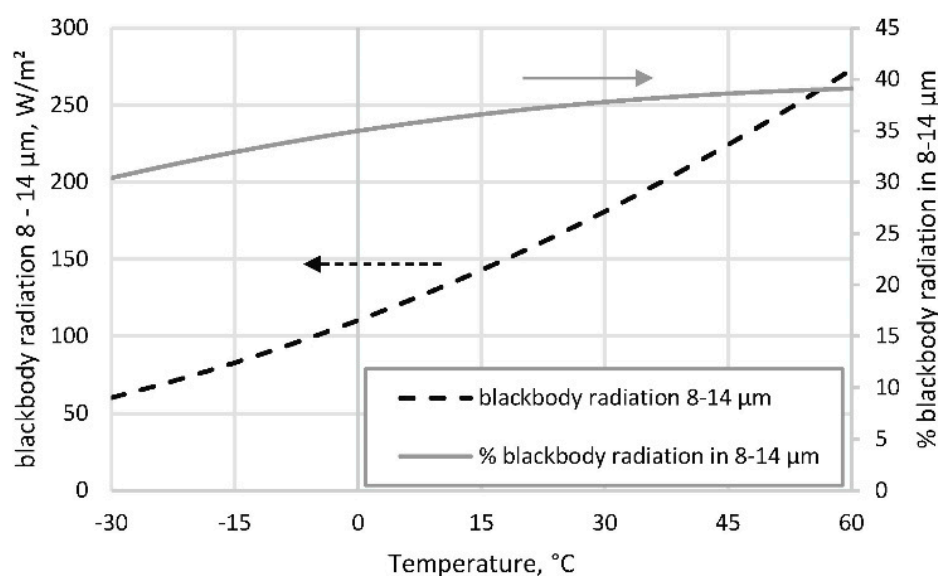

Figure 43. Intensity of blackbody thermal radiation within the 8–14 μm and % of thermal radiation within the atmospheric window vs. surface temperature [194].

Accordingly, the following summer characteristics are those where radiative cooling would have a limited impact listed in [34]:

- Locations in which most of the summer nighttime hours are humid and hot over 80% relative humidity, with temperatures over 24 °C.
- Locations where most summer nighttime temperatures are very warm (above 27 °C).
- Compact buildings with low cooling loads in maritime climates.
- Locations with a lot of hot summer days and fewer short summer nights.

8.2. Affordability Issues

The use of PRC systems in comparison to three different system configurations—cool roofs, conventional radiators, and photonic radiators—is discussed in this section regarding the potential cost savings.

Building cooling systems for commercial use are expensive to install, and examples of PRC commercialization in buildings involve cool roofs. Levinson et al. [195] calculated prototypical energy savings and heating costs per unit of conditioned roof space and concluded that modifying 80% of the 2.58 billion square feet of conditioned roof space on commercial buildings in the United States would save $735 million in annual energy costs. Hossein et al. [196] used DOE-2.1E (a building energy analysis software that predicts energy usage and costs for all types of buildings which makes use of a description of the building layout, construction, operating schedules, and HVAC systems) to show that a cool roof could reduce the total annual energy cost of retail buildings by up to $60/100 m^2 of roof area for cool roofs operating in cold climates.

The rooftop radiator, radiative cooling panels, thermal storage, insulation, and connecting piping are a few of the conventional radiator system's expected components, all of which have high initial costs. According to cost information from the late 1990s, a system involving a water radiator coupled with a cooling panel, which was assessed at the Athens Renewable Energy Facility, is said to cost 116 €/m^2. Further, Heliocoil and polycarbonate are two novel radiators tested in Sde-Boqer, priced at 60 and 50 €/m^2, respectively [197]. An economic analysis of a field trial of a closed water-based PRC system in hot climatic conditions revealed that it's payback time was approximately 6.8 years. Rooftop spray cooling systems are a favorite among commercial technologies due to their low cost when compared to covering a significant portion of the roof with radiators and using pipes for water flow. Installation costs for the spray cooling system for the Whitecap rooftop system were estimated to be $400 per 1000 ft^2 (roughly 90 m^2) of roof area [198,199].

The cost of production-scale photonic products is currently unknown for novel photonic systems, as the technology is still in the laboratory prototype stage. The cost advantages of photonic radiation systems were compared to several reference systems, including volume air volume (VAV) systems and custom emitters with high-end and medium surface properties, in a simulation run by [34]. In comparison with VAV systems, the novel photonic system reduced electricity usage by 24 to 103 MWh. An acceptable maximum incremental cost of switching from night cooling to photonic radiant cooling should range from $8.25 and $11.50/m^2. Furthermore, it has a short five-year payback period [34].

The application of PRC systems in buildings, perhaps while primarily daytime PRC would be needed, appears to still be in its infancy from the discussion above, and the low cooling potential per unit area means that the energy savings may not be sufficient to justify the high initial cost. Mass production and the enhancement of the novel material's optical properties, with nanoparticles seemingly offering the best features, are primarily responsible for the potential cost savings.

9. Conclusions

The content of this paper uses a brief summary of research conducted at Åbo Akademi University as a starting point to had better describe thermal radiation heat transfer through double glass windows and passive cooling skylights. Using DPRC skylights to reduce energy usage can contribute to a reduction in overall energy use. The existing ÅA skylight

prototype will be designed further to reflect more sunlight than a typical roof, which will result in less solar energy being absorbed. This shall lead to a drop in temperature inside the building. In general, the surface of conventional roofs can reach temperatures of up to 65 °C or higher on a hot summer afternoon. This skylight allows a building's inside temperature to remain cooler in the same circumstances by reducing heat flow from the rooftop into the outer space; this can save energy and money in buildings with air conditioning or improve human comfort in buildings without air conditioning.

Primarily, this review provides a synopsis of the evolution of DPRC technology, beginning with the fundamentals of PRC and progressing to the designs, materials, functionalities, and effectiveness of various radiative coolers (both nocturnal and diurnal applications). Foregoing studies concentrated on nocturnal radiative cooling with black and/or infrared selective emitters [21]. Recent advances in nanophotonic emitters and metamaterials have been used to demonstrate DPRC. Certainly, there is evidence for metamaterial/nanophotonic-based radiative cooling in many different configurations, including simple and multilayer films, intricate nanostructured surfaces, and randomly arranged nanospheres. However, the expensive procedures required for the nanofabrication techniques required to create selective emitters include electron beam lithography (EBL), reactive ion etching, roll-to-roll nanoimprint lithography, and others [30]. This study examined several techniques and concludes that nanoparticles or nanospheres are the most commercially viable because they can be produced in large numbers, are simple and cost-effective to produce, and can be applied to different surfaces. In any case, it is challenging to choose the right material and optimize nanospheres sizes and filling fractions in order to achieve effective radiative cooling [31].

The current review can conclude with the following findings:

There are many uses for especially DPRC, including personal thermal management, power generation, photovoltaic system/solar cell cooling, and energy-efficient buildings, as described in the above sections. The effectiveness of PRC systems in the real world will, however, depend on further research in the following key areas:

- The solar reflectivity and thermal IR emissivity of a radiative cooler are currently very close to being equal to one. However, heat losses, such as convection and conduction through the cooler, must be deployed to enhance PRC performance. Therefore, addressing the heat-loss issue is the most effective way to improve the radiant cooler's overall performance [30].
- In the case of applications below ambient temperature, it is still difficult to find a long-lasting convection cover shield that does not greatly affect outgoing radiation. Without effective suppression of the non-radiative heat transfer modes, even an ideal IR selective radiator cannot provide enough cooling at sub-ambient temperatures [30,42].
- It is necessary to conduct more research on the regional applicability of radiative cooling, especially with regard to diurnal radiative cooling. The influence of sky conditions, a thorough integration of geographical locations, climatic conditions, and other factors, is a crucial parameter for PRC improvement [21].
- It is crucial to reduce the impact of wind, water vapor, dirt accumulation, rain, and other environmental factors on the effectiveness of the new generation of radiative coolers. A deeper understanding of surface topology and attributes is still required. A closed surface is less susceptible to wind and dirt, for example, while a hydrophobic surface is less susceptible to water vapor and rain [21,30].
- Glass-type or other suitable window materials with high transmittance in the atmospheric window wavelength range need to be developed and produced via low-cost routes.

Data Availability Statement: Not applicable.

Conflicts of Interest: Authors declare that they have no conflict of interest.

References

1. Yi, Z.; Lv, Y.; Xu, D.; Xu, J.; Qian, H.; Zhao, D.; Yang, R. Energy Saving Analysis of a Transparent Radiative Cooling Film for Buildings with Roof Glazing. *Energy Built Environ.* **2021**, *2*, 214–222. [CrossRef]
2. Zhao, D.; Aili, A.; Zhai, Y.; Xu, S.; Tan, G.; Yin, X.; Yang, R. Radiative Sky Cooling: Fundamental Principles, Materials, and Applications. *Appl. Phys. Rev.* **2019**, *6*, e5087281. [CrossRef]
3. Sun, J.; Wang, J.; Guo, T.; Bao, H.; Bai, S. Daytime Passive Radiative Cooling Materials Based on Disordered Media: A Review. *Sol. Energy Mater. Sol. Cells* **2022**, *236*, 111492. [CrossRef]
4. Liu, J.; Zhang, J.; Tang, H.; Zhou, Z.; Zhang, D.; Ye, L.; Zhao, D. Recent Advances in the Development of Radiative Sky Cooling Inspired from Solar Thermal Harvesting. *Nano Energy* **2021**, *81*, e105611. [CrossRef]
5. Suhendri; Hu, M.; Su, Y.; Darkwa, J.; Riffat, S. Implementation of Passive Radiative Cooling Technology in Buildings: A Review. *Buildings* **2020**, *10*, 215. [CrossRef]
6. Muhammed, A. Design of Spectrally Selective Surfaces. Ph.D. Thesis, Sabanci University, Tuzla, Turkey, 2020; pp. 1–9.
7. Mahdavinejad, M.; Javanrudi, K. Assessment of Ancient Fridges: A Sustainable Method to Storage Ice in Hot-Arid Climates. *Asian Cult. Hist.* **2012**, *4*, 133–139. [CrossRef]
8. Zhao, B.; Hu, M.; Ao, X.; Chen, N.; Pei, G. Radiative Cooling: A Review of Fundamentals, Materials, Applications, and Prospects. *Appl. Energy* **2019**, *236*, 489–513. [CrossRef]
9. Lu, X.; Xu, P.; Wang, H.; Yang, T.; Hou, J. Cooling Potential and Applications Prospects of Passive Radiative Cooling in Buildings: The Current State-of-the-Art. *Renew. Sustain. Energy Rev.* **2016**, *65*, 1079–1097. [CrossRef]
10. Hossain, M.M.; Gu, M. Radiative Cooling: Principles, Progress, and Potentials. *Adv. Sci.* **2016**, *3*, 1500360. [CrossRef]
11. Sun, X.; Sun, Y.; Zhou, Z.; Alam, M.A.; Bermel, P. Radiative Sky Cooling: Fundamental Physics, Materials, Structures, and Applications. *Nanophotonics* **2017**, *6*, 997–1015. [CrossRef]
12. Vall, S.; Castell, A. Radiative Cooling as Low-Grade Energy Source: A Literature Review. *Renew. Sustain. Energy Rev.* **2017**, *77*, 803–820. [CrossRef]
13. Bagiorgas, H.S.; Mihalakakou, G. Experimental and Theoretical Investigation of a Nocturnal Radiator for Space Cooling. *Renew. Energy* **2008**, *33*, 1220–1227. [CrossRef]
14. Al-Nimr, M.; Tahat, M.; Al-Rashdan, M. Night Cold Storage System Enhanced by Radiative Cooling–A Modified Australian Cooling System. *Appl. Therm. Eng.* **1999**, *19*, 1013–1026. [CrossRef]
15. Meir, M.G.; Rekstad, J.B.; LØvvik, O.M. A Study of a Polymer-Based Radiative Cooling System. *Sol. Energy* **2002**, *73*, 403–417. [CrossRef]
16. Fu, Y.; Yang, J.; Su, Y.S.; Du, W.; Ma, Y.G. Daytime Passive Radiative Cooler Using Porous Alumina. *Sol. Energy Mater. Sol. Cells* **2019**, *191*, 50–54. [CrossRef]
17. Yin, X.; Yang, R.; Tan, G.; Fan, S. Terrestrial Radiative Cooling: Using the Cold Universe as a Renewable and Sustainable Energy Source. *Science* **2020**, *370*, 786–791. [CrossRef]
18. Chen, L.; Zhang, K.; Ma, M.; Tang, S.; Li, F.; Niu, X. Sub-Ambient Radiative Cooling and Its Application in Buildings. *Build. Simul.* **2020**, *13*, 1165–1189. [CrossRef]
19. Santamouris, M.; Feng, J. Recent Progress in Daytime Radiative Cooling: Is It the Air Conditioner of the Future? *Buildings* **2018**, *8*, 168. [CrossRef]
20. Fält, M. The Utilization of Participating Gases and Long Wave Thermal Radiation In a Passive Cooling Skylight. Ph.D. Thesis, Åbo Akademi University, Turku, Finland, 2016.
21. Cui, Y.; Luo, X.; Zhang, F.; Sun, L.; Jin, N.; Yang, W. Progress of Passive Daytime Radiative Cooling Technologies towards Commercial Applications. *Particuology* **2022**, *67*, 57–67. [CrossRef]
22. Bijarniya, J.P.; Sarkar, J.; Maiti, P. Review on Passive Daytime Radiative Cooling: Fundamentals, Recent Researches, Challenges and Opportunities. *Renew. Sustain. Energy Rev.* **2020**, *133*, 110263. [CrossRef]
23. Liu, J.; Zhou, Z.; Zhang, J.; Feng, W.; Zuo, J. Advances and Challenges in Commercializing Radiative Cooling. *Mater. Today Phys.* **2019**, *11*, 100161. [CrossRef]
24. Trenberth, K.E.; Fasullo, J.T.; Kiehl, J. Earth's Global Energy Budget. *Bull. Am. Meteorol. Soc.* **2009**, *90*, 311–323. [CrossRef]
25. Alimonti, G. Our Energy Future Starts from Actual Energy Limits. *EPJ Web Conf.* **2018**, *189*, e00003. [CrossRef]
26. Bao, H.; Yan, C.; Wang, B.; Fang, X.; Zhao, C.Y.; Ruan, X. Double-Layer Nanoparticle-Based Coatings for Efficient Terrestrial Radiative Cooling. *Sol. Energy Mater. Sol. Cells* **2017**, *168*, 78–84. [CrossRef]
27. Eriksson, T.S.; Granqvist, C.G. Radiative Cooling Computed for Model Atmospheres. *Appl. Opt.* **1982**, *21*, 4381. [CrossRef] [PubMed]
28. Head, A.K. Methods and Means for Producing Refrigeration by Selective Radiation. U.S. Patent No. 3,043,112, 10 July 1962.

29.　Nilsson, T.M.J.; Niklasson, G.A.; Granqvist, C.G. A Solar Reflecting Material for Radiative Cooling Applications: ZnS Pigmented Polyethylene. *Sol. Energy Mater. Sol. Cells* **1992**, *28*, 175–193. [CrossRef]

30.　Zeyghami, M.; Goswami, D.Y.; Stefanakos, E. A Review of Clear Sky Radiative Cooling Developments and Applications in Renewable Power Systems and Passive Building Cooling. *Sol. Energy Mater. Sol. Cells* **2018**, *178*, 115–128. [CrossRef]

31.　Ko, B.; Lee, D.; Badloe, T.; Rho, J. Metamaterial-Based Radiative Cooling: Towards Energy-Free All-Day Cooling. *Energies* **2019**, *12*, 89. [CrossRef]

32.　Nilsson, N.A.; Eriksson, T.S.; Granqvist, C. Cooling: Initial Results on Corrugated Polyethylene. *Sol. Energy Mater.* **1985**, *12*, 327–333. [CrossRef]

33.　Nilsson, T.M.J.; Niklasson, G.A. Radiative Cooling during the Day: Simulations and Experiments on Pigmented Polyethylene Cover Foils. *Sol. Energy Mater. Sol. Cells* **1995**, *37*, 93–118. [CrossRef]

34.　Fernandez, N.; Wang, W.; Alvine, K. *Energy Savings Potential of Radiative Cooling Technologies*; Pacific Northwest National Laboratory, Department of Energy USA: Washington, DC, USA, 2015; p. 72.

35.　Chen, M.; Pang, D.; Chen, X.; Yan, H.; Yang, Y. Passive Daytime Radiative Cooling: Fundamentals, Material Designs, and Applications. *EcoMat* **2022**, *4*, 12153. [CrossRef]

36.　Zhu, L.; Raman, A.; Fan, S. Color-Preserving Daytime Radiative Cooling. *Appl. Phys. Lett.* **2013**, *103*, e4835995. [CrossRef]

37.　Zhu, L.; Raman, A.; Wang, K.X.; Anoma, M.A.; Fan, S. Radiative Cooling of Solar Cells. *Optica* **2014**, *1*, 32. [CrossRef]

38.　Zhai, Y.; Ma, Y.; David, S.N.; Zhao, D.; Lou, R.; Tan, G.; Yang, R.; Yin, X. Scalable-Manufactured Randomized Glass-Polymer Hybrid Metamaterial for Daytime Radiative Cooling. *Science* **2017**, *355*, 1062–1066. [CrossRef] [PubMed]

39.　Chae, D.; Lim, H.; So, S.; Son, S.; Ju, S.; Kim, W.; Rho, J.; Lee, H. Spectrally Selective Nanoparticle Mixture Coating for Passive Daytime Radiative Cooling. *ACS Appl. Mater. Interfaces* **2021**, *13*, 21119–21126. [CrossRef] [PubMed]

40.　Benlattar, M.; Ibourk, I.; Adhiri, R. Simple Double-Layer Coating for Efficient Daytime and Nighttime Radiative Cooling. *Atmos.* **2021**, *12*, 1198. [CrossRef]

41.　Lin, K.T.; Han, J.; Li, K.; Guo, C.; Lin, H.; Jia, B. Radiative Cooling: Fundamental Physics, Atmospheric Influences, Materials and Structural Engineering, Applications and Beyond. *Nano Energy* **2021**, *80*, e105517. [CrossRef]

42.　Zhang, J.; Yuan, J.; Liu, J.; Zhou, Z.; Sui, J.; Xing, J.; Zuo, J. Cover Shields for Sub-Ambient Radiative Cooling: A Literature Review. *Renew. Sustain. Energy Rev.* **2021**, *143*, 110959. [CrossRef]

43.　Zeyghami, M.; Khalili, F. Performance Improvement of Dry Cooled Advanced Concentrating Solar Power Plants Using Daytime Radiative Cooling. *Energy Convers. Manag.* **2015**, *106*, 10–20. [CrossRef]

44.　Zevenhoven, R.; Fält, M.; Gomes, L.P. Thermal Radiation Heat Transfer: Including Wavelength Dependence into Modelling. *Int. J. Therm. Sci.* **2014**, *86*, 189–197. [CrossRef]

45.　Rephaeli, E.; Raman, A.; Fan, S. Ultrabroadband Photonic Structures to Achieve High-Performance Daytime Radiative Cooling. *Nano Lett.* **2013**, *13*, 1457–1461. [CrossRef] [PubMed]

46.　Etzion, Y.; Erell, E. Thermal Storage Mass in Radiative Cooling Systems. *Build. Environ.* **1991**, *26*, 389–394. [CrossRef]

47.　Erell, E.; Etzion, Y. Radiative Cooling of Buildings with Flat-Plate Solar Collectors. *Build. Environ.* **2000**, *35*, 297–305. [CrossRef]

48.　Onubogu, N.O.; Chong, K.K.; Tan, M.H. Review of Active and Passive Daylighting Technologies for Sustainable Building. *Int. J. Photoenergy* **2021**, *2021*, 8802691. [CrossRef]

49.　Sharp, F.; Lindsey, D.; Dols, J.; Coker, J. The Use and Environmental Impact of Daylighting. *J. Clean. Prod.* **2014**, *85*, 462–471. [CrossRef]

50.　Light, N. Daylighting. In *Lighting Historic Buildings*; McGraw-Hill: New York, NY, USA, 1997; ISBN 0070498644.

51.　Lotfabadi, P. Analyzing Passive Solar Strategies in the Case of High-Rise Building. *Renew. Sustain. Energy Rev.* **2015**, *52*, 1340–1353. [CrossRef]

52.　Zain-Ahmed, A.; Sopian, K.; Othman, M.Y.H.; Sayigh, A.A.M.; Surendran, P.N. Daylighting as a Passive Solar Design Strategy in Tropical Buildings: A Case Study of Malaysia. *Energy Convers. Manag.* **2002**, *43*, 1725–1736. [CrossRef]

53.　Gago, E.J.; Muneer, T.; Knez, M.; Köster, H. Natural Light Controls and Guides in Buildings. Energy Saving for Electrical Lighting, Reduction of Cooling Load. *Renew. Sustain. Energy Rev.* **2015**, *41*, 1–13. [CrossRef]

54.　Cuce, E.; Riffat, S.B. A State-of-the-Art Review on Innovative Glazing Technologies. *Renew. Sustain. Energy Rev.* **2015**, *41*, 695–714. [CrossRef]

55.　Jelle, B.P.; Hynd, A.; Gustavsen, A.; Arasteh, D.; Goudey, H.; Hart, R. Fenestration of Today and Tomorrow: A State-of-the-Art Review and Future Research Opportunities. *Sol. Energy Mater. Sol. Cells* **2012**, *96*, 1–28. [CrossRef]

56.　Hee, W.J.; Alghoul, M.A.; Bakhtyar, B.; Elayeb, O.; Shameri, M.A.; Alrubaih, M.S.; Sopian, K. The Role of Window Glazing on Daylighting and Energy Saving in Buildings. *Renew. Sustain. Energy Rev.* **2015**, *42*, 323–343. [CrossRef]

57.　Zevenhoven, R.; Martin, F. Passive Cooling Against the Night Sky. *J. Sustain. Res. Eng.* **2014**, *1*, 49–54.

58.　Kim, J.T.; Todorovic, M.S. Tuning Control of Buildings Glazing's Transmittance Dependence on the Solar Radiation Wavelength to Optimize Daylighting and Building's Energy Efficiency. *Energy Build.* **2013**, *63*, 108–118. [CrossRef]

59.　Protocol, M. Code Changes on A2L Refrigerants. In *International Code Council (ICC) Building Safety Journal*; International Code Council (ICC): Washington, DC, USA, 2021; pp. 1–4.

60.　Fält, M.; Zevenhoven, R. Combining the Radiative, Conductive and Convective Heat Flows in and Around a Skylight. In Proceedings of the World Renewable Energy Congress, Linköping, Sweden, 8–13 May 2011; Volume 57, pp. 4027–4032. [CrossRef]

61. United Nations Environment Programme. *The Kigali Amendment to the Montreal Protocol: HFC Phase-Down, OzonAction Fact Sheet*; Factsheet; UN Environment: Nairobi, Kenya, 2016; pp. 1–7.

62. Hellma Materials. VIS/IR Applications. In *CVD Ceramics Catalogue*; Hellma Materials GmbH: Jena, Germany, 2020.

63. Gangisetty, G.; Zevenhoven, R. Selection of Nano-Particulate Material for Improved Passive Cooling Skylight Performance. In Proceedings of the 35th International Conference on Efficiency, Cost, Optimization, Simulation, and Environmental Impact of Energy Systems (ECOS), Copenhagen, Denmark, 4–7 July 2022; pp. 1211–1222.

64. Harris, D.C. Thermal, Structural, and Optical Properties of Cleartran® Multispectral Zinc Sulfide. *Opt. Eng.* **2008**, *47*, 114001. [CrossRef]

65. Khan, U.; Zevenhoven, R. Passive Cooling through the Atmospheric Window for Vehicle Temperature Control. *Arch. Thermodyn.* **2021**, *42*, 25–44. [CrossRef]

66. Huang, Z.; Ruan, X. Nanoparticle Embedded Double-Layer Coating for Daytime Radiative Cooling. *Int. J. Heat Mass Transf.* **2017**, *104*, 890–896. [CrossRef]

67. Kou, J.; Jurado, Z.; Chen, Z.; Fan, S.; Minnich, A.J. Daytime Radiative Cooling Using Near-Black Infrared Emitters. *ACS Photonics* **2017**, *4*, 626–630. [CrossRef]

68. Zou, C.; Ren, G.; Hossain, M.M.; Nirantar, S.; Withayachumnankul, W.; Ahmed, T.; Bhaskaran, M.; Sriram, S.; Gu, M.; Fumeaux, C. Metal-Loaded Dielectric Resonator Metasurfaces for Radiative Cooling. *Adv. Opt. Mater.* **2017**, *5*, 1700460. [CrossRef]

69. Atiganyanun, S.; Plumley, J.B.; Han, S.J.; Hsu, K.; Cytrynbaum, J.; Peng, T.L.; Han, S.M.; Han, S.E. Effective Radiative Cooling by Paint-Format Microsphere-Based Photonic Random Media. *ACS Photonics* **2018**, *5*, 1181–1187. [CrossRef]

70. Catalanotti, S.; Cuomo, V.; Piro, G.; Ruggi, D.; Silvestrini, V.; Troise, G. The Radiative Cooling of Selective Surfaces. *Sol. Energy* **1975**, *17*, 83–89. [CrossRef]

71. Gentle, A.R.; Smith, G.B. Radiative Heat Pumping from the Earth Using Surface Phonon Resonant Nanoparticles. *Nano Lett.* **2010**, *10*, 373–379. [CrossRef] [PubMed]

72. Miyazaki, H.; Okada, K.; Jinno, K.; Ota, T. Fabrication of Radiative Cooling Devices Using Si2N2O Nano-Particles. *J. Ceram. Soc. Jpn.* **2016**, *124*, 1185–1187. [CrossRef]

73. Miyazaki, H.; Yoshida, S.; Sato, Y.; Suzuki, H.; Ota, T. Fabrication of Radiative Cooling Materials Based on Si2N 2O Particles by the Nitridation of Mixtures of Silicon and Silicon Dioxide Powders. *J. Ceram. Soc. Jpn.* **2013**, *121*, 242–245. [CrossRef]

74. Suryawanshi, C.N.; Lin, C.T. Radiative Cooling: Lattice Quantization and Surface Emissivity in Thin Coatings. *ACS Appl. Mater. Interfaces* **2009**, *1*, 1334–1338. [CrossRef] [PubMed]

75. Eriksson, T.S.; Granqvist, C.G. Infrared Optical Properties of Electron-Beam Evaporated Silicon Oxynitride Films. *Appl. Opt.* **1983**, *22*, 3204. [CrossRef]

76. Taft, E.A. Characterization of Silicon Nitride Films. *J. Electrochem. Soc.* **1971**, *118*, 1341. [CrossRef]

77. Granqvist, C.G.; Hjortsberg, A. Surfaces for Radiative Cooling: Silicon Monoxide Films on Aluminum. *Appl. Phys. Lett.* **1980**, *36*, 139–141. [CrossRef]

78. Eriksson, T.S.; Jiang, S.-J.; Granqvist, C.G. Surface coatings for radiative cooling applications: Silicon dioxide and silicon nitride made by reactive rf-sputtering. *Sol. Energy Mater.* **1985**, *12*, 319–325. [CrossRef]

79. Diatezua, D.M.; Thiry, P.A.; Dereux, A.; Caudano, R. Silicon Oxynitride Multilayers as Spectrally Selective Material for Passive Radiative Cooling Applications. *Sol. Energy Mater. Sol. Cells* **1996**, *40*, 253–259. [CrossRef]

80. Berdahl, P. Radiative Cooling with MgO and/or LiF Layers. *Appl. Opt.* **1984**, *23*, 370. [CrossRef]

81. Jordan, D.B.; Ogren, W.L. The CO2/O2 specificity of ribulose 1,5-bisphosphate carboxylase/oxygenase. *Planta* **1984**, *161*, 308–313. [CrossRef] [PubMed]

82. Lushiku, E.M.; Eriksson, T.S.; Hjortsberg, A.; Granqvist, C.G. Radiative Cooling to Low Temperatures with Selectively Infrared-Emitting Gases. *Sol. Wind Technol.* **1984**, *1*, 115–121. [CrossRef]

83. Hjortsberg, A.; Granqvist, C.G. Radiative Cooling with Selectively Emitting Ethylene Gas. *Appl. Phys. Lett.* **1981**, *39*, 507–509. [CrossRef]

84. Lushiku, E.M.; Hjortsberg, A.; Granqvist, C.G. Radiative Cooling with Selectively Infrared-Emitting Ammonia Gas. *J. Appl. Phys.* **1982**, *53*, 5526–5530. [CrossRef]

85. Parker, D.S.; Sherwin, J.R. *Evaluation of the NightCool Nocturnal Radiation Cooling Concept: In Scale Test Buildings Stage Gate 1B*; Technical Report; U.S. Department of Energy: Washington, DC, USA, 2008. [CrossRef]

86. Kimball, B.A.; Idso, S.B.; Aase, J.K. A Model of Thermal Radiation from Partly Cloudy and Overcast Skies. *Water Resour. Res.* **1982**, *18*, 931–936. [CrossRef]

87. Hollick, J. Nocturnal Radiation Cooling Tests. *Energy Procedia* **2012**, *30*, 930–936. [CrossRef]

88. Fält, M.; Zevenhoven, R. Radiative Cooling in Northern Europe for the Production of Freezer Temperatures. In Proceedings of the 23rd International Conference on Efficiency, Cost, Optimization, Simulation, and Environmental Impact of Energy Systems, (ECOS) 2010, Lausanne, Switzerland, 14–17 June 2010; Volume 3, pp. 413–419.

89. Liu, Z.; Tan, H.; Ma, G. Experimental Investigation on Night Sky Radiant Cooling Performance of Duct-Type Heat Exchanger. *Int. J. Vent.* **2017**, *16*, 255–267. [CrossRef]

90. Pearlmutter, D.; Berliner, P. Experiments with a 'Psychrometric' Roof Pond System for Passive Cooling in Hot-Arid Regions. *Energy Build.* **2017**, *144*, 295–302. [CrossRef]

91. Hosseinzadeh, E.; Taherian, H. An Experimental and Analytical Study of a Radiative Cooling System with Unglazed Flat Plate Collectors. *Int. J. Green Energy* **2012**, *9*, 766–779. [CrossRef]
92. Sodha, M.S.; Singh, U.; Srivastava, A.; Tiwari, G.N. Experimental Validation of Thermal Model of Open Roof Pond. *Build. Environ.* **1981**, *16*, 93–98. [CrossRef]
93. Nahar, N.M.; Sharma, P.; Purohit, M.M. Performance of Different Passive Techniques for Cooling of Buildings in Arid Regions. *Build. Environ.* **2003**, *38*, 109–116. [CrossRef]
94. Tang, R.; Etzion, Y. Comparative Studies on the Water Evaporation Rate from a Wetted Surface and That from a Free Water Surface. *Build. Environ.* **2004**, *39*, 77–86. [CrossRef]
95. Tang, R.; Etzion, Y. On Thermal Performance of an Improved Roof Pond for Cooling Buildings. *Build. Environ.* **2004**, *39*, 201–209. [CrossRef]
96. Spanaki, A.; Tsoutsos, T.; Kolokotsa, D. On the Selection and Design of the Proper Roof Pond Variant for Passive Cooling Purposes. *Renew. Sustain. Energy Rev.* **2011**, *15*, 3523–3533. [CrossRef]
97. Goldstein, E.A.; Raman, A.P.; Fan, S. Sub-Ambient Non-Evaporative Fluid Cooling with the Sky. *Nat. Energy* **2017**, *2*, 17143. [CrossRef]
98. Zhao, D.; Aili, A.; Zhai, Y.; Lu, J.; Kidd, D.; Tan, G.; Yin, X.; Yang, R. Subambient Cooling of Water: Toward Real-World Applications of Daytime Radiative Cooling. *Joule* **2019**, *3*, 111–123. [CrossRef]
99. Lee, B.T.; Paul, R.K.; Lee, K.H.; Kim, H.D. Synthesis of Si2N2O Nanowires in Porous Si2N2O-Si3N4 Subtrate Using Si Powder. *J. Mater. Res.* **2007**, *22*, 615–620. [CrossRef]
100. Hossain, M.M.; Jia, B.; Gu, M. A Metamaterial Emitter for Highly Efficient Radiative Cooling. *Adv. Opt. Mater.* **2015**, *3*, 1047–1051. [CrossRef]
101. Tazawa, M.; Jin, P.; Yoshimura, K.; Miki, T.; Tanemura, S. New Material Design with V1-XWxO2 Film for Sky Radiator to Obtain Temperature Stability. *Sol. Energy* **1998**, *64*, 3–7. [CrossRef]
102. Kimball, B.A. Cooling Performance and Efficiency of Night Sky Radiators. *Sol. Energy* **1985**, *34*, 19–33. [CrossRef]
103. Granqvist, C.G.; Hjortsberg, A. Radiative Cooling to Low Temperatures: General Considerations and Application to Selectively Emitting SiO Films. *J. Appl. Phys.* **1981**, *52*, 4205–4220. [CrossRef]
104. Hu, M.; Pei, G.; Wang, Q.; Li, J.; Wang, Y.; Ji, J. Field Test and Preliminary Analysis of a Combined Diurnal Solar Heating and Nocturnal Radiative Cooling System. *Appl. Energy* **2016**, *179*, 899–908. [CrossRef]
105. Etzion, Y.; Erell, E. Low-Cost Long-Wave Radiators for Passive Cooling of Buildings. *Archit. Sci. Rev.* **1999**, *42*, 79–85. [CrossRef]
106. Berdahl, P.; Martin, M.; Sakkal, F. Performances Thermiques Des Panneaux a Refroidissement Radiatif. *Int. J. Heat Mass Transf.* **1983**, *26*, 871–880. [CrossRef]
107. Dobson, R.T. Thermal Modelling of a Night Sky Radiation Cooling System. *J. Energy South Afr.* **2005**, *16*, 56–67. [CrossRef]
108. Dimoudi, A.; Androutsopoulos, A. The Cooling Performance of a Radiator Based Roof Component. *Sol. Energy* **2006**, *80*, 1039–1047. [CrossRef]
109. Gentle, A.; Smith, P.G. Performance Comparisons of Sky Window Spectral Selective and High Emittance Radiant Cooling Systems under Varying Atmospheric Conditions. In Proceedings of the SEFI 48th Annual Conference Engaging Engineering Education, Canberra, ACT, Australia, 1–3 December 2010; pp. 1–8.
110. Okoronkwo, C.A.; Nwigwe, K.N.; Ogueke, N.V.; Anyanwu, E.E.; Onyejekwe, D.C.; Ugwuoke, P.E. An Experimental Investigation of the Passive Cooling of a Building Using Nighttime Radiant Cooling. *Int. J. Green Energy* **2014**, *11*, 1072–1083. [CrossRef]
111. Rincón, J.; Almao, N.; González, E. Experimental and Numerical Evaluation of a Solar Passive Cooling System under Hot and Humid Climatic Conditions. *Sol. Energy* **2001**, *71*, 71–80. [CrossRef]
112. Fält, M.; Zevenhoven, R. Experimentation and Modeling of an Active Skylight. In Proceedings of the 28th 23rd International Conference on Efficiency, Cost, Optimization, Simulation, and Environmental Impact of Energy Systems (ECOS) 2015, Pau, France, 29 June–3 July 2015.
113. Al-Zubaydi, A.Y.T.; Dartnall, W.J. Design and Modelling of Water Chilling Production System by the Combined Effects of Evaporation and Night Sky Radiation. *J. Renew. Energy* **2014**, *2014*, e624502. [CrossRef]
114. Gentle, A.R.; Smith, G.B. Angular Selectivity: Impact on Optimised Coatings for Night Sky Radiative Cooling. *Nanostructured Thin Film. II* **2009**, *12*, e825722. [CrossRef]
115. Zhou, L.; Song, H.; Liang, J.; Singer, M.; Zhou, M.; Stegenburgs, E.; Zhang, N.; Xu, C.; Ng, T.; Yu, Z.; et al. A Polydimethylsiloxane-Coated Metal Structure for All-Day Radiative Cooling. *Nat. Sustain.* **2019**, *2*, 718–724. [CrossRef]
116. Cunha, N.F.; AL-Rjoub, A.; Rebouta, L.; Vieira, L.G.; Lanceros-Mendez, S. Multilayer Passive Radiative Selective Cooling Coating Based on Al/SiO2/SiNx/SiO2/TiO2/SiO2 Prepared by Dc Magnetron Sputtering. *Thin Solid Film.* **2020**, *694*, e137736. [CrossRef]
117. Farooq, A.S.; Zhang, P.; Gao, Y.; Gulfam, R. Emerging Radiative Materials and Prospective Applications of Radiative Sky Cooling—A Review. *Renew. Sustain. Energy Rev.* **2021**, *144*, 110910. [CrossRef]
118. Shi, N.N.; Tsai, C.C.; Camino, F.; Bernard, G.D.; Yu, N.; Wehner, R. Keeping Cool: Enhanced Optical Reflection and Radiative Heat Dissipation in Saharan Silver Ants. *Science* **2015**, *349*, 298–301. [CrossRef] [PubMed]
119. Tsai, C.C.; Shi, N.; Pelaez, J.; Pierce, N.; Yu, N. Butterflies Regulate Wing Temperatures Using Radiative Cooling. In Proceedings of the 2017 Conference on Lasers and Electro-Optics (CLEO), San Jose, CA, USA, 14–19 May 2017. [CrossRef]
120. Shi, N.N.; Tsai, C.C.; Craig, C.; Yu, N. Nano-Structured Wild Moth Cocoon Fibers as Radiative Cooling and Waveguiding Optical Materials. In Proceedings of the Conference on Lasers and Electro-Optics, Munich, Germany, 25–29 June 2017; pp. 1–2. [CrossRef]

121. Raman, A.P.; Anoma, M.A.; Zhu, L.; Rephaeli, E.; Fan, S. Passive Radiative Cooling below Ambient Air Temperature under Direct Sunlight. *Nature* **2014**, *515*, 540–544. [CrossRef] [PubMed]
122. Liu, T.; Takahara, J. Ultrabroadband Absorber Based on Single-Sized Embedded Metal-Dielectric-Metal Structures and Application of Radiative Cooling. *Opt. Express* **2017**, *25*, A612. [CrossRef] [PubMed]
123. Wu, D.; Liu, C.; Xu, Z.; Liu, Y.; Yu, Z.; Yu, L.; Chen, L.; Li, R.; Ma, R.; Ye, H. The Design of Ultra-Broadband Selective near-Perfect Absorber Based on Photonic Structures to Achieve near-Ideal Daytime Radiative Cooling. *Mater. Des.* **2018**, *139*, 104–111. [CrossRef]
124. Gentle, A.R.; Smith, G.B. A Subambient Open Roof Surface under the Mid-Summer Sun. *Adv. Sci.* **2015**, *2*, 2–5. [CrossRef] [PubMed]
125. Zhang, Z.; Tong, S.; Yu, H. Life Cycle Analysis of Cool Roof in Tropical Areas. *Procedia Eng.* **2016**, *169*, 392–399. [CrossRef]
126. Testa, J.; Krarti, M. A Review of Benefits and Limitations of Static and Switchable Cool Roof Systems. *Renew. Sustain. Energy Rev.* **2017**, *77*, 451–460. [CrossRef]
127. Lee, G.J.; Kim, Y.J.; Kim, H.M.; Yoo, Y.J.; Song, Y.M. Colored, Daytime Radiative Coolers with Thin-Film Resonators for Aesthetic Purposes. *Adv. Opt. Mater.* **2018**, *6*, e00707. [CrossRef]
128. Bretz, S.E.; Akbari, H. Long-Term Performance of High-Albedo Roof Coatings. *Energy Build.* **1997**, *25*, 159–167. [CrossRef]
129. Akbahi, H.; Behre, A.; Levinson, R.; Graveline, S.; Foley, K.; Delgado, A.H.; Paroli, R.M. *Aging and Weathering of Cool Roofing Membranes*; Lawrence Berkeley National Laboratory: Berkeley, CA, USA, 2005; pp. 1–11.
130. Oleson, K.W.; Bonan, G.B.; Feddema, J. Effects of White Roofs on Urban Temperature in a Global Climate Model. *Geophys. Res. Lett.* **2010**, *37*, e042194. [CrossRef]
131. Yang, P.; Chen, C.; Zhang, Z.M. A Dual-Layer Structure with Record-High Solar Reflectance for Daytime Radiative Cooling. *Sol. Energy* **2018**, *169*, 316–324. [CrossRef]
132. Levinson, R.; Berdahl, P.; Akbari, H. Erratum: Solar Spectral Optical Properties of Pigments—Part I: Model for Deriving Scattering and Absorption Coefficients from Transmittance and Reflectance Measurements (Solar Energy Materials and Solar Cells (2005) 89:4 (319-349)). *Sol. Energy Mater. Sol. Cells* **2012**, *107*, 337. [CrossRef]
133. Levinson, R.; Berdahl, P.; Akbari, H. Solar Spectral Optical Properties of Pigments—Part II: Survey of Common Colorants. *Sol. Energy Mater. Sol. Cells* **2005**, *89*, 351–389. [CrossRef]
134. Chen, M.; Pang, D.; Yan, H. Colored Passive Daytime Radiative Cooling Coatings Based on Dielectric and Plasmonic Spheres. *Appl. Therm. Eng.* **2022**, *216*, e119125. [CrossRef]
135. Ono, M.; Chen, K.; Li, W.; Fan, S. Self-Adaptive Radiative Cooling Based on Phase Change Materials. *Opt. Express* **2018**, *26*, A777. [CrossRef]
136. Mandal, J.; Fu, Y.; Overvig, A.C.; Jia, M.; Sun, K.; Shi, N.N.; Zhou, H.; Xiao, X.; Yu, N.; Yang, Y. Hierarchically Porous Polymer Coatings for Highly Efficient Passive Daytime Radiative Cooling. *Sceince* **2018**, *362*, 315–319. [CrossRef]
137. Chae, D.; Kim, M.; Jung, P.H.; Son, S.; Seo, J.; Liu, Y.; Lee, B.J.; Lee, H. Spectrally Selective Inorganic-Based Multilayer Emitter for Daytime Radiative Cooling. *ACS Appl. Mater. Interfaces* **2020**, *12*, 8073–8081. [CrossRef]
138. You, P.; Li, X.; Huang, Y.; Ma, X.; Pu, M.; Guo, Y.; Luo, X. High-Performance Multilayer Radiative Cooling Films Designed with Flexible Hybrid Optimization Strategy. *Materials* **2020**, *13*, 2885. [CrossRef] [PubMed]
139. Lee, E.; Luo, T. Black Body-like Radiative Cooling for Flexible Thin-Film Solar Cells. *Sol. Energy Mater. Sol. Cells* **2019**, *194*, 222–228. [CrossRef]
140. Kecebas, M.A.; Menguc, M.P.; Kosar, A.; Sendur, K. Passive Radiative Cooling Design with Broadband Optical Thin-Film Filters. *J. Quant. Spectrosc. Radiat. Transf.* **2017**, *198*, 1339–1351. [CrossRef]
141. Fan, J.; Fu, C.; Fu, T. Yttria-Stabilized Zirconia Coating for Passive Daytime Radiative Cooling in Humid Environment. *Appl. Therm. Eng.* **2020**, *165*, 114585. [CrossRef]
142. Li, N.; Wang, J.; Liu, D.; Huang, X.; Xu, Z.; Zhang, C.; Zhang, Z.; Zhong, M. Selective Spectral Optical Properties and Structure of Aluminum Phosphate for Daytime Passive Radiative Cooling Application. *Sol. Energy Mater. Sol. Cells* **2019**, *194*, 103–110. [CrossRef]
143. Xu, Z.; Li, N.; Liu, D.; Huang, X.; Wang, J.; Wu, W.; Zhang, H.; Liu, H.; Zhang, Z.; Zhong, M. A New Crystal Mg11(HPO3)8(OH)6 for Daytime Radiative Cooling. *Sol. Energy Mater. Sol. Cells* **2018**, *185*, 536–541. [CrossRef]
144. Cheng, Z.M.; Shuai, Y.; Gong, D.Y.; Wang, F.Q.; Liang, H.X.; Li, G.Q. Optical Properties and Cooling Performance Analyses of Single-Layer Radiative Cooling Coating with Mixture of TiO2 Particles and SiO2 Particles. *Sci. China Technol. Sci.* **2021**, *64*, 1017–1029. [CrossRef]
145. Liu, Y.; Bai, A.; Fang, Z.; Ni, Y.; Lu, C.; Xu, Z. A Pragmatic Bilayer Selective Emitter for Efficient Radiative Cooling under Direct Sunlight. *Materials* **2019**, *12*, 1208. [CrossRef]
146. Song, W.Z.; Wang, X.X.; Qiu, H.J.; Wang, N.; Yu, M.; Fan, Z.; Ramakrishna, S.; Hu, H.; Long, Y.Z. Single Electrode Piezoelectric Nanogenerator for Intelligent Passive Daytime Radiative Cooling. *Nano Energy* **2021**, *82*, 105695. [CrossRef]
147. Torgerson, E.; Hellhake, J. Polymer Solar Filter for Enabling Direct Daytime Radiative Cooling. *Sol. Energy Mater. Sol. Cells* **2020**, *206*, 110319. [CrossRef]
148. Jeong, S.Y.; Tso, C.Y.; Ha, J.; Wong, Y.M.; Chao, C.Y.H.; Huang, B.; Qiu, H. Field Investigation of a Photonic Multi-Layered TiO2 Passive Radiative Cooler in Sub-Tropical Climate. *Renew. Energy* **2020**, *146*, 44–55. [CrossRef]

149. Han, D.; Ng, B.F.; Wan, M.P. Preliminary Study of Passive Radiative Cooling under Singapore's Tropical Climate. *Sol. Energy Mater. Sol. Cells* **2020**, *206*, 110270. [CrossRef]

150. Dong, M.; Chen, N.; Zhao, X.; Fan, S.; Chen, Z. Nighttime Radiative Cooling in Hot and Humid Climates. *Opt. Express* **2019**, *27*, 31587. [CrossRef] [PubMed]

151. 3M 3M™ Enhanced Specular Reflector (ESR) 3M 3M. 2018, Volume 2. Available online: https://multimedia.3m.com/mws/media/1389248O/application-guide-for-esr.pdf (accessed on 10 January 2018).

152. Erell, E.; Etzion, Y. Analysis and Experimental Verification of an Improved Cooling Radiator. *Renew. Energy* **1999**, *16*, 700–703. [CrossRef]

153. Benlattar, M.; Oualim, E.M.; Harmouchi, M.; Mouhsen, A.; Belafhal, A. Radiative Properties of Cadmium Telluride Thin Film as Radiative Cooling Materials. *Opt. Commun.* **2005**, *256*, 10–15. [CrossRef]

154. Benlattar, M.; Oualim, E.M.; Mouhib, T.; Harmouchi, M.; Mouhsen, A.; Belafhal, A. Thin Cadmium Sulphide Film for Radiative Cooling Application. *Opt. Commun.* **2006**, *267*, 65–68. [CrossRef]

155. Naghshine, B.B.; Saboonchi, A. Optimized Thin Film Coatings for Passive Radiative Cooling Applications. *Opt. Commun.* **2018**, *410*, 416–423. [CrossRef]

156. Bathgate, S.N.; Bosi, S.G. A Robust Convection Cover Material for Selective Radiative Cooling Applications. *Sol. Energy Mater. Sol. Cells* **2011**, *95*, 2778–2785. [CrossRef]

157. Khedari, J.; Waewsak, J.; Thepa, S.; Hirunlabh, J. Field Investigation of Night Radiation Cooling under Tropical Climate. *Renew. Energy* **2000**, *20*, 183–193. [CrossRef]

158. Craig, S.; Harrison, D.; Cripps, A.; Knott, D. BioTRIZ Suggests Radiative Cooling of Buildings Can Be Done Passively by Changing the Structure of Roof Insulation to Let Longwave Infrared Pass. *J. Bionic Eng.* **2008**, *5*, 55–66. [CrossRef]

159. Chen, Z.; Zhu, L.; Raman, A.; Fan, S. Radiative Cooling to Deep Sub-Freezing Temperatures through a 24-h Day-Night Cycle. *Nat. Commun.* **2016**, *7*, 1–5. [CrossRef] [PubMed]

160. Tso, C.Y.; Chan, K.C.; Chao, C.Y.H. A Field Investigation of Passive Radiative Cooling under Hong Kong's Climate. *Renew. Energy* **2017**, *106*, 52–61. [CrossRef]

161. Fält, M.; Pettersson, F.; Zevenhoven, R. Modified Predator-Prey Algorithm Approach to Designing a Cooling or Insulating Skylight. *Build. Environ.* **2017**, *126*, 331–338. [CrossRef]

162. Son, S.; Jeon, S.; Chae, D.; Lee, S.Y.; Liu, Y.; Lim, H.; Oh, S.J.; Lee, H. Colored Emitters with Silica-Embedded Perovskite Nanocrystals for Efficient Daytime Radiative Cooling. *Nano Energy* **2021**, *79*, 105461. [CrossRef]

163. Addeo, A.; Monza, E.; Peraldo, M.; Bartoli, B.; Coluzzi, B.; Silvestrini, V.; Troise, G. Selective Covers for Natural Cooling Devices. *Nuovo Cim. C* **1978**, *1*, 419–429. [CrossRef]

164. Gulmine, J.V.; Janissek, P.R.; Heise, H.M.; Akcelrud, L. Polyethylene Characterization by FTIR. *Polym. Test.* **2002**, *21*, 557–563. [CrossRef]

165. Hu, M.; Pei, G.; Li, L.; Zheng, R.; Li, J.; Ji, J. Theoretical and Experimental Study of Spectral Selectivity Surface for Both Solar Heating and Radiative Cooling. *Int. J. Photoenergy* **2015**, *2015*, 807875. [CrossRef]

166. Engelhard, T.; Jones, E.D.; Viney, I.; Mastai, Y.; Hodes, G. Deposition of Tellurium Films by Decomposition of Electrochemically-Generated H2Te: Application to Radiative Cooling Devices. *Thin Solid Film.* **2000**, *370*, 101–105. [CrossRef]

167. Ali, A.H.H.; Saito, H.; Taha, I.M.S.; Kishinami, K.; Ismail, I.M. Effect of Aging, Thickness and Color on Both the Radiative Properties of Polyethylene Films and Performance of the Nocturnal Cooling Unit. *Energy Convers. Manag.* **1998**, *39*, 87–93. [CrossRef]

168. Pieters, J.G.; Deltour, J.M. Performances of Greenhouses with the Presence of Condensation on Cladding Materials. *J. Agric. Eng. Res.* **1997**, *68*, 125–137. [CrossRef]

169. Pollet, I.V.; Pieters, J.G. Condensation and Radiation Transmittance of Greenhouse Cladding Materials, Part 3: Results for Glass Plates and Plastic Films. *J. Agric. Eng. Res.* **2000**, *77*, 419–428. [CrossRef]

170. Parsons, A.M.; Sharp, K. The Effects of Multiple Covers with Condensation and Optical Degradation of a Polyethylene Windscreen on the Performance of a Sky Cooling System. *Int. J. Sustain. Energy* **2019**, *38*, 469–485. [CrossRef]

171. Gentle, A.R.; Dybdal, K.L.; Smith, G.B. Polymeric Mesh for Durable Infra-Red Transparent Convection Shields: Applications in Cool Roofs and Sky Cooling. *Sol. Energy Mater. Sol. Cells* **2013**, *115*, 79–85. [CrossRef]

172. Golaka, A.; Exell, R.H.B. An Investigation into the Use of a Wind Shield to Reduce the Convective Heat Flux to a Nocturnal Radiative Cooling Surface. *Renew. Energy* **2007**, *32*, 593–608. [CrossRef]

173. Mastai, Y.; Diamant, Y.; Aruna, S.T.; Zaban, A. TiO2 Nanocrystalline Pigmented Polyethylene Foils for Radiative Cooling Applications: Synthesis and Characterization. *Langmuir* **2001**, *17*, 7118–7123. [CrossRef]

174. Liu, J.; Zhang, D.; Jiao, S.; Zhou, Z.; Zhang, Z.; Gao, F. Daytime Radiative Cooling with Clear Epoxy Resin. *Sol. Energy Mater. Sol. Cells* **2020**, *207*, 110368. [CrossRef]

175. Bhatia, B.; Leroy, A.; Shen, Y.; Zhao, L.; Gianello, M.; Li, D.; Gu, T.; Hu, J.; Soljačić, M.; Wang, E.N. Passive Directional Sub-Ambient Daytime Radiative Cooling. *Nat. Commun.* **2018**, *9*, 7293. [CrossRef] [PubMed]

176. Hannah, K.; Andrej, L. Optical and Thermal Filtering Nanoporous Materials for Sub-ambient Radiative Cooling. *J. Opt.* **2018**, *20*, 084002. [CrossRef]

177. Leroy, A.; Bhatia, B.; Kelsall, C.C.; Castillejo-Cuberos, A.; Di Capua, M.H.; Zhao, L.; Zhang, L.; Guzman, A.M.; Wang, E.N. High-Performance Subambient Radiative Cooling Enabled by Optically Selective and Thermally Insulating Polyethylene Aerogel. *Sci. Adv.* **2019**, *5*, 9480. [CrossRef] [PubMed]

178. Zhang, J.; Zhou, Z.; Tang, H.; Xing, J.; Quan, J.; Liu, J.; Yu, J.; Hu, M. Mechanically Robust and Spectrally Selective Convection Shield for Daytime Subambient Radiative Cooling. *ACS Appl. Mater. Interfaces* **2021**, *13*, 14132–14140. [CrossRef]

179. Royne, A.; Dey, C.J.; Mills, D.R. Cooling of Photovoltaic Cells under Concentrated Illumination: A Critical Review. *Sol. Energy Mater. Sol. Cells* **2005**, *86*, 451–483. [CrossRef]

180. Skoplaki, E.; Palyvos, J.A. On the Temperature Dependence of Photovoltaic Module Electrical Performance: A Review of Efficiency/Power Correlations. *Sol. Energy* **2009**, *83*, 614–624. [CrossRef]

181. Wang, Z.; Kortge, D.; Zhu, J.; Zhou, Z.; Torsina, H.; Lee, C.; Bermel, P. Lightweight, Passive Radiative Cooling to Enhance Concentrating Photovoltaics. *Joule* **2020**, *4*, 2702–2717. [CrossRef]

182. Li, W.; Shi, Y.; Chen, K.; Zhu, L.; Fan, S. A Comprehensive Photonic Approach for Solar Cell Cooling. *ACS Photonics* **2017**, *4*, 774–782. [CrossRef]

183. Riverola, A.; Mellor, A.; Alonso Alvarez, D.; Ferre Llin, L.; Guarracino, I.; Markides, C.N.; Paul, D.J.; Chemisana, D.; Ekins-Daukes, N. Mid-Infrared Emissivity of Crystalline Silicon Solar Cells. *Sol. Energy Mater. Sol. Cells* **2018**, *174*, 607–615. [CrossRef]

184. Safi, T.S.; Munday, J.N. Improving Photovoltaic Performance through Radiative Cooling in Both Terrestrial and Extraterrestrial Environments. *Opt. Express* **2015**, *23*, A1120. [CrossRef]

185. Chen, M.; Yan, H.; Zhou, P.; Chen, X.Y. Performance Analysis of Solar Thermophotovoltaic System with Selective Absorber/Emitter. *J. Quant. Spectrosc. Radiat. Transf.* **2020**, *253*, 107163. [CrossRef]

186. Chen, M.; Chen, X.; Yan, H.; Zhou, P. Theoretical Design of Nanoparticle-Based Spectrally Emitter for Thermophotovoltaic Applications. *Phys. E Low-Dimens. Syst. Nanostruct.* **2021**, *126*, 114471. [CrossRef]

187. Raman, A.P.; Li, W.; Fan, S. Generating Light from Darkness. *Joule* **2019**, *3*, 2679–2686. [CrossRef]

188. Fan, L.; Li, W.; Jin, W.; Orenstein, M.; Fan, S. Maximal Nighttime Electrical Power Generation via Optimal Radiative Cooling. *Opt. Express* **2020**, *28*, 25460. [CrossRef]

189. Ishii, S.; Dao, T.D.; Nagao, T. Radiative Cooling for Continuous Thermoelectric Power Generation in Day and Night. *Appl. Phys. Lett.* **2020**, *117*, 10190. [CrossRef]

190. Taylor, S.; Yang, Y.; Wang, L. Vanadium Dioxide Based Fabry-Perot Emitter for Dynamic Radiative Cooling Applications. *J. Quant. Spectrosc. Radiat. Transf.* **2017**, *197*, 76–83. [CrossRef]

191. Sun, K.; Riedel, C.A.; Wang, Y.; Urbani, A.; Simeoni, M.; Mengali, S.; Zalkovskij, M.; Bilenberg, B.; De Groot, C.H.; Muskens, O.L. Metasurface Optical Solar Reflectors Using AZO Transparent Conducting Oxides for Radiative Cooling of Spacecraft. *ACS Photonics* **2018**, *5*, 495–501. [CrossRef]

192. Bijarniya, J.P.; Sarkar, J.; Maiti, P. Environmental Effect on the Performance of Passive Daytime Photonic Radiative Cooling and Building Energy-Saving Potential. *J. Clean. Prod.* **2020**, *274*, 123119. [CrossRef]

193. Zhu, L.; Fan, S. Near-Complete Violation of Detailed Balance in Thermal Radiation. *Phys. Rev. B Condens. Matter Mater. Phys.* **2014**, *90*, 220301. [CrossRef]

194. Zevenhoven, R.; Fält, M. Radiative Cooling through the Atmospheric Window: A Third, Less Intrusive Geoengineering Approach. *Energy* **2018**, *152*, 27–33. [CrossRef]

195. Levinson, R.; Akbari, H. Potential Benefits of Cool Roofs on Commercial Buildings: Conserving Energy, Saving Money, and Reducing Emission of Greenhouse Gases and Air Pollutants. *Energy Effic.* **2010**, *3*, 53–109. [CrossRef]

196. Hosseini, M.; Akbari, H. Effect of Cool Roofs on Commercial Buildings Energy Use in Cold Climates. *Energy Build.* **2016**, *114*, 143–155. [CrossRef]

197. Erell, E.; Yannas, S.; Molina, J.L. *Roof Cooling Techniques*; Routledge: London, UK, 2005. [CrossRef]

198. Enderlin, A.R. ScholarWorks @ UARK Radiative Cooling to the Night Sky Radiative Cooling to the Night Sky. Bachelor Thesis, Department of Chemical Engineering, University of Arkansas, Fayetteville, AK, USA, 2015.

199. U.S. Department of Energy. *Technology Installation Review: WhiteCapTM Roof Spray Cooling System*; U.S. Department of Energy: Washington, DC, USA, 1998.